Thermal-Hydraulic Turbine Dynamometer

To: Dr. Patrick Lemieux

CVTeam

Ryan Baskett

Alexander Campbell

Andrew Puntorno-Carlberg

Mechanical Engineering Department

California Polytechnic State University

San Luis Obispo

2015

Statement of Disclaimer

Table of Contents

1. Introduction:

The purpose of this project is to design and implement a variable system to control loading and measure power generation through Cal Poly's Wind Turbine. Our product will be used by Dr. Lemieux for research into wind power technology - the effects of rotor size and tip speed in various wind conditions. Currently, the Cal Poly Wind Turbine is equipped with a 2-meter rotor and a direct drive shaft to an electric generator. The current setup poses two problems for efficient power generation: the small rotor is unable to produce significant power in low-speed wind conditions, and the direct drive does not have the ability to regulate rotor speed in order to maximize efficiency. Implementing a variable system will allow a larger, 10-meter, rotor to be fitted to the tower which could provide power in low wind conditions while regulating the tip speed of the rotor in varying wind speeds.

Our sponsor requested that we aim to achieve these goals using a Hydraulic Continuously Variable Transmission (CVT), so that was our original goal. This would have provided him with means to conduct additional research on CVT's. Our team attempted to do so; however, this approach proved to be beyond our financial resources and was not a viable option for implementation. This report will show our research into CVT's and our suggested design for future projects with more funding, as well as our alternative design to achieve our sponsors more immediate needs.

1.1 Background:

When it comes to the transmission of power from rotor to generator, the majority of wind turbines currently implement a planetary gear transmission, example shown in Figure 1, which uses large helical gears to transmit the power produced by the rotor.

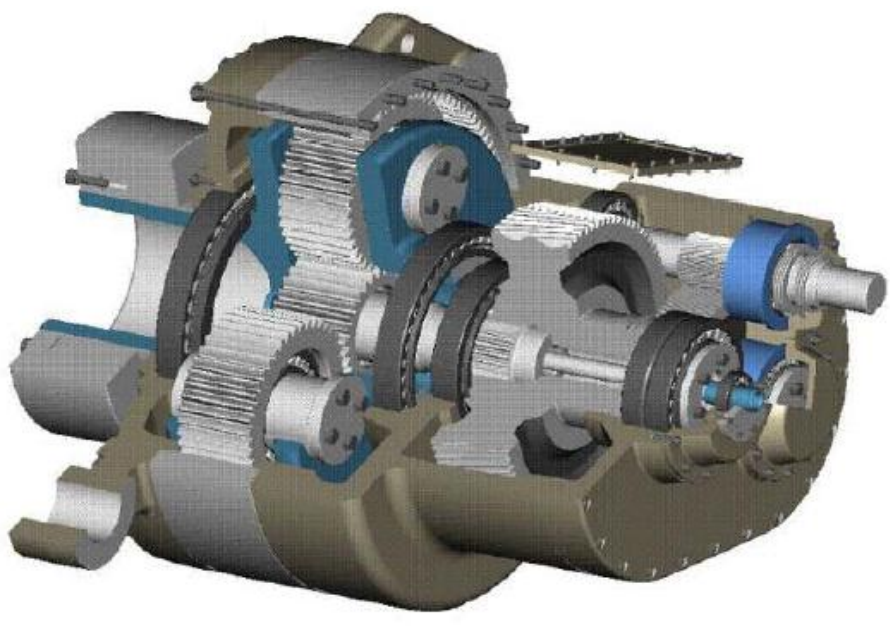

Figure 1. A typical planetary gearbox used in Wind Turbine Designs.

A mechanical gear box has the ability to change the rotor speed in varying wind conditions, but it has a drawback as described by Ragheb in his paper **Wind Turbine Gearbox Technologies,** "The typical design lifetime of a utility wind turbine is 20 years, but the gearboxes, which convert rotor blades rotational speed of between 5 and 22 rpm to the generator-required speed of around 1,000 to 1,600

rpm, commonly fail within an operational period of 5 years, and have to be replaced" (Ragheb & Ragheb, 2010). The short lifetime and high cost of a mechanical gearbox can intrude on the profitability of using a wind turbine to generate power. Other ideas and products to replace the short lifespan planetary gearboxes include direct drive transmissions which utilize annular multipole generators, seen in Figure 2, which split the torque between several generators in order to relieve the stress on the gears, and a wide variety of CVTs.

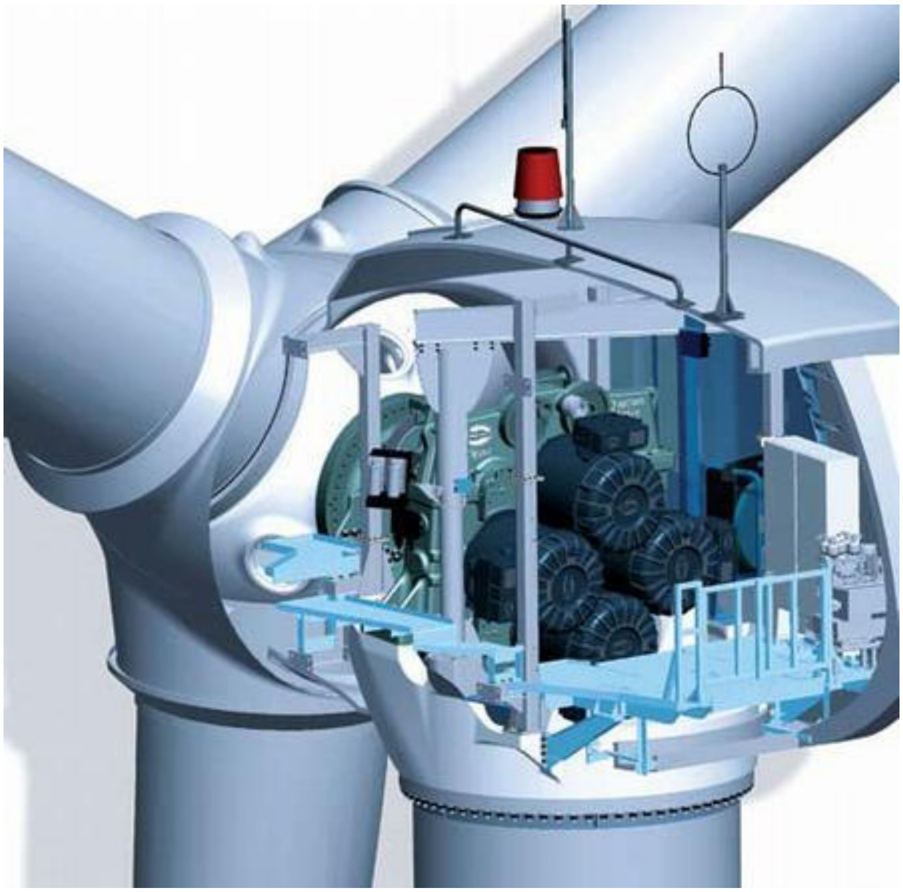

Figure 2. Annular generator transmission used in wind turbines.

The alternative methods of power transmission listed above have seen adequate success in being implemented into production wind turbines. The underlying problem with using CVTs in the past has been their inability to handle excessive torque. This is due to most CVTs requiring the use of a source pulley which can require a large frictional force to withstand the rotor torque. This problem is overcome by using a hydrostatic CVT because it does not use a source pulley, but rather uses a hydraulic pump and motor to transfer torque. The concept of using hydraulic pumps and motors like this dates back to the 1970's with Patent US 4149092 A (United States Patent No. US4149092, 1979); however, the actual application of it is quite recent - only occurring in the last few years (Europe Patent No. EP2535581A2). There are several patents on the application of hydrostatic transmissions in wind turbines that we have reviewed and have taken into account.

The reason for the lack of implementing hydrostatic CVTs in wind turbines can be attributed to some inherent characteristics with their design. Hydrostatic CVTs are less efficient than conventional

mechanical gear systems by sometimes more than 20%. The low efficiency of hydrostatic CVTs is primarily caused by the losses due to pump and motor leakage since the systems are usually under high pressures (on the orders of thousands of psi). Another characteristic of hydrostatic CVTs is that they have a high capital cost. Pumps and motors that are capable of transmitting the power produced by a commercial wind turbine are frequently built to order and come at an extremely high cost. The high pressure that these transmissions operate at also requires high strength seals and bearings which add to the cost of the systems.

1.2 Project Objectives:

The objective of the CVTeam is to modify the current Cal Poly wind turbine by replacing the current direct drive power transmission system with a variable system that has the capability to control load and measure power output. The new system must be able to operate with both the 2m and 10m rotors currently being considered and it must be able to control the rotor speed to maximize efficiency. The system must also be safe, consist primarily of off-the-shelf components, and avoid any major alterations to the current nacelle.

1.2.1 Package Dimensions

Due to the limited space within the nacelle and our sponsor's desire to avoid alterations, we will use the overall package dimensions as our first engineering specification. Since the overall dimensions of the system can have numerous configurations we will focus on the most restrictive size requirement, the axial length of our components inside the nacelle. While this length will be our primary specification, we will also take other package dimensions into consideration during our design selection phase.

1.2.2 Loading Capacity

In order for the system to operate with both rotors it must be able to apply a load equivalent to the direct drive system for the current rotor and, for the new, larger rotor, it must be able to apply a load equivalent to a 10:1 gear ratio (a load 10-times greater than the direct drive system). Hence, our next engineering specification is loading capacity.

1.2.3 Power Capacity

Currently, the generator being used by the Cal Poly wind turbine is rated for about 3kW and the braking system slows down the rotor when reaching an rpm that would produce around 4kW. Using this information, the CVTeam will design a system that expects to safely handle and measure up to 4kW of power.

1.2.4 Efficiency

The overall goal of this project is to produce a system that can control loading and measure power being produced; therefore, system efficiency is only a consideration as far as handling its general side-effects. Efficiency itself is not a concern of the CVTeam as long as it can be measured; however, lost efficiency in any hydraulic system is dumped directly into the working fluid in the form of thermal energy, so in that regard, efficiency must be managed and handled appropriately as to not overheat the working fluid or surrounding components.

1.2.5 Support Structure Factor of Safety

Since the CVT system will consist primarily of off-the-shelf components, we will be required to design and manufacture a custom support structure. To ensure the safety of our system we will require a minimum factor of safety of 2.0 for all support structure components.

You can see all of the above engineering specifications along with their corresponding tolerance, risk, and compliance tabulated in Table 1 below.

Table 1. Cal Poly Hydrostatic Wind Turbine CVT Formal Requirements

Spec. #	Parameter Description	Required or Target	Tolerance	Risk*	Compliance**
1	Package Dimensions	length ≤ 30 in	Max	H	A, S, I
2	Gear Ratio Range	1:1 to ~10:1	Min	H	A, T, I
3	Power Capacity	6 kW	Min	M	A, T
4	Efficiency	≈ 80%	Min	M	A,T
5	Support Structure F.S.	2	Min	L	A

**High (H), Medium (M), Low (L)

* Analysis (A), Test (T), Similarity to Existing Design (S), Inspection (I)

1.3 Quality Function Deployment

A House of Quality figure can be seen below in Appendix A which uses the Quality Function Deployment (QFD) method to turn qualitative demands into measurable goals. The QFD displays the requirements and considerations for the CVT's function and compares them to measurable engineering specifications which will be used to reach those requirements. The engineering specifications described in the QFD are weighted in importance based on the amount of requirements they help to fulfill. The QFD also relates the engineering specifications to each other so that the result of changing one specification can be predicted. The final comparison that the QFD helps to make is the comparison of the CVT project with other products currently on the market. Using the QFD we can visualize the strengths and weaknesses of our design with the strengths and weaknesses of other designs.

2. Initial Design Development (CVT):

2.1 Concepts

The design of a Hydrostatic CVT for the wind turbine is dependent on two parts: 1. nacelle geometry and component configuration, and 2. pump and motor type. The design choices made for the nacelle geometry greatly affects the design choices for pump and motor type since the space made available by the nacelle geometry is what determines the pump and motor size. While these two criteria are directly linked, we underwent the first stage of the design selection process for the nacelle geometry and pump/motor type independently, thus ensuring that no options were exclude prematurely.

2.1.1 Nacelle Geometry

The arrangement of the internal components (mainly the generator) of the nacelle is the sole variable that determines the space available for the CVT. We considered the following configurations of the generator:

- No change to geometry
- Offsetting the pump and motor with a mechanical transmission
- Rotating the generator 180°
- Moving the generator farther back in the nacelle
- Rotating the generator 180° and moving the generator back in the nacelle
- Move generator outside of the nacelle

The configurations of the generator that involve rotating it 180° or removing the generator from the nacelle completely relies on the fact that the hydrostatic CVT does not require any specific orientation between the pump and motor in order to function. The power transmission between the pump and motor only requires hydraulic lines to be installed which allow the pump and motor to be in independent locations.

No Change to Geometry

The current layout of the nacelle has the rotor connected to a drive shaft which is coupled directly to another drive shaft which leads to the generator. The coupler which would be removed is a little less than 6 inches long. To utilize this geometry, the pump, motor, and their accompanying components would need to be contained within the 6" space.

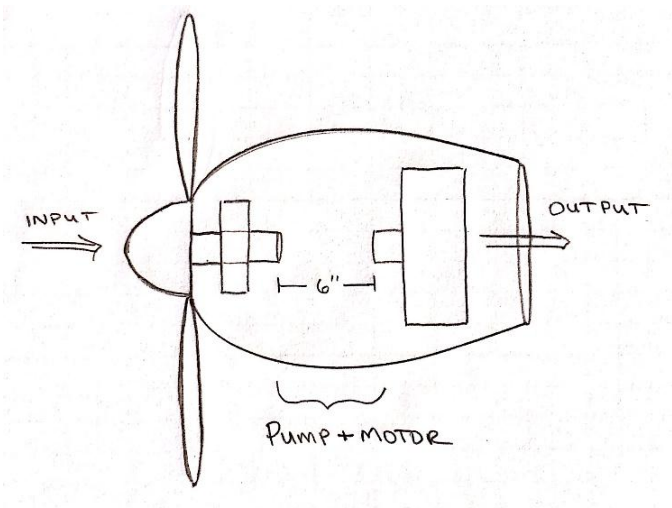

Figure 3. Current Nacelle Geometry

Offsetting the Pump and Motor with a Mechanical Transmission

The mechanical transmission design uses bevel gears to put the axial direction of the pump and motor perpendicular to the shafts of the rotor and generator. While this design is advantageous because it utilizes the space towards the sides of the nacelle, it would require a lubricated, enclosed gear box to maintain the gears. Also, depending on the size of the final pump and motor, the space towards the sides of the nacelle may not be sufficient to contain all of the components.

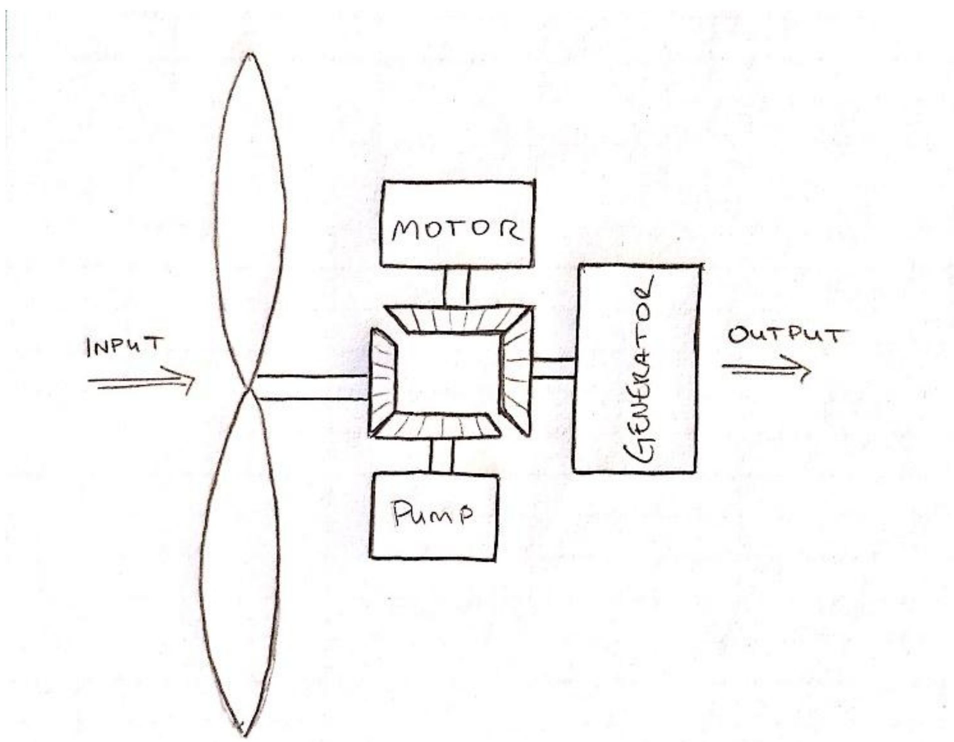

Figure 4. Sketch of Mechanical Transmission Offset

Rotating and/or Moving Back the Generator

Rotating the generator backwards allows the space between the generator and the rear of the fairing to be used to house the motor. This means the space where the coupler was present can be solely used to contain the pump. Moving the generator back towards the rear of the nacelle will widen the distance between the drive shafts for the pump and motor, but likely will only give a few more inches. Combining both methods of rotating and moving back the generator allows for the rear of the nacelle to be used and provides a few more inches in front of the generator for pump fitment.

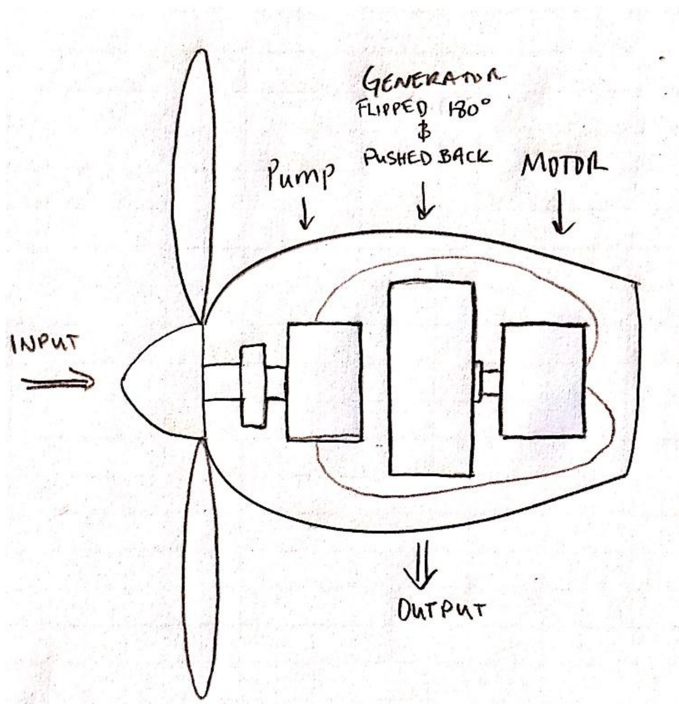

Figure 5. Sketch of Flipped and Moved Back Generator

Moving Generator Out of the Nacelle

Removing the generator from the nacelle completely provides the maximum space of all the geometry concepts. Having the generator on the ground leaves the entire nacelle space to be used for the pump, which widens the options for more pump sizes. The generator and the motor would need a container to protect the components from the weather since it would be located outside of any fairings, but the ability to create a container of any size means that motor size would not be restrictive.

Additionally, hydraulic lines would need to be installed to transport hydraulic fluid up and down the full height of the tower. While the head loss associated with the large increase in line length is a concern, initial calculations have shown that the pressure drop across the line will be on the order of 1-6% of the total operating pressure. To prove that moving the generator out of the nacelle is a viable option, calculations on head loss and pressure drop can be seen in Appendix B and C.

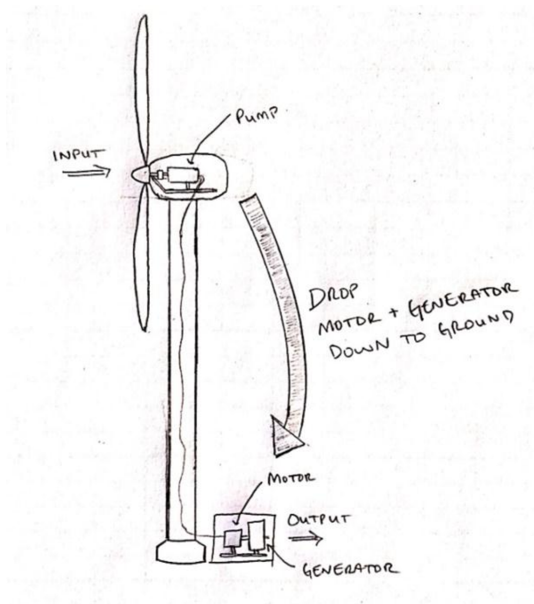

Figure 6. Sketch of Moving the Generator Out of the Nacelle

2.1.2 Pump and Motor Type

The type of pump and motor used in the design has a large effect on the overall efficiency, cost, and maximum power transfer capabilities of the system. The following pump and motor types were chosen to be analyzed:

- Axial Piston
- Radial Piston
- Rotary Vane
- Lobe
- Internal Gear
- External Gear

All pump and motor types chosen for analysis are positive displacement which maintains a constant volumetric flow rate for a certain displacement.

Axial Piston Pump

An axial piston pump is a positive displacement pump which consists of several pistons arranged in a circular pattern parallel to the driveshaft. Axial piston pumps have the highest efficiency compared to the five other pump types we considered. Axial pumps are also the most common type of positive displacement pump; as such, there are many commercially available models to choose from and they are less expensive than other pump types of comparable size and quality.

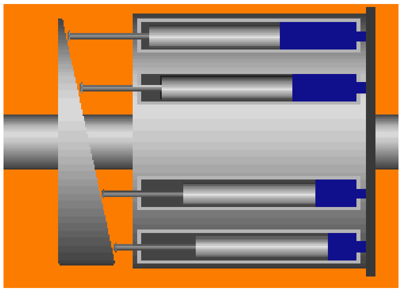

Radial Piston Pump

Radial piston pumps are similar to axial piston pumps, except their pistons are arranged in a radial manner. This geometric difference allows them to have a considerable shorter axial length for a comparable displacement while still having a high efficiency. The main drawback of radial piston pumps is their lack of availability and their prohibitive cost.

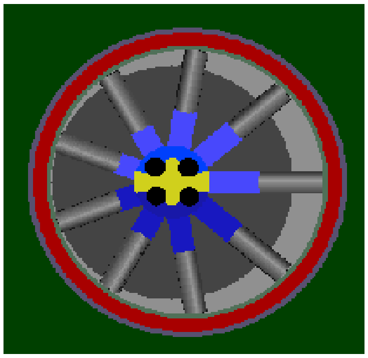

Rotary Vane Pump

A rotary vane pump consists of a rotor with radially mounted vanes that create chambers between the rotor and the side of the pump cavity. Rotary vane pumps are easily variable and they are relatively compact; however, they are not ideal for high viscosity fluids and low operating speeds.

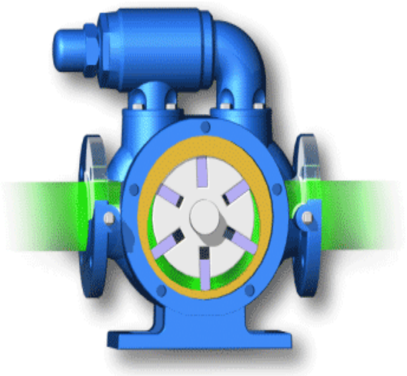

Lobe Pump

Lobe pumps consist of lobes with meshing faces that create chambers between the interior cavity and the lobes. Lobe pumps are ideal for application where there are particulates in the fluid, but they require a high operating speed to maintain a desirable efficiency.

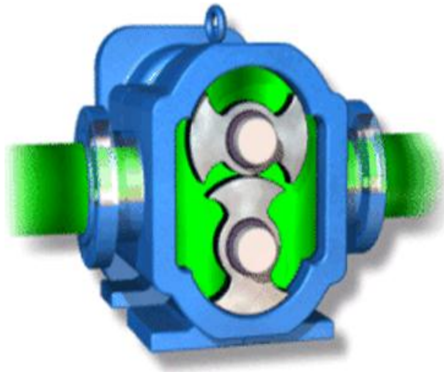

Internal Gear Pump

Gear pumps are quite common and have a variety of applications. They use the rotation and meshing of gears to pump fluids; as the gears rotate, they create a void in the intake side to allow fluid to rush in, once inside, the fluid is pushed through the pump as the gears mesh together. Internal gear pumps consist of a driving gear in the center that rotates around external teeth to create voids and push fluid through; these pumps are simple and easy to maintain and can handle fluids of very high viscosity.

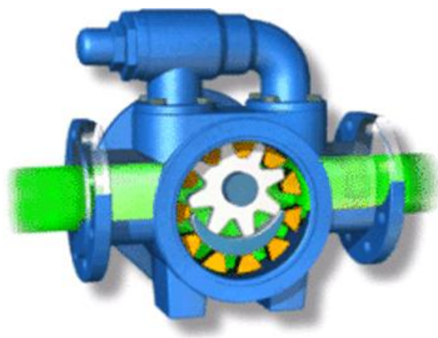

External Gear Pump

External gear pumps are very similar to internal gear pumps except the operate using two gears - the drive gear and the idler gear. These pumps are also very common and are used mainly for hydraulic power applications. They can handle highly viscous fluids but are usually limited to a working pressure of around 200 bars and an operating speed of around 3000 rpm.

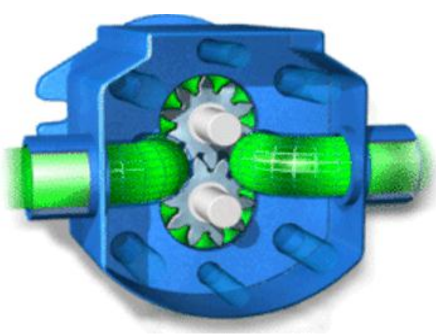

2.2 Concept Selection (CVT):

2.2.1 Pugh & Decision Matrices

Our first step in selecting a concept was to generate Pugh matrices to narrow down our option by comparing each design element with specific objectives or key features necessary to achieve said objectives. Since the primary aspects of our design that most heavily influence our final concept are the geometrical arrangement and the type of pump and motor we created Pugh matrices for each respective design element.

Table 2 is our geometrical arrangement Pugh matrix. While this Pugh matrix did not produce a definitive winner in our geometrical arrangements, it highlighted some key considerations. From

Table 2 we were able to eliminate the option of offsetting the pump and motor with beveled gears. We were also able to determine that moving the generator outside of the nacelle provide the most benefits from the list of geometrical arrangements.

Table 2. Geometric Arrangement Selection Pugh Matrix

Geometry						
Concept / Criteria	No Change	Flipping 180	Moving Back	Flip and Move Back	Offset w/ Gears	Move Generator Outside
Cost of Alteration	D	S	S	S	-	-
Space Made Available	A	+	+	+	+	+
Ease of Implementation	T	-	-	-	-	-
Alterations to Nacelle	U	S	S	S	S	S
Moment on Tower	M	S	S	S	S	+
Sum (+)	0	1	1	1	1	2
Sum (-)	0	1	1	1	2	2
Sum (S)	0	3	3	3	2	1

Unlike the geometrical arrangement Pugh matrix, our pump and motor type Pugh matrix, Table 3, did produce a definitive winner, the radial piston pump. Table 3 shows that the radial piston and axial piston pumps have definitive advantages over all other types in efficiency, however the radial piston pump has a shorter axial length. Thus, for our application the radial piston pump is ideal.

Table 3. Pump & Motor Selection Pugh Matrix

Pump/Motor Type						
Concept / Criteria	Axial Piston	Radial Piston	Vane	Lobe	Internal Gear	External Gear
Cost	D	-	-	-	S	S
Axial Length	A	+	+	+	+	+
Efficiency	T	S	-	-	-	-
Gear Ratio	U	+	+	-	-	-
Maintenance	M	S	-	S	S	S
Sum (+)	0	2	2	1	1	1
Sum (-)	0	1	3	3	2	2
Sum (S)	0	2	0	1	2	2

While our Pugh matrices provided useful observations, they do not take into account the degree to which a concept satisfies a criteria, nor do they account for the relative importance of each criteria compared to the others. For these reasons, our next step in selecting a design was to narrow down our options further with decision matrices, which takes both of these factors into consideration. As with the Pugh matrices, we broke our design matrices into geometric arrangement, and pump and motor type. In Table 4 it can be seen that moving the generator and hydraulic motor outside of the nacelle is the ideal geometric arrangement.

Table 4. Geometric Arrangement Selection Decision Matrix

Geometry													
Concept / Criteria	Weight	No Change		Flipping 180		Moving Back		Flip and Move Back		Offset w/ Gears		Move Generator Outside	
		% Satisfaction	Weighted	% Satisfaction	Weighted	% Satisfaction	Weighted	% Satisfaction	Weighted	% Satisfaction	Weighted	% Satisfaction	Weighted
Cost of Alteration	0.15	100	15	100	15	100	15	100	15	45	6.75	65	9.75
Space Made Available	0.5	0	0	40	20	60	30	75	37.5	50	25	100	50
Ease of Implementation	0.15	100	15	95	14.25	90	13.5	80	12	20	3	70	10.5
Moment on Tower	0.2	50	10	50	10	50	10	50	10	40	8	100	20
Weighted Total	1	40		59.25		68.5		74.5		42.75		90.25	

Table 5 suggests that the ideal motor is a radial piston pump, and the ideal pump is an axial piston pump. While the radial piston pump has a higher overall score in

Table 5 the criteria of axial length is not a concern for the motor if it is placed outside of the nacelle as suggested by the results of Table 4; therefore, an axial piston pump is a better choice for the motor due to its lower price and market availability. Combining the results of these two tables, we have a final design consisting of a radial piston pump inside the nacelle, and an axial piston motor coupled to the generator outside of the nacelle.

Table 5. Pump & Motor Selection Decision Matrix

Pump & Motor													
Concept / Criteria	Weight	Axial Piston		Radial Piston		Vane		Lobe		Internal Gear		Externa l Gear	
		% Satisfaction	Weighted	% Satisfaction	Weighted	% Satisfaction	Weighted	% Satisfaction	Weighted	% Satisfaction	Weighted	% Satisfaction	Weighted
Cost	0.2	100	20	75	15	75	15	75	15	80	16	80	16
Axial Length	0.2	50	10	80	16	80	16	80	16	80	16	80	16
Efficiency	0.3	91	27.3	90	27	85	25.5	85	25.5	85	25.5	90	27
Gear Ratio	0.25	100	25	100	25	60	15	40	10	40	10	40	10
Maintenance	0.05	90	4.5	90	4.5	60	3	70	3.5	70	3.5	70	3.5
Weighted Total	1	86.8		87.5		74.5		70		71		72.5	

2.3 Selected Concept (CVT):

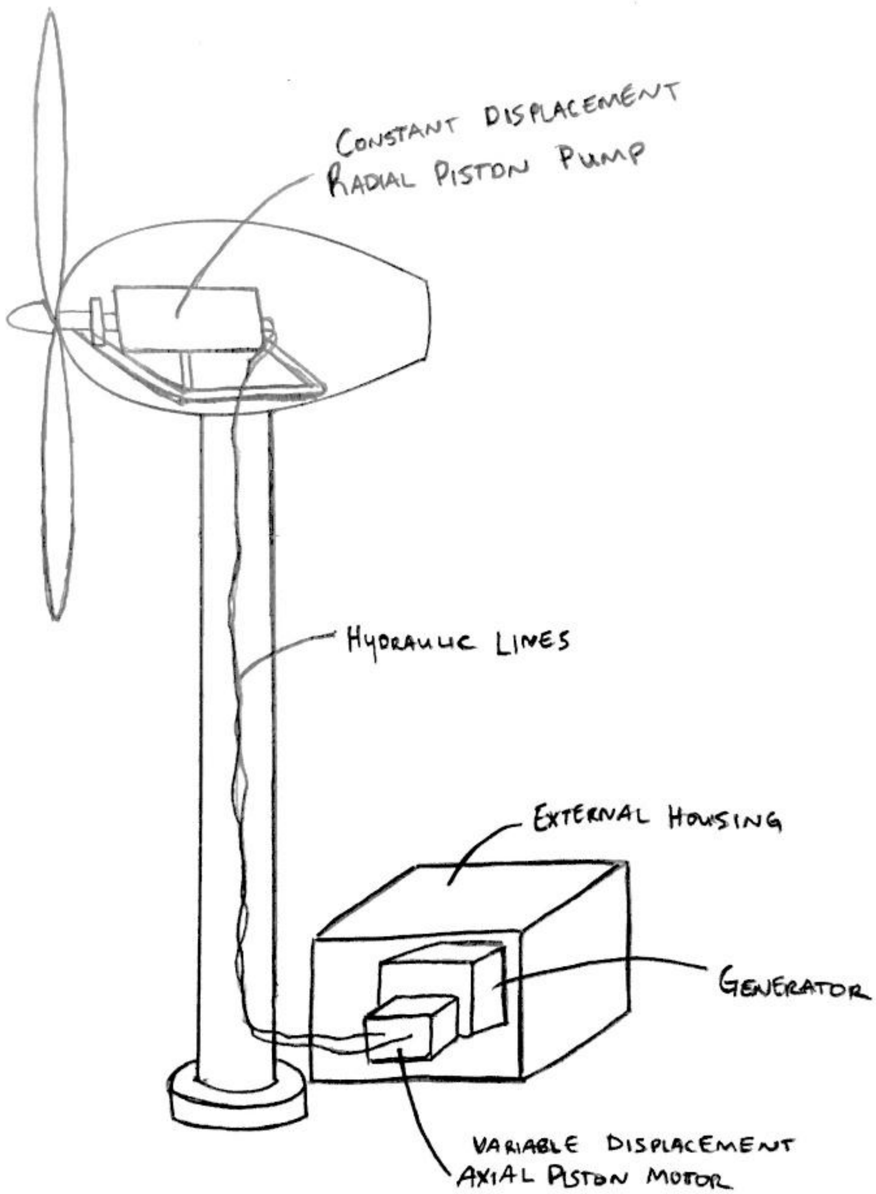

Figure 6. Selected Concept

After much deliberation we recommend the above concept - a fixed displacement radial piston pump linked with hydraulic lines to a variable, axial piston motor and generator that will be contained in an external housing. While other combinations of geometric arrangements and pump/motor types may be feasible, we have not been able to find any such combination that would not require substantial alterations to the nacelle.

Additionally, the above concept has the added benefit of decreasing the overall weight of components within the nacelle, which alleviates concerns of structural failure do to shock loading upon raising and lowering of the tower.

For the motor, we recommend a variable bent-axis piston motor - these motors are reliable and less expensive than other options and we believe it will be advantageous to vary the motor from the ground rather than varying the pump at the top of the tower due to size limitations within the nacelle. When it came to pump selection, piston pumps stood out among the rest because of their ability to handle the low rpm provided by the rotor. We selected a radial piston pump because of the limited axial space available in the nacelle, but we are still investigating whether or not there are axial piston pumps that will fit without alterations being made to the nacelle.

The amount of fluid power transferred in a hydraulic system is a function of both flowrate and pressure. To achieve the desired fluid power at a manageable working pressure, two options are available. The first option is a large displacement pump and motor which can provide a large flowrate at the low rotor speed. While this option maintains the simplicity of the hydrostatic CVT system, it is prohibitively costly and heavy. The second option is to use a small displacement pump attached to a mechanical transmission, which increases the speed of the input shaft into the pump. The mechanical gearbox would allow the use of a smaller pump to produce the same flow rate. The benefit of this option is the use of a smaller pump which would drastically decrease the cost and size of the system. Unfortunately this option would increase the relative complexity of the system, introducing more efficiency losses in the mechanical gearbox as well as more components which could potentially fail.

3. Alternative Design Development

(Thermal-Hydraulic Turbine Dynamometer):

3.1 Concept:

After reviewing each design involving hydraulic CVT's, our team determined that a traditional CVT was not financially feasible for this project, so we decided to pursue an alternative design. The selected CVT concept is still valid and all research and designs will be left with our sponsor in case there ever comes a time when funding for completion of this project is available. For now, we want a design that will provide our sponsor with the means to continue his research, while still leaving room for a CVT to be completed in the future. Realizing that it was not necessary to capture the generated power produced by the turbine, we came up with what we refer to as the "Thermal-Hydraulic Turbine Dynamometer" concept – a design consisting of a pump, a heat exchanger, a method of measuring potential power produced, a throttling device, and a few other components to regulate flow and pressure. With this design, the need for a motor and generator are eliminated (along with much of the cost) and the load can be controlled by the throttle device while the energy that would be produced as electrical power is, instead, released as heat and measured by other means. Details of this concept are as follows.

3.1.1 Idea Generation:

Our design can be simplified down to four main functions: power absorption, energy transfer, application of load, and measurement of power produced by the system. There are several methods of accomplishing each function, below is our analysis and comparison of these methods.

3.1.2 Power Absorption:

It is necessary to take the mechanical power from the rotor and transfer it into something we can measure. Since our sponsor wants to, someday, incorporate a CVT into this turbine, we decided to transform the mechanical power to hydraulic power and begin building the first stages of a CVT. Although a bent-axis piston pump was already donated to us, we performed the following analysis to validate our selection.

FUNCTION: Transfer of Power													
Concept / Criteria	Weight	Bent-Axis Piston		Radial Piston		Vane		Lobe		Internal Gear		External Gear	
		% Satisfaction	Weighted	% Satisfaction	Weighted	% Satisfaction	Weighted	% Satisfaction	Weighted	% Satisfaction	Weighted	% Satisfaction	Weighted
Cost	0.4	100	40	25	10	25	10	25	10	25	10	25	10
Axial Length	0.2	50	10	80	16	80	16	80	16	80	16	80	16
Efficiency	0.1	91	9.1	90	27	85	25.5	85	25.5	85	25.5	90	27
Gear Ratio	0.25	100	25	100	25	60	15	40	10	40	10	40	10
Maintanance	0.05	90	4.5	90	4.5	60	3	70	3.5	70	3.5	70	3.5
Weighted Total	1	88.6		82.5		69.5		65		65		66.5	

3.1.3 Energy Transfer:

With power coming into our system, our options for transferring the power out of the system are to convert the energy to heat and release it through a heat exchanger, add a motor to convert back to mechanical power and release through a generator (completing a CVT), or keep the heat in our system and allow it to be transferred by natural convection and radiation from the system components.

FUNCTION: Release of Energy									
Concept / Criteria	Weight	Air-Oil Heat Ex.		Concentric Tube Heat Ex.		Generator		No Release	
		% Satisfaction	Weighted	% Satisfaction	Weighted	% Satisfaction	Weighted	% Satisfaction	Weighted
Cost	0.3	90	27	25	7.5	10	3	100	30
Capacity	0.35	90	31.5	90	31.5	100	35	0	0
Size	0.2	75	15	75	15	50	10	100	20
Weighted Total	0.15	80	12	65	9.75	25	3.75	100	15
Weighted Total		85.5		63.75		51.75		65	

3.1.4 Application of Load:

For our sponsor's research, there needs to be a way to apply a load to the rotor. This can be done mechanically with some sort of braking system applied directly to the rotor/shaft, or it can be done hydraulically by creating an increased upstream pressure on the system, causing a load on the pump to resist the motion of the rotor.

FUNCTION: Application of Load									
Concept / Criteria	Weight	Throttle Valve		Needle Valve		Counterbalance Valve		Mechanical Resistance	
		% Satisfaction	Weighted	% Satisfaction	Weighted	% Satisfaction	Weighted	% Satisfaction	Weighted
Cost	0.3	80	24	90	27	80	24	50	15
Load Capability	0.5	90	45	100	50	90	45	100	50
Controllability	0.1	100	10	75	7.5	50	5	25	2.5
Variability	0.1	90	9	100	10	50	5	25	2.5
Weighted Total	1	88		94.5		79		70	

3.1.5 Measurement of Power:

There are several ways to measure the power produced by the turbine: a pressure transducer calibrated and characterized so we know how much power would be produced depending on the pressure in the system, a thermocouple that would measure the heat coming out of the system, a load cell under the pump measuring torque coming from the rotor, or a torque gauge applied directly to the shaft. All of these would also require a means of measuring the shaft speed or the flowrate in the system, either of which could be used to calculate the other based on an approximate volumetric efficiency.

FUNCTION: Measure Load									
Concept / Criteria	Weight	Pressure Transducer		Thermocouple		Load Cell		Torque Gauge	
		% Satisfaction	Weighted	% Satisfaction	Weighted	% Satisfaction	Weighted	% Satisfaction	Weighted
Cost	0.2	80	16	100	20	50	10	25	5
Accuracy	0.5	90	45	50	25	95	47.5	100	50
Reliability	0.1	80	8	50	5	90	9	100	10
Response Time	0.2	95	19	50	10	95	19	95	19
Weighted Total	1	88		60		85.5		84	

4. Final Design Concept:

The design selected to be built was the alternative design discussed earlier. The large price which accompanies a fully functional hydrostatic continuously variable transmission outweighed the benefits for this particular research application. The to-be-built design will feature a hydraulic pump which will be driven by the rotor, a needle valve which adjusts pressure and flow rate within the hydraulic system, two pressure reducers to decrease hydraulic pressure, and a heat exchanger to dissipate the thermal energy. Since this is a high pressure application, redundancies and safety devices will be incorporated to prevent any damage to the device or anyone within the vicinity. These safety features will include pressure transducers to measure critical points in the hydraulic system and pressure relief valves to relieve pressure if the threshold for pressure is overcome.

4.1 Pump:

The pump used for the design was donated to the project by the Cal Poly Rose Float team. The pump is a variable, axial piston motor, Rexroth A6VM250. The A6VM is a hydraulic motor, but by using the proper precautions can be used as a pump. The pump has variable capabilities with a maximum

displacement of 250 cubic centimeters, but for the first iteration of the design we will keep the pump fixed at 250cc and allow Dr. Lemieux to add variability in the future if he chooses.

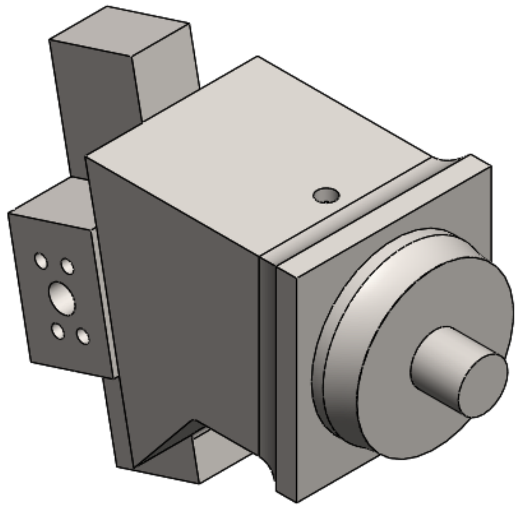

Figure 7. Rexroth A6VM-250 Variable Piston Motor.

The pump's inlet and outlet uses standard Code 62 1.25" flanges; there are also two drain ports on the top and bottom of the pump which use M22-1.5 threads. Although the inlet and outlet uses standard SAE flanges, the bolts to mount the flanges are not standard. The bolts to mount the flanges are M14x2 threads.

The pump is the heaviest component of the design weighing approximately 220 lbs. without hydraulic fluid. To secure the pump in position a steel bracket will be built. The bracket will mount to the designed mounting points on the front of the pump and attach to the nacelle frame using the same points which the generator used for mounting. The design of the pump mounting bracket followed the basic design of most brackets on the market. A basic stress analysis was done to ensure the bracket would not fail under load, which led to a final steel thickness of 0.25" for all parts.

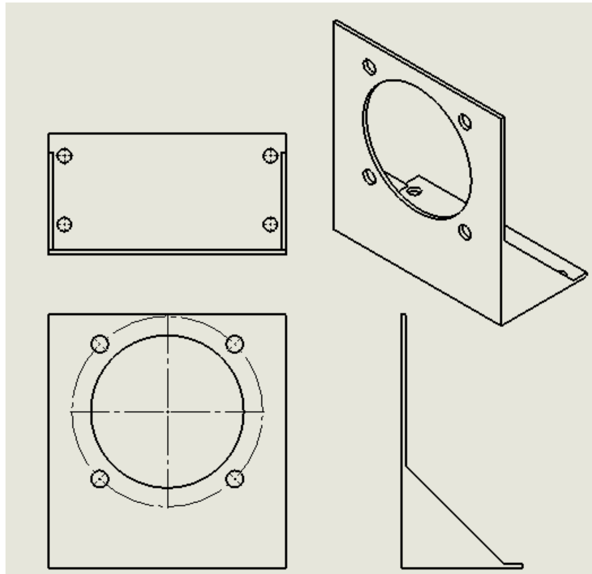

Figure 8. Pump mounting bracket.

4.2 Valves:

Most valves used for the design are manufactured by Sun Hydraulics. Sun Hydraulic's valves are "cartridge" valves which mean that all valves share a common manifold into which they are installed. Using these valves allows Dr. Lemieux to easily change valves without uninstalling any major components if a different valve is needed. The three types of valves which will be used from Sun Hydraulic are a load bearing needle valve, two pressure reducing valves, and two pressure relief valves.

The load bearing needle valve is a Sun Hydraulics model NFCD which will allow a maximum pressure of 5,000psi to be placed on the pump at a maximum flow rate of 20gpm. The manifold that will be used is the model GAD/S which uses ¾" NPTF threads. The manifold is a special option made out of steel to withstand the higher pressures.

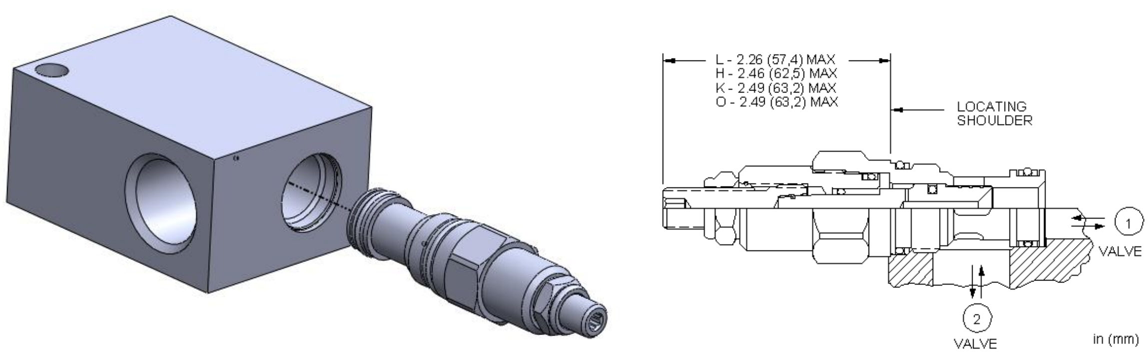

Figure 9. Sun Hydraulic NFCD needle valve and GAD/S manifold.

Two pressure reducing valves will be used to lower the pressure in the hydraulic system after the load bearing needle valve. The pressure has to be reduced from a maximum of 5,000 psi to below 250 psi in order to work properly with the heat exchanger. The first pressure reducing valve is Sun Hydraulic's model PRFR/LAN which has a pressure range of 750 psi to 3,000 psi. The pressure reducing valves

used are designed to output a desired pressure regardless of upstream hydraulic pressure. The first valve will be used to drop the upstream pressure to 1,000 psi downstream prior to the second pressure reducing valve. The second pressure reducing valve is Sun Hydraulic's model PRFR/LSN which has a pressure range of 50 psi to 200 psi. This second pressure reducing valve will decrease the pressure to the needed amount for the heat exchanger. The use of two pressure reducing valves is a purposeful redundancy within the design. The valves are tested by Sun Hydraulic to work properly under 5,000 psi, so the use of only the PRFR/LSN valve should be adequate to reduce pressure. Due to the inaccessibility of the wind turbine, we believed placing two pressure reducing valves would be a worthwhile drop in risk so that if one was to fail the other would still function to drop the pressure significantly. This eliminates most risk of overloading the heat exchanger or causing leaks from excess pressure should a pressure reducing valve fail.

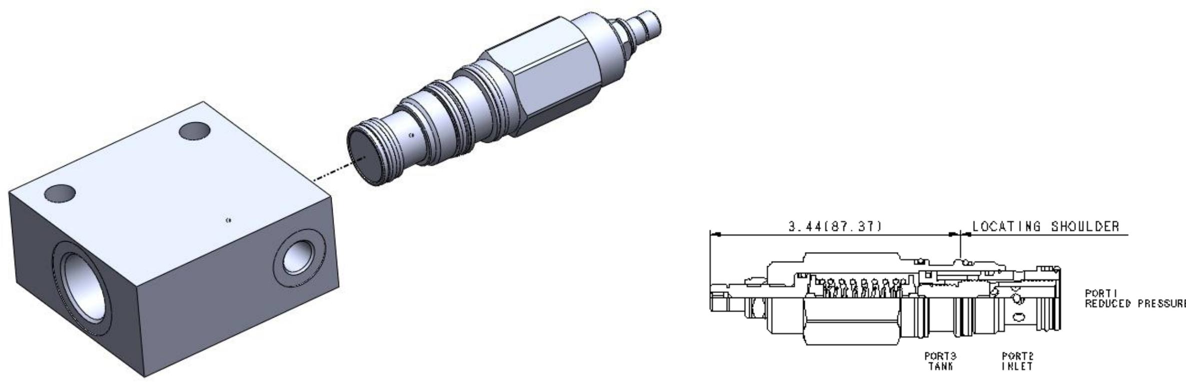

Figure 10. Sun Hydraulic PRFR pressure reducing valve and BCD manifold.

Both pressure reducing valves will be mounted to the model BCD manifold from Sun Hydraulic. Both manifolds will be constructed from steel to be able to withstand high hydraulic pressures. Each pressure reducing valve has a third port which is used to drain any leakage which occurs within the valve mechanism. The drainage port is connected directly to the hydraulic reservoir. The main ports of the manifold use ¾" NPTF threads and the drain port uses a ¼" NPTF thread.

Relief valves are used as a fail-safe to prevent excess pressure in crucial parts of the hydraulic system. For this design there are two crucial parts which will have relief valves installed: after the outlet of the pump and before the heat exchanger. The first relief valve will be placed between the outlet of the pump and the load bearing needle valve. The pressure which will trigger the relief valve will be slightly over our maximum allowable pressure of 5,000 psi. This pressure relief setting will guarantee that our needle valve, hoses, and fittings will not exceed their maximum pressure. The relief valve used for this section will be Sun Hydraulic's model RDDA/LCN which has an adjustment range of 1,000 psi to 6,000 psi. The second relief valve will be placed between the second pressure reducing valve and the heat exchanger. This pressure relief valve will be triggered at 250 psi to ensure that the heat exchanger does not exceed its maximum pressure. The second relief valve will be Sun Hydraulic's model RDDA/LEN which has an adjustment range of 100 psi to 400 psi. Both pressure relief valves will use a model FED manifold but the manifold located directly after the pump will be made from steel due to its high pressure application. The manifolds use ¾" NPTF threads for all three ports.

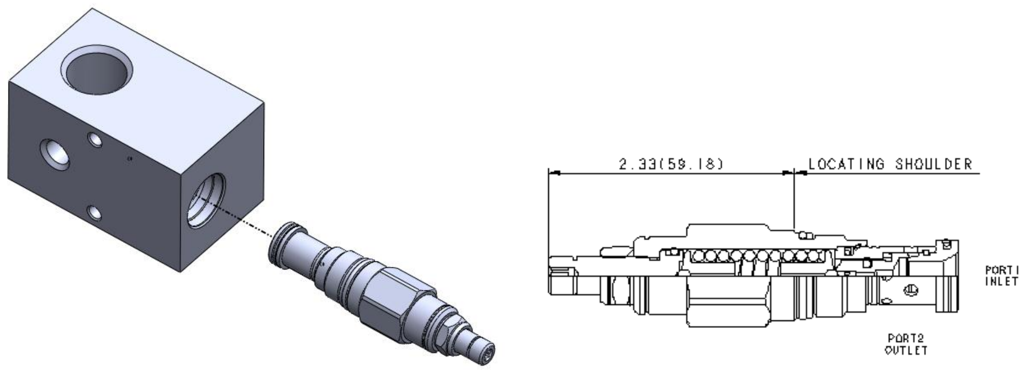

Figure 11. Sun Hydraulic RDDA pressure relief valve and FED manifold.

The FED manifold also includes a ¼" NPTF threaded port to allow a gauge to be installed. We will use these extra ports to install our pressure transducers.

An additional needle valve will also be installed between the heat exchanger outlet and the hydraulic reservoir. This needle valve allows the user to adjust how much flushing hydraulic fluid is rerouted to the pump. As mentioned earlier, the pump has two additional ports for the purpose of draining, but the top one will be used for flushing. Flushing refers to pushing cooled hydraulic oil through the drainage of the pump to facilitate pump cooling. The needle valve will work to redirect a user decided amount of fluid to flushing the pump. The adjustment of this needle valve will be done when the rotor of the wind turbine is changed, and the amount of flushing required is related to pump speed.

4.3 Heat Exchanger:

The heat exchanger was sized to allow the amount of heat transfer needed to cool the hydraulic oil prior to being returned to the hydraulic reservoir or to flushing the pump. The heat exchanger chosen for this application is the AKG model C-18 oil-to-air heat exchanger. Due to restrictions in the placement of the heat exchanger, the heat exchanger will be mounted in the "shadow" of the tower which holds the nacelle. Some fluid modeling was done to ensure that the heat exchanger will receive enough air flow in the wake of the tower. The brackets which hold the heat exchanger will be discussed later in the Rear Bird Plate section, but the brackets for the heat exchanger were designed to place the heat exchanger at a proper distance behind the tower. The C-18 uses #16 SAE thread type for both the inlet and outlet ports. The C-18 also has a bypass built in which will allow the hydraulic fluid to escape around the dissipating elements if the hydraulic fluid exceeds the maximum pressure of the heat exchanger. In the event of a bypass the heat exchanger would be spared from damage but the hydraulic oil will remain hot as it goes to the reservoir and into flushing the pump.

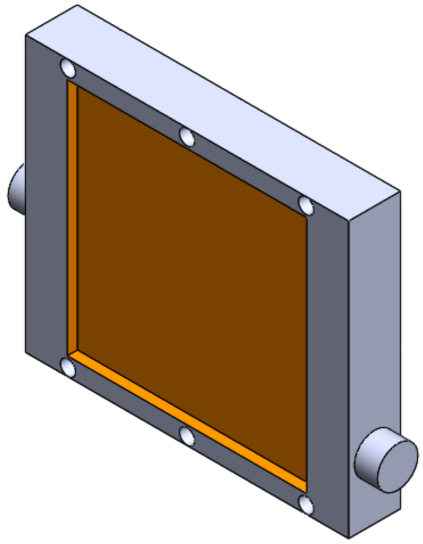

Figure 12. AGK C-18 heat exchanger. Orange represents the cooling elements.

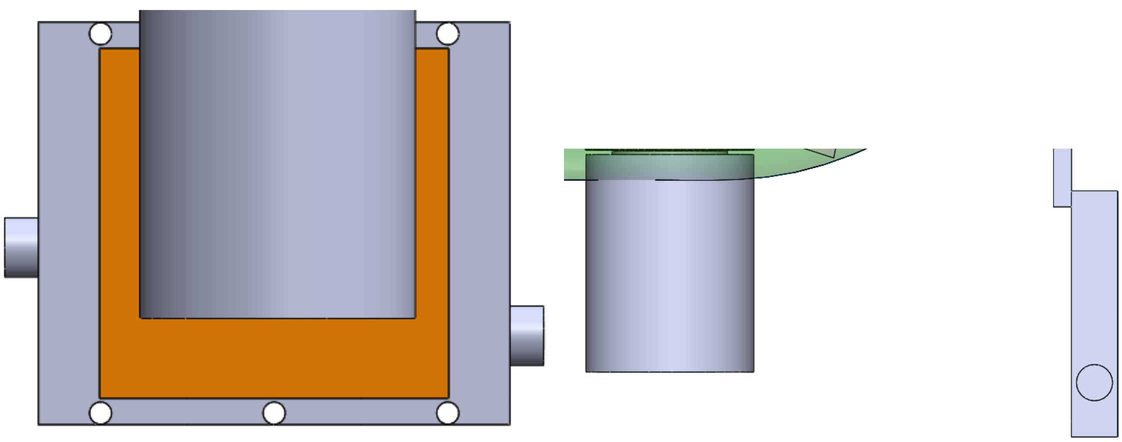

Figure 13. C-18 heat exchanger as seen from the front with tower included and from the side.

4.5 Fittings:

All fittings were chosen on a case by case basis to meet key qualities including reliability, cost effiveness, and ease of use. In hydraulic systems there are eight main fitting types to choose from: National Pipe Tapered Fuel (NPTF), National Pipe Straight Mechanical (NPSM), JIC 37°, flareless compression, Straight Thread O-Ring (ORB/SAE), and O-Ring Face Seal (ORFS). Each type has its own benefits and its own pressure rating. Discount Hydraulic Hose provides a helpful table which show each individual pressure rating as show below in Table 6.

Table 6. Pressure ratings for the main hydraulic thread and flange types.

Dash Size	Nominal Tube/Pipe Size	SAE 100R2	National Pipe Tapered Fuel (NPTF)		National Pipe Straight Mechanical (NPSM)	JIC 37° Flare Hydraulic SAE J514		Flareless Compression SAE J514
			Male	Female	Female Swivel	Male	Female Swivel	
-02	1/8"		10000	5000	6000			
-04	1/4"	5000	9500	4500	5000	8500	5500	6000
-05	5/16"	4250				8500	5000	
-06	3/8"	4000	8000	3500	4000	7000	4000	6000
-08	1/2"	3500	6000	3500	3500	6000	4000	6000
-10	5/8"	2750				5500	3000	5000
-12	3/4"	2250	5000	3000	3500	4000	3000	4500
-14	7/8"	2000				4000	3000	
-16	1"	2000	4000	2500	3000	3500	2500	4000

Dash Size	Nominal Tube/Port Size	SAE 100R2	Straight Thread O-Ring (ORB) SAE J1926-1			O-Ring Face Seal (ORFS) SAE J1453		Code 61 Flange SAE J518	Code 62 Flange SAE J518
			Male	Male Adj.	Female	Male	Female Swivel		
-04	1/4"	5000	7500	4500	4500	9000	9000		
-05	5/16"	4250	7500	3500	3500				
-06	3/8"	4000	7500	4000	3500	9000	9000		
-08	1/2"	3500	7500	4000	3000	9000	8000	5000	6000
-10	5/8"	2750	7500	4000	2500	9000	8000		
-12	3/4"	2250	5000	3500	1800	6000	6000	5000	6000
-14	7/8"	2000	5000	3000	1700				
-16	1"	2000	4500	2500	1600	6000	6000	5000	6000
-20	1-1/4"	1625	4500	2000	1500	4500	4500	4000	6000

4.6 Hydraulic Hoses:

The hydraulic hoses used for this project were based on availability, pressure rating, and adaptability to fittings. As discussed earlier, some fittings which are harder to find dictate the hose size used such as a ¾" swivel fitting needing a ¾" hose. The first restriction on hose size is found from the 1.25" flange fitting attached to the pump. Most hoses can be used with fittings one size larger or smaller than its size, so a 1.25" flange can use a minimum hose size of 1". Due to these restrictions the majority of hoses used are ¾" inner diameter with some being 1" inner diameter. Pump and valve drainage ports, as well as other low flow sections of the system, will use ⅜" inner diameter hose.

Hydraulic hoses and fittings must be crimped together using special tools to ensure full strength. Because we require a third party to assemble the hose assemblies, we must rely on a company's hose and fitting selection for our choices in hoses. The 1", ¾", and ⅜" hoses were found at Discount Hydraulic Hose (who also offer assembly and a wide variety of fittings). For the 1" hose we decided to use the Hydraulax EN 856 4SH which offers a working pressure of 5,515 psi and allows W-series "bite" fittings which is more reliable. The ¾" hose is the same model as the 1" but in a smaller size; it offers a working pressure of 6,095 psi. The ⅜" hose is the Hydraulax SAE 100R1AT which is a cheaper, low pressure hose and only offers a 2,250 psi working pressure. Each hose we use also has a minimum bend radius which was kept in mind during the design of the complete system assembly. The dimensions, pressure ratings, and minimum radius were provided by Discount Hydraulic Hose as shown below in Table 7.

Table 7. Hydraulic hose specifications. The top table represents the 3/4" and 1" hoses selected and the bottom represents the 3/8" hose.

Hose Number	Inside Diameter	Outside Diameter	Maximum Working Pressure (MWP)	Minimum Burst Pressure	Minimum Bend Radius
4SH-12	**3/4"**	**1.21"**	**6,095**	**24,380**	**9.5"**
4SH-16	1"	1.50"	5,515	22,060	12"
4SH-20	1-1/4"	1.85"	5,000	20,000	16.5"
4SH-24	1-1/2"	2.11"	4,200	16,800	20"
4SH-32	2"	2.63"	3,625	14,500	25"

Hose Number	Inside Diameter	Outside Diameter	Maximum Working Pressure (MWP)	Minimum Burst Pressure	Minimum Bend Radius
R1-04	1/4"	0.53"	2,750 psi	11,000 psi	4"
R1-06	**3/8"**	**0.69"**	**2,250 psi**	**9,000 psi**	**5"**
R1-08	1/2"	0.82"	2,000 psi	8,000 psi	7"
R1-10	5/8"	0.94"	1,500 psi	6,000 psi	8"
R1-12	3/4"	1.10"	1,250 psi	5,000 psi	9.5"
R1-16	1"	1.41"	1,000 psi	4,000 psi	12"

4.7 Rear Bird Plate:

A major requirement for this project, as discussed early on in this report, is to not alter the nacelle's fiberglass body in any way. This means that all exterior mounting requirements and exterior hoses must be routed through the rear of the nacelle. The plate which covers the rear opening of the nacelle is called the rear bird plate. The only major component located outside of the nacelle body is the heat exchanger and the hoses that are connected to it. The rear bird plate must be able to fully support the heat exchanger and its hoses, so brackets were designed to rigidly mount the rear bird plate to the frame of the nacelle. These mounts and the bird plate can be seen below in Figure 14.

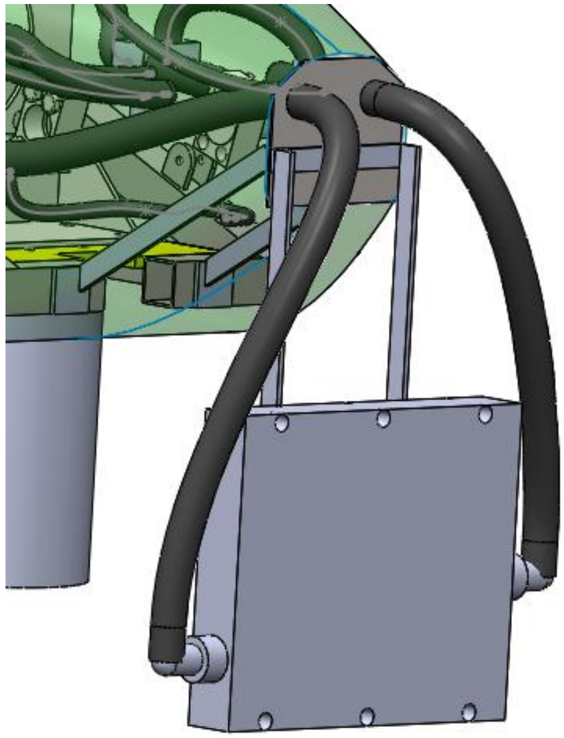

Figure 14. Rear view of the bird plate mount to the frame and the mounting for the heat exchanger and its hoses.

The rear bird plate, heat exchanger mounts, and rear bird plate mounts will be made from 6061 aluminum for weight and corrosive benefits. The rear bird plate also must allow air flow through the nacelle body so it will have sections removed, which are not pictured above.

4.8 Hydraulic Reservoir:

The hydraulic reservoir must store all hydraulic fluid pumped through the system, drained from the pump, or drained from the valves in order to be pumped once again into the system. For this purpose, the reservoir must be able to hold the volume of fluid needed by the system while being able to change position during periods where the tower is lowered. For the volume of fluid that the reservoir is required to hold, we were unable to find a reservoir on the market which will fit within the tight confines of the nacelle. In order to have a reservoir which can store the amount of fluid required we will need to manufacture our own which will follow the shape of the nacelle and take advantage all available space available. The reservoir design is shown below in Figure 15.

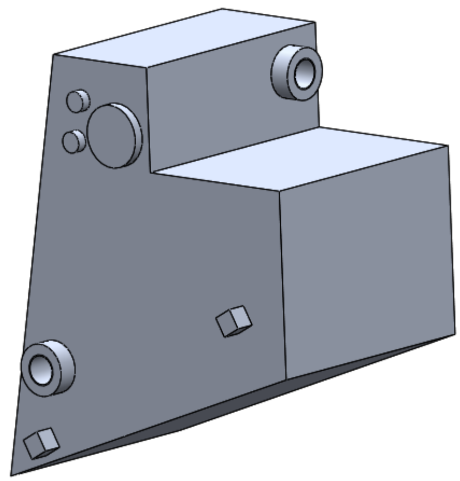

Figure 15. Hydraulic reservoir design.

The body of the reservoir will be constructed from 0.1" aluminum sheet metal for weight and corrosive advantages. The tank will have weld in bungs of varying thread sizes in order to accommodate the different hose fittings that lead to the reservoir. On the sides of the reservoir are blind, threaded weld on bungs which will serve as the mounting point of the reservoir to the rear bird plate mounts.

Reservoirs are either made to be pressurized or vented to atmosphere. Having a pressurized reservoir could be beneficial to us since it could serve as a precaution to guard against pump cavitation, but designing and building a pressurized reservoir is much more difficult and expensive than building a vented reservoir. Because of the low speeds that the pump will be operating at we chose to design the reservoir as vented to atmosphere. The low pump speeds makes cavitation a very low risk.

5. System Analysis

5.1 Model Predictions

5.1.1 Cut In Speed

The cut in speed of a rotor is the speed of the wind needed to turn the rotor and its attached transmission. To calculate the cut in speed of each rotor, the torque produced by the rotor was plotted against the minimum load torque provided by the system for a range of wind speeds. The torque produced by the rotor comes from actuator disk theory, while the load torque is a combination of several factors discussed in the Model Development section. The largest contribution to the minimum load torque at low speed was the constant torque; however, the torque required to overcome the pressure drop in the system also contributed sizably to the minimum load. To calculate the torque required to overcome the systems minimum pressure drop, a flow rate was needed. To determine the flow rate a constant tip speed ratio assumption was used to calculate the shaft speed and flow rate for the corresponding wind speeds. Figure 16 (below) shows the minimum load torque and the corresponding rotor torque for the large rotor planned to be installed. The intersection point of these two curves shows the predicted cut in wind speed of the system, which is less than 1m/s (2.25mph) even at the highest viscosity expected in the system.

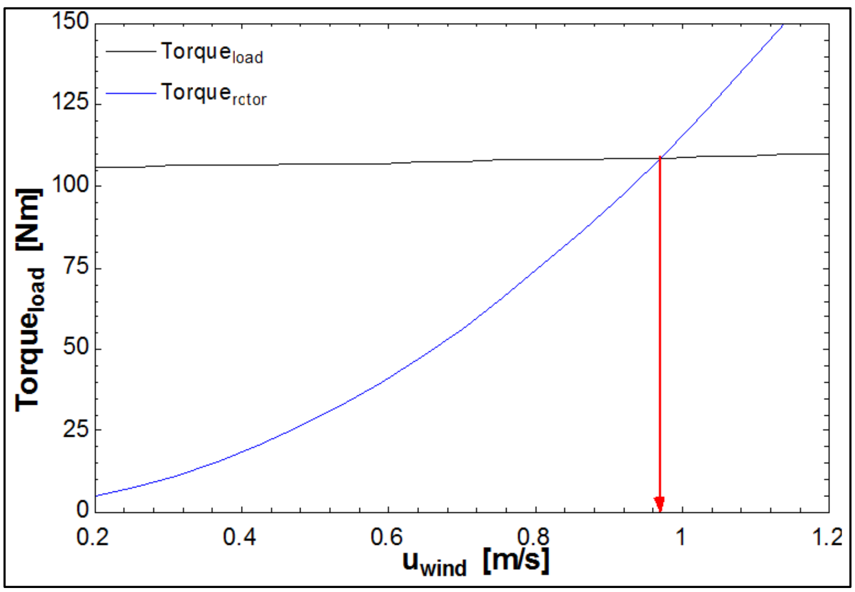

Figure 16. Large Rotor Cut In Speed

Similarly to Figure 16, Figure 17 shows the cut in wind speed for the small rotor. As can be seen, the cut in wind speed is considerably higher for the small rotor. Even when the viscosity is set to the expected operating conditions, as in Figure 17, the cut in speed is still approximately 11m/s (24.6mph). Since there were many assumptions made in the model the results shown in Figure 17 many differ substantially from the actual performance of the system. That being said, the model still provides some insight into the effects of slight variations on the systems configuration. Figure 18 shows the cut in speed for the small rotor under the same conditions in Figure 17, except several non-critical components were bypassed. The reduction in cut in speed from this small variation was just over 1.5 m/s (3.4mph). This shows that slight changes and adjustments to the system during the

construction and testing phase of the project might be able to greatly reduce the cut in speed for the small rotor.

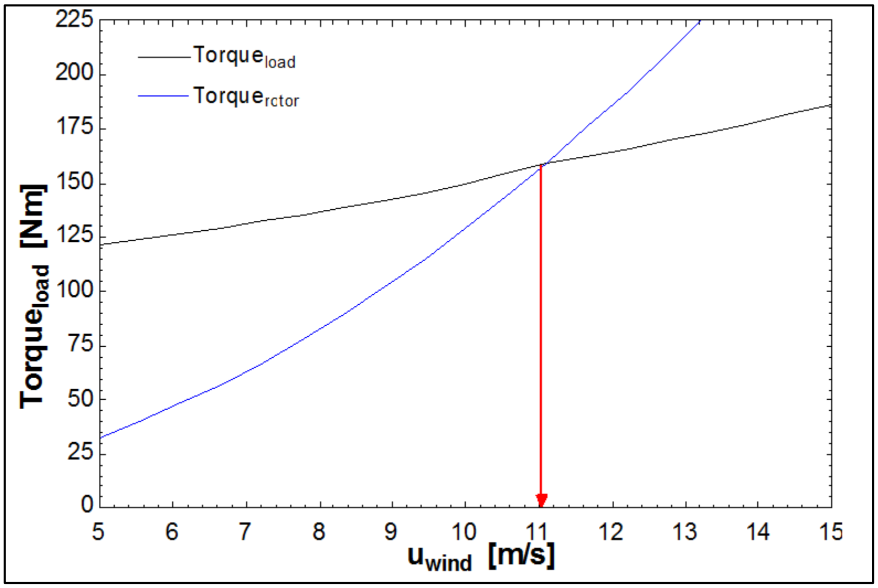

Figure 17. Small Rotor Cut In Speed

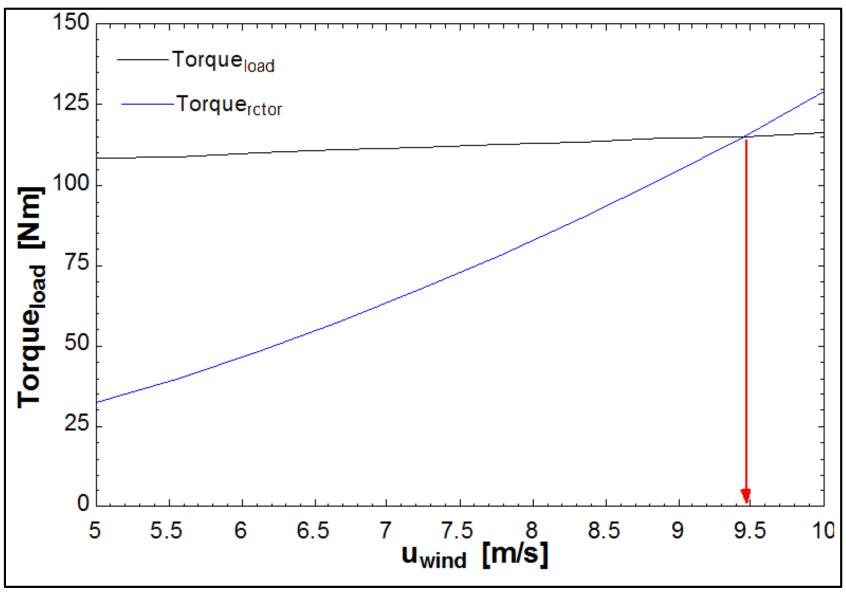

Figure 18. Small Rotor Cut In Speed with Bypass

5.1.2 Cut Out Speed

The process for estimating a cut out speed is exactly the same as above; however, now the maximum load torque is used. The maximum load torque is comprised of several factors, but by far the largest contribution to the maximum load torque is the pressure drop across the system which is set to not exceed the maximum pressure of the system, 34,500kPa (5000psi). Figure 19 shows the estimated cut out speed of the larger rotor, which is approximately 3.7m/s (8.3mph). Currently, the limiting factor in this cut out speed is the pressure rating of the throttle valve. Since pressure limit of all the

components upstream of the throttle valve exceed 41,400kPa (6000psi), replacing the throttle valve with a higher rated valve would considerable increase the cut out speed; however, throttle valves rated over 34,500kPa (5000psi) exceed the current budget.

In Figure 20, it can be seen that the small rotor cut out speed is in excess of 34m/s (76mph). Therefore the small rotor can safely operate even in the most extreme local wind conditions.

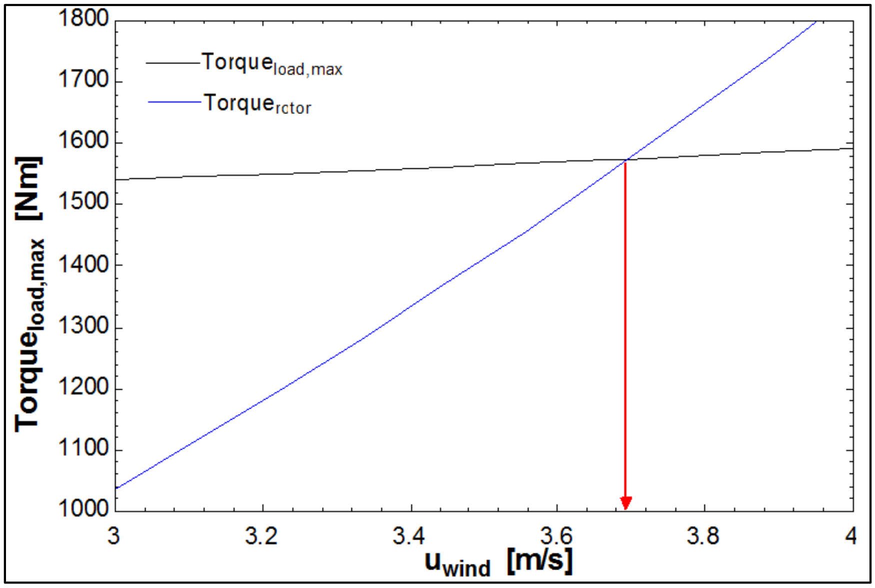

Figure 19. Large Rotor Cut Out Speed

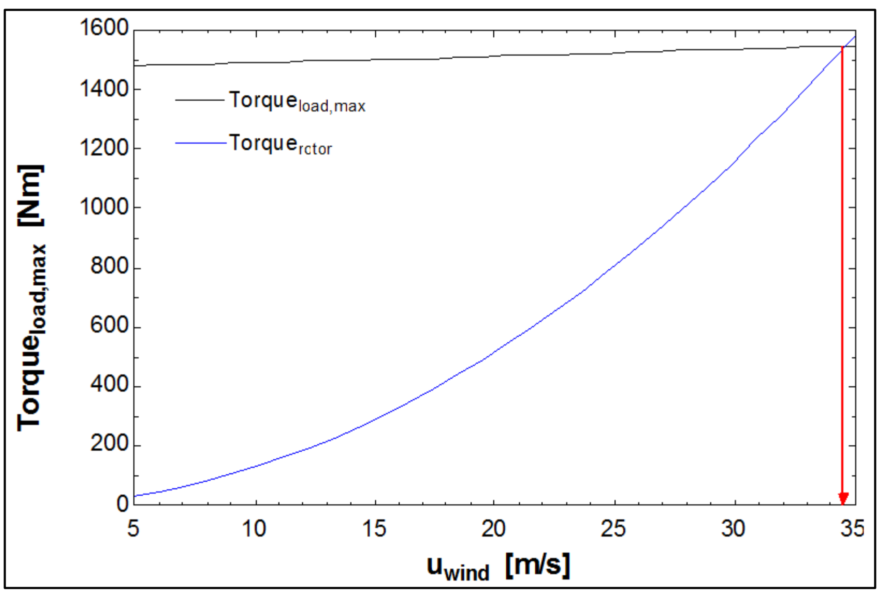

Figure 20. Small Rotor Cut Out Speed

5.1.3 Steady State Temperature

The steady state temperature was determined by plotting the temperature of the hydraulic oil leaving the reservoir and returning to the reservoir after flowing through the system operating at maximum power. The point on the plot corresponding to the steady state temperature is when the outlet

temperature equals the inlet temperature. Figure 21 shows the highest estimated steady state temperature for the large rotor, approximately 57°C (135 °F).

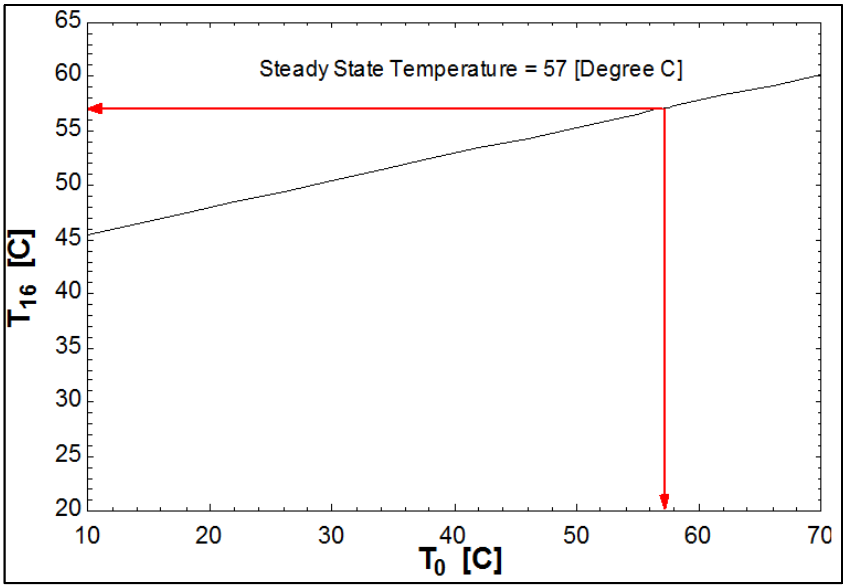

Figure 21. Steady State Temperature

5.1.4 Maximum Pressure

Figure 22 is a plot of the maximum pressure in the system versus the rotor speed for the large rotor. As can be seen in the plot the pressure increases exponentially with rotor speed.

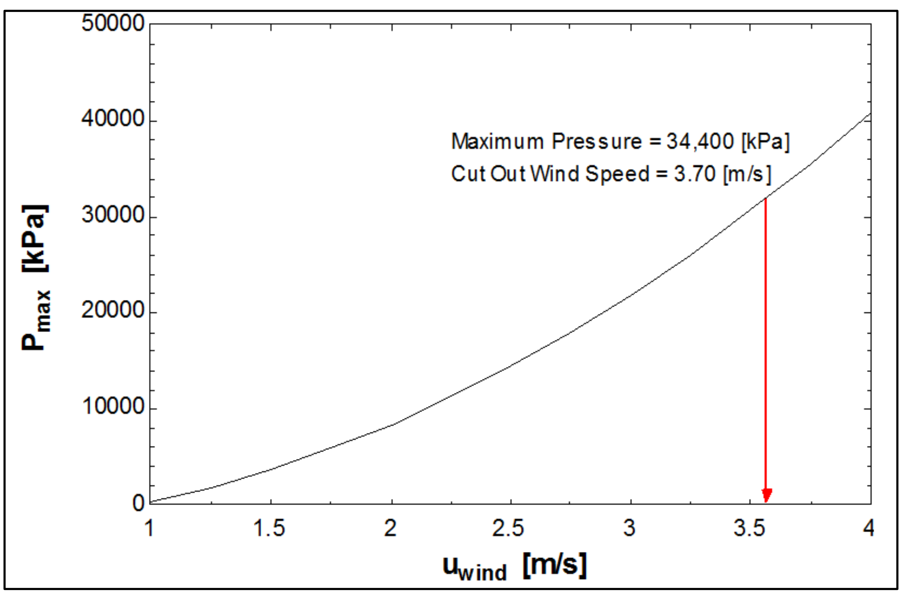

Figure 22. Maximum System Pressure

5.1.5 Maximum Temperature

Figure 23 is a plot of the maximum temperature in the system versus the rotor speed for the large rotor. Similarly to the pressure the temperature also increases exponentially with rotor speed.

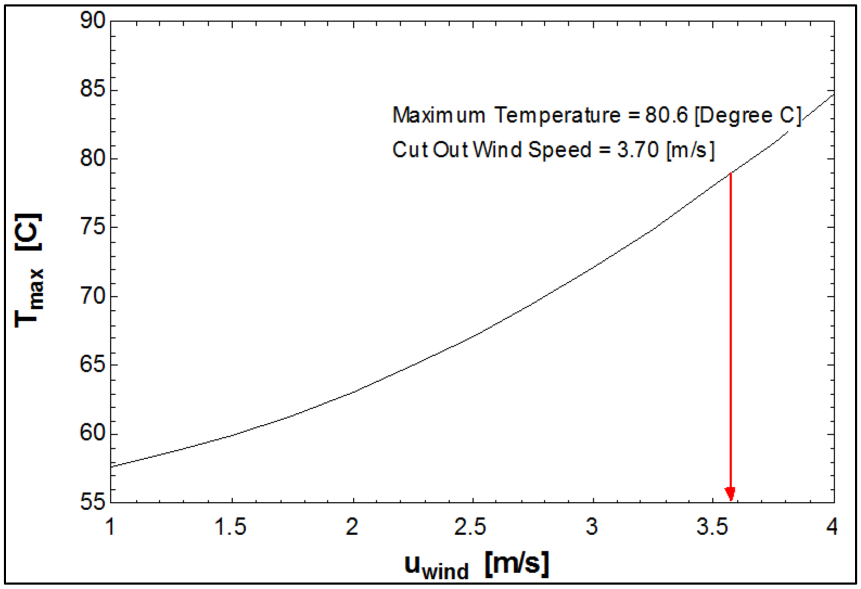

Figure 23. Maximum System Temperature

5.2 Development of the Model

5.2.1 Actuator Disk Theory

The first step in the development of a system model was to estimate the range of input power and rotor speed that the pump would be subjected to. Since the purpose of this system is to absorb the power produced by the Cal Poly wind turbine, modeling the performance of the wind turbine provided useful insight into the required operating range of the system. To determine the performance of the wind turbine a relatively simple analysis was conducted using Actuator Disk Theory.

Based on a range of wind speeds and rotor parameters given by our sponsor, Dr. Lemieux, a range of shaft power was determined for both rotors using Equation 1.

$$\dot{W}_{shaft} = \frac{1}{2} C_{power} \rho \pi R^2 u_{wind}^3 \tag{1}$$

Where,

$C_{power} \triangleq The\ power\ coefficent, given\ as\ 0.45$

$\rho \triangleq The\ density\ of\ air, calculated\ at\ 65°F$

$R \triangleq The\ radius\ of\ the\ rotor, given\ as\ 10m\ and\ 2m\ for\ the\ two\ differnet\ rotors$

$u_{wind} \triangleq The\ wind\ speed$

Assuming a constant tip speed ratio (λ) provided by Dr. Lemieux a range of corresponding rotor speeds was determined using Equation 2.

$$\lambda = \frac{R\omega_{rotor}}{u_{wind}} \tag{2}$$

Where,

$\lambda \triangleq The\ tip\ speed\ ratio, given\ as\ 7$

After the shaft power was determined for a full range or shaft speeds, the next step was to conduct an analysis of the hydraulic pump.

5.2.2 Steady-State Pump Analysis

The four most important interrelated parameters of a positive displacement pump are applied torque, shaft speed, flowrate, and pressure differential. The purpose of our system can be simply stated as a hydraulic dynamometer that provides a variable shaft torque at a range of shaft speeds. Therefore, by buildings a hydraulic system to couple with the positive displacement pump the aforementioned variable shaft torque can be adjusted by changing the system pressure requirements, which in turn change the pumps pressure differential and flowrate accordingly.

In order to characterize the performance of the positive-displacement bent-axis piston pump several assumptions had to be made about the pump which will be discussed in detail later in the analysis section of this report. For now, the most important aspects of the operation of a positive displacement pump are input torque, shaft speed, flow rate, and pressure differential. These parameters were related using the steady-state analysis laid out by Gerhard Reethof in chapter 4 of Fluid Power Control, Characteristics of Positive Displacement Pumps and Motors (Reethof, Characteristics of Postive Displacment Pumps and Motors, 1960). As Reethof states,

The torque required to drive a positive-displacement pump at a constant speed can be divided into four factors:

$$\tau_a = \tau_t + \tau_r + \tau_f + \tau_c \tag{4.1}$$

Where,
τ_a = actual torque required
τ_t = ideal torque due to the pressure differential, (P_1-P_2), and the physical dimensions of the unit only (without friction)
τ_r = = friction torque due to viscous shearing of the fluid in the narrow passages between moving and stationary parts of the pump
τ_f = friction torque due to mechanical friction which is directly proportional to the pressure differential. This may originate in seals if the sealing forces are proportional to P, or in bearings where the resistance is proportional to P.
τ_c = constant friction torque that is independent of both pressure differential and speed

The delivery of the pump can be expressed in a similar manner as:

$$Q_a = Q_t - Q_l - Q_r \tag{4.2}$$

Where,
Q_a = actual delivery
Q_t = ideal delivery (volume rate of flow) of the pump, which is a function of its physical dimensions and its shaft speed (assuming zero leakage and cavitation)
Q_l = viscous-leakage flow, proportional to the pressure differential between the inlet and the outlet
Q_r = loss in delivery due to cavitation or entrained gases or vapor

For the purposes of modeling the applied load on the rotor, the actual torque term was calculated based on each of the four torque terms. The ideal torque (τ_t) was found using Equation 4.8, the viscous

shearing friction torque (τ_r) was found from Equation 4.29, the mechanical friction torque (τ_f) was found from Equation 4.31, and the constant friction torque (τ_c) was approximated using Figure 24 taken from *Fundamentals of Fluid Power Control* by J Watton (Watton, 2009).

$$\tau_t = D_p(P_1 - P_2) \tag{4.8}$$

Where,
$D_p = the\ pump\ displacement\ per\ radian, 39.8\ cc/rad$

$$\tau_r = C_D D_p \omega_{rotor} \mu \tag{4.29}$$

$$\tau_f = C_f(P_1 - P_2)D_p \tag{4.31}$$

Figure 24 shows the constant friction torque of a smaller, but geometrically similar piston pump. Since the pump used to create this curve is smaller, the friction torque used in the model was scaled up to give a more reasonable approximation.

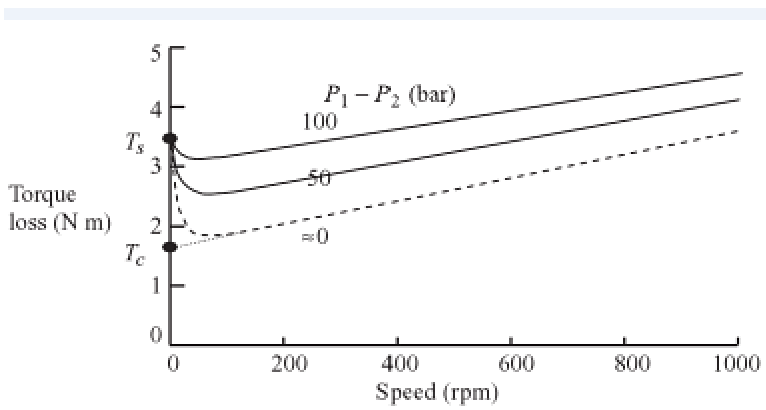

Figure 24 Constant Friction Torque of a Piston Pump

For both Equations 4.29 and 4.31 coefficients are needed to characterize the pump's performance; however, budgetary and time constraints limited the ability to test for these coefficients. Therefore, both the drag coefficient (C_D) and the friction-torque coefficient (C_f) were approximated based on ranges provided in chapter 4 of Fluid Power Control (Reethof, Characteristics of Postive Displacment Pumps and Motors, 1960), C_D=0.07 and C_f=10^5.

In the above torque equations, all of the parameters were known except for the pressure differential and the speed. Assuming a constant speed, the pressure differential was then determined based on the pressure in the reservoir and system pressure drop which is dependent on the flowrate.

Since the pressure differential across the pump must equal the pressure drop across the system at the same flow rate, the next logical step was to quantify the flow rate produced by the pump at the shaft speed being considered. To determine the actual flow rate in the system, all three flowrate terms in Equation 4.2 were determined. The ideal flow (Q_t) was calculated using Equation 4.10, the leakage

flow (Q_l) was calculated using Equation 4.4, and the cavitation flow was assumed to be zero since the only pressure drop from the reservoir to the pump inlet is a short section of tubing and the likelihood of cavitation is minimal.

$$Q_t = D_p \omega_{rotor} \tag{4.10}$$

$$\acute{\eta}_{vp} = 1 - \frac{Q_l}{Q_t} \tag{4.4}$$

While the leakage flow could also be determined using a slip coefficient or quantities relating to the piston and cylinder interface, none of the necessary values were known. Therefore, a volumetric efficiency ($\acute{\eta}_{vp}$) of 60% was used. The volumetric efficiency was based on known efficiencies for similar pumps operating near the range of shaft speeds.

5.2.3 Modified Bernoulli

To calculate the overall pressure drop, the system was broken into several sub-sections seen in Figure 25.

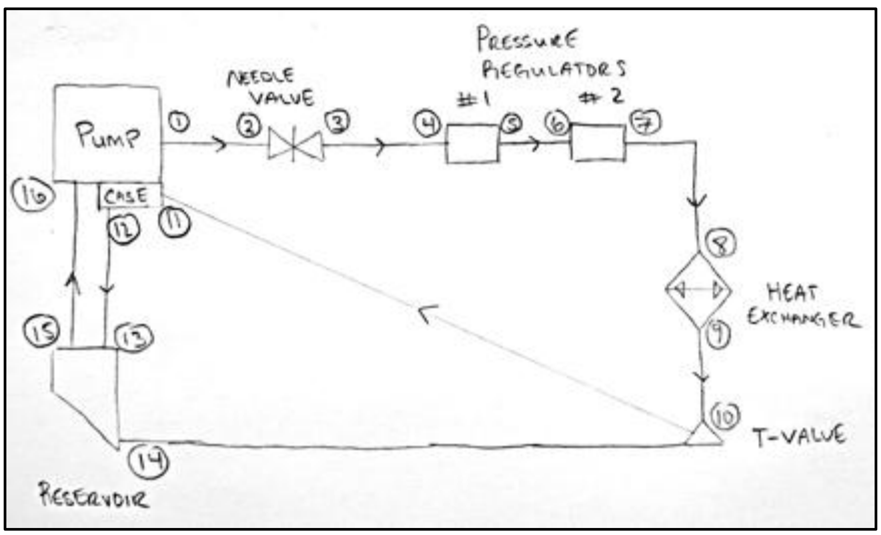

Figure 25. System Schematic

The pressure drop for each subsection was determined using empirical data, when available. When no empirical data was available for a subsection, the pressure drop was determined using the Modified Bernoulli Equation:

$$\frac{P_1}{\rho} + \frac{1}{2}\alpha V_1^2 + gZ_1 = \frac{P_2}{\rho} + \frac{1}{2}\alpha V_2^2 + gZ_2 + h_{Loss} \tag{3}$$

Rearranging the above equation and expanding the head loss term yields:

$$\Delta P = \rho\left[g(Z_2 - Z_1) + \frac{\alpha}{2}(\bar{V}_2^2 - \bar{V}_1^2) + \frac{\bar{V}^2}{2}\left[f\left(\frac{L + L_e}{D}\right) + K_{loss}\right]\right] \tag{4}$$

All of the loss coefficients (K_{loss}) for the system were calculated using built in EES values and the approximate system dimensions taken from the CAD drawing. Two components in the system, the case drain and the filter, were quantified using the effective length (L_e) method. For both of these values the effective lengths were estimated from empirical pressure drops for similar components. Furthermore, the flowrates through both of these components are controlled by the needle valve before the reservoir so if either of the assumed effective lengths prove to be poor assumptions, there will be minimal impact on the models effectiveness since the needle valve can be adjusted to compensate for any differences.

The friction factor (f) for each subsystem was calculated using the Churchill correlation feature built into EES which accounts for both laminar flow, turbulent flow, and also provides an estimate for the transition region.

According to an article on Nuetrium.net (Neutrium, 2012), "the Churchill correlation shows very good agreement with the Darcy equation for laminar flow, accuracy through the transitional flow regime is unknown, in the turbulent regime a difference of around 0.5-2% is observed between the Churchill equation and the Colebrook equation."

To calculate the friction factor from the Churchill correlation, two inputs are required; the relative roughness (ε/D) and the Reynolds number (Re_D). While there are some steel components in the system with a $\varepsilon \approx 0.00015$ [ft] according to Streeter (Streeter, 1966) the relative roughness of the system was set to 0, since the majority of the system can be considered smooth pipe. Additionally most of the steel components pressure drops are accounted for by either empirical data or loss coefficients.

The Reynolds number for the system was calculated using:

$$Re_D = \frac{\rho V D}{\mu} \tag{5}$$

In an early model of the system the viscosity was calculated for each section using the mean temperature across that section; however, this proved to be an unwieldy and cumbersome portion of the model. After simplifying the model to use a constant viscosity based on the mean temperature of the system it was found that the component with the largest pressure drop, and therefore largest temperature difference, showed only a 3% pressure drop difference at the extreme operating condition, highest pressure drop at low flowrate. Furthermore, all three components which experience the largest pressure drops, the two pressure regulators and the needle valve, all can be adjusted to account for viscosity changes so modeling the viscosity change for each section is not necessary to adequately represent the system.

5.2.4 Flow Factor

While the majority of components pressure drops were determined using Equation 4 or empirical data, the flow rate and pressure drop relation for two needle valves in the system was determined using the flow factor equation:

$$Q = K\sqrt{\Delta P} \tag{6}$$

Where,

$Q \triangleq The flow\ rate\ through\ the\ valve\ in \left[\frac{m^3}{s}\right]$

$K \triangleq The\ flow\ factor\ in \left[\frac{m^{(7/2)}}{kg^{(1/2)}}\right]$

$\Delta P \triangleq The\ pressure\ drop\ across\ the\ valve\ in\ [Pa]$

The flow rate factor is an empirically derived relation, and the relation for the specific component we are using in the system was not provided by the manufacture. While researching typical flow rate factors for comparable components, a sample lab report from the University of Minnesota (Lab 3: Pressure Flow Relation Across a Needle Valve) on determining the flow rate and pressure drop relationship was found. The flow rates in their system were on the same order of magnitude as the expected flow rates in this system, and there was a full range of flow factors for varying needle positions. Since all of the flow rate factors provided fell within a range of typical needle valve flow factors, the relationship outlined in the lab report was used to model both flow factors.

5.2.5 Empirical Data

For several components in the system, the manufactures provided data for the pressure drop over a range of flow rates. For each component information about the testing conditions was gathered, this information was then used to correct the empirical data to the expected conditions of the system.

Pressure Regulators

For both of the Sun Hydraulic pressure regulators in the system, the regulated outlet pressure was treated as an input variable to the model. Although the actual outlet pressure for one particular setting varies with flow rate as seen in Figure 26 the system will undergo extensive calibration before it is installed, and it will be possible to correct the pressure regulator controls to maintain a relatively constant outlet pressure regardless of any flow rate of viscosity changes.

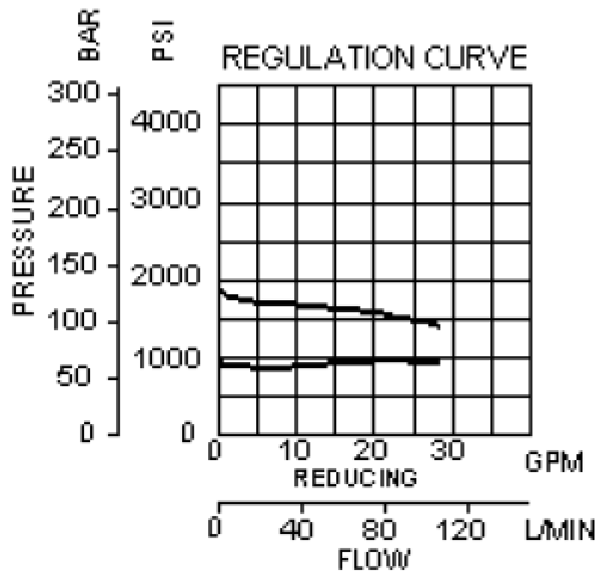

Figure 26. Pressure Regulator Outlet Pressure Variation

While the regulated outlet pressure can be controlled when the inlet pressure is high, for input pressures less than set regulation pressure (i.e. a fully open valve) the pressure drop across the valve is determined from Figure 27.

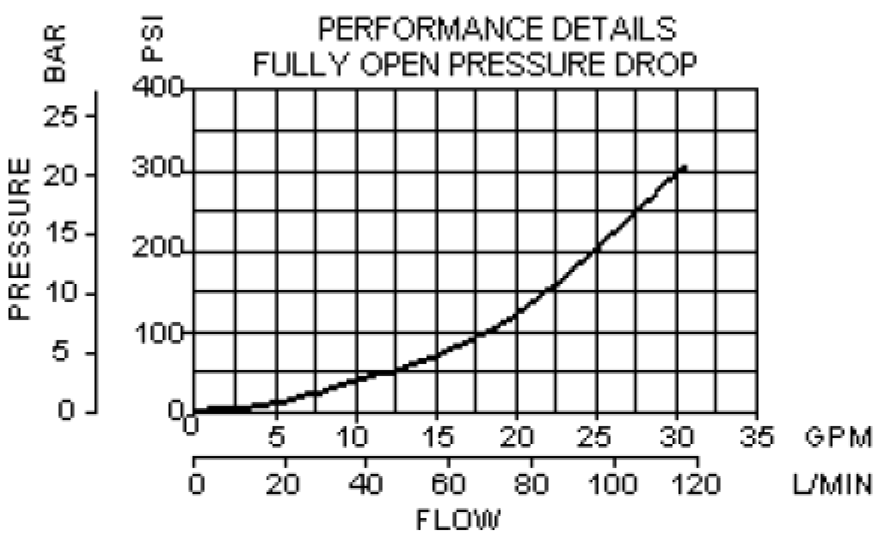

Figure 27. Fully Open Pressure Drop

Within the EES model a user defined function is used to determine the pressure drop across each pressure regulator. If the inlet pressure is greater than the set regulation pressure than the outlet pressure is set to the regulation pressure and the pressure drop across the valve is determine by the difference between the inlet and regulation pressure. If the inlet pressure is less than the set regulation pressure than the pressure drop across the valve is found with a lookup table containing the data taken

from Figure 27 using the plot digitizer tool. In early versions of the model the pressure drop data was corrected for the density and viscosity of the hydraulic oil being used if it differed from the test conditions; however, the current oil being used in the system is the same as oil used in the test with a similar expected temperature range.

Heat Exchanger

The AKG C-18 oil cooler's pressure drop versus flow rate data was provided in Figure 28 along with its performance data. As can be seen in Figure 28, only four data points were taken during this test, which caused some difficulties in extrapolating the pressure drop in an EES lookup table at low flow rates. Additionally, the test was performed with 50 SUS viscosity oil while the system will be using oil that is approximately 150 SUS. To correct for the viscosity differences Figure 29 was used to find a pressure drop correction factor. In response to the insuffcent amout of test data, the corrected pressure drop data was plotted in Excel and then a power series trend line was fitted to the data. This trend line, seen in Figure 30, was then inputed into the EES model and used to calculate the pressure drop across the heat exchanger.

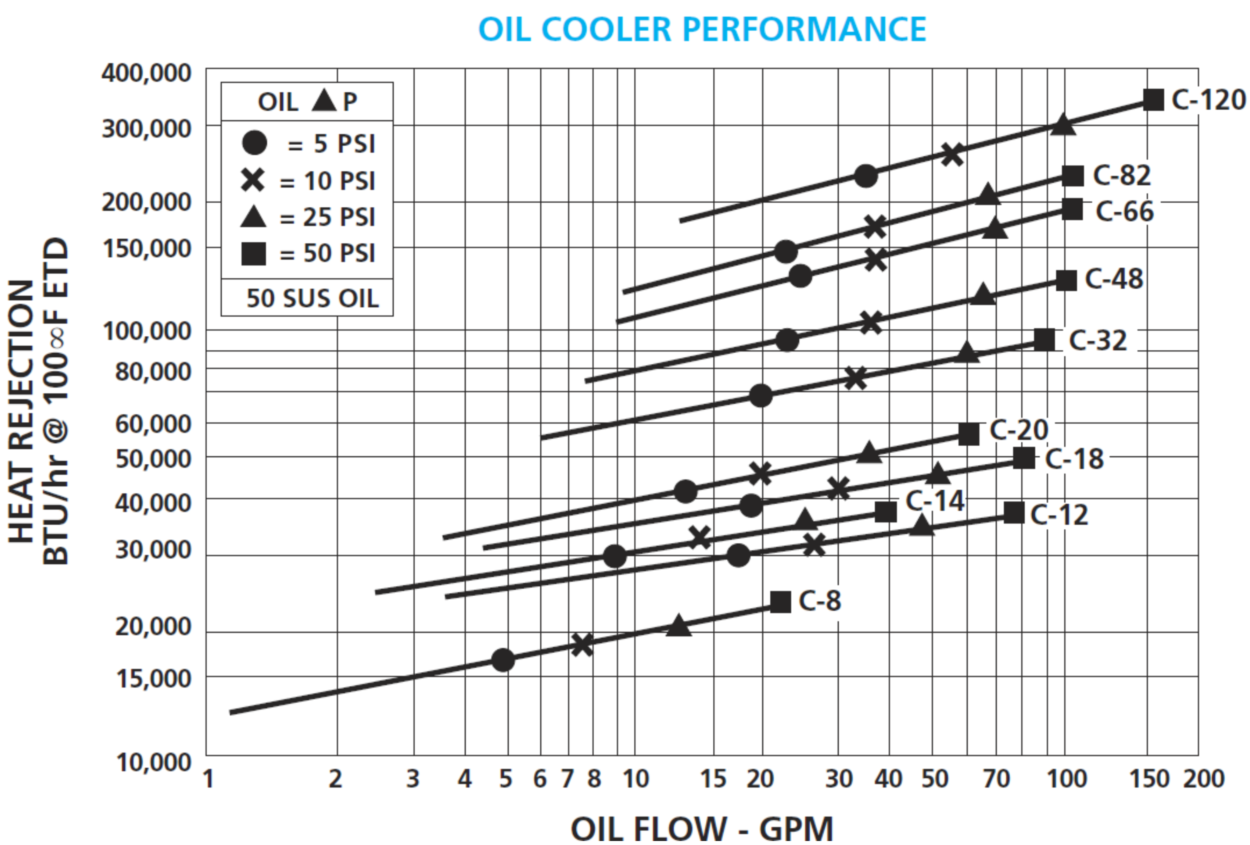

Figure 28. Oil Cooler Performance

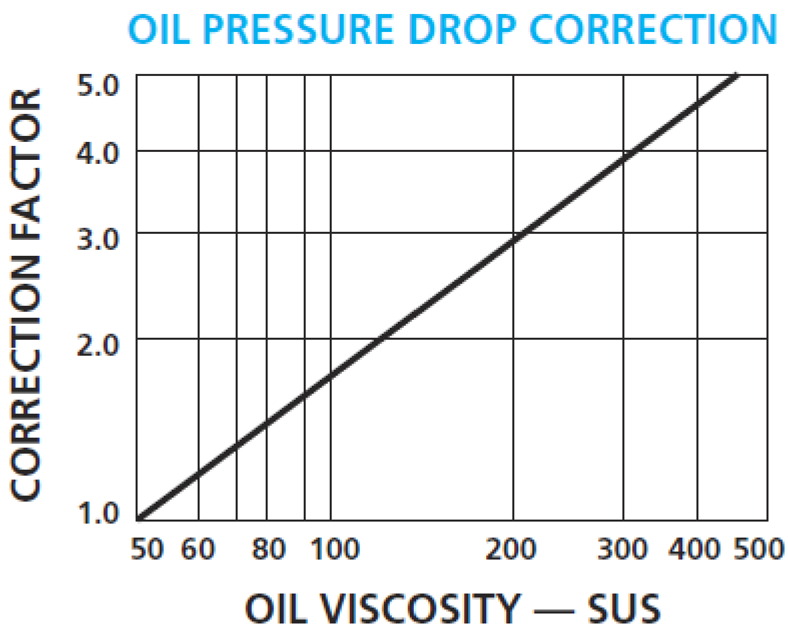

Figure 29. Oil Pressure Drop Correction

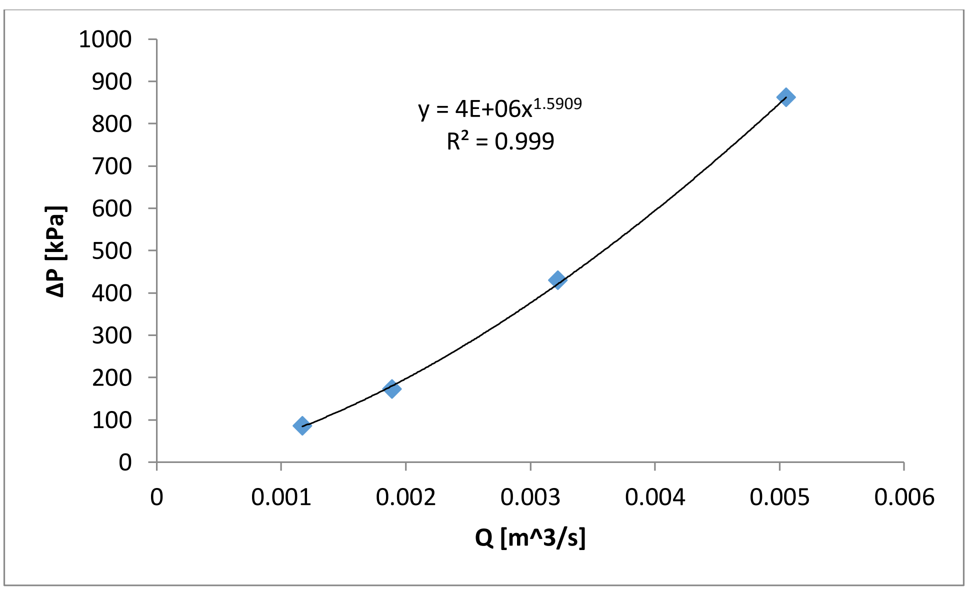

Figure 30. Corrected Pressure Drop Across Heat Exchanger

5..2.6 First Law of Thermodynamics

The first law of thermodynamics for incompressible fluids, Equation 7, was used to calculate the temperature rise throughout the system.

$$q - w = \dot{m} c_p \Delta T \tag{7}$$

With the exception of the heat exchanger, the entire system was assumed to be adiabatic. While heat transfer will take place throughout the system, the adiabatic assumption provides a conservative estimate of the steady-state temperature of the system. Furthermore, all of the energy expended in each component do to the pressure drop was assumed to be transferred into the fluid in the form of heat generation. Thus Equation 7 can be rewritten as Equation 8 below.

$$-Q\Delta P = \dot{m} c_p \Delta T \tag{8}$$

5.2.7 NTU Method

Using the heat exchanger performance data found in Figure 28 the product of the overall heat transfer coefficient and the heat transfer area (UA) was calculated to be 230 W/K. This UA value was calculated at an oil flow rate of 7 GPM which lies in the middle of the expected oil flow range of the system, using the log mean temperature difference method. Fouling of the heat exchanger was also factored into the UA based on a fouling factor of 0.00018 m^2K/W found on engineeringpage.com (Engineeringpage.com, 2015).

The value of UA was then used in EES to calculate the number of transfer units (NTUs) based on the minimum heat capacity rate for each run using Equation 9 below.

$$NTU = \frac{UA}{C_{min}} \tag{9}$$

Using the NTU value, effectiveness for the heat exchanger was then calculated using EES built in function for effectiveness of unmixed cross flow heat exchangers. With the effectiveness and two inlet temperatures, the heat transfer across the heat exchanger was then calculated form Equation 10.

$$q = \varepsilon C_{min}(T_{h,i} - T_{c,i}) \tag{10}$$

6. Model Validation

To ensure reasonable predictions of the systems performance, the model has been kept simple and it relies heavily on well-established relations, such as actuator disk theory, the modified Bernoulli equation, the first law of thermodynamics, and the NTU method. Additionally, empirical data is used whenever possible thus ensuring considerable accuracy for those select components.

Unfortunately model validation has been constrained by the limited budget and compressed time scale of this project. For this reason, the validation of the model is still ongoing. To validate the application of the modified Bernoulli equation, the first law of thermodynamics, and the NTU method would require flowing hydraulic oil through a similar system. Since our team has neither the time nor the financial resources to acquire the necessary testing equipment it was determined that the best course

of action would be to validate these models with the actual components needed for the system. Considering the precedent for the use of the above mentioned relationships, we can assume with some certainty that the system will perform similarly to the predictions.

The mathematical characterization of positive displacement pumps outlined by Reethof (Reethof, Characteristics of Postive Displacment Pumps and Motors, 1960) is not as robust of a model as the other relationships used. However, when considering the lack of available test data for any bent axis piston pump at the desired operating speeds the use of these characterizing equations and coefficients was vital to producing a functioning model. Similarly to the other relationships used in the model, Reethof's characterization cannot be validated without the acquisition of some system components.

The only mathematical model that can be validated without the purchasing of components is actuator disk theory. Since the current Cal Poly wind turbine is functional there is test data, relating its power output to the wind conditions, which can be used to validate the actuator disk theory model. While all components of the model should be validated, actuator disk theory will suffice to provide estimated rotor input speed and power until the uncertainties of the other assumptions can be eliminated through testing.

In order to refine the major assumptions of the model, a testing procedure was created to characterize the vital system components. Below is the aforementioned testing procedure which outlines the objective of the experiment, gives background into the models being validated, and outlines the procedures needed to operate the equipment and acquire data.

6.1 Objective

The objective of this experiment is to validate and correct the wind turbine thermal-hydraulic dynamometer model. There are three aspects of the model, which have been deemed most crucial to investigate with this experiment. The first is the steady-state pump analysis (Reethof, Characteristics of Positive-Displacement Pumps and Motors, 1960), since this component has the largest overall effect on the model predictions and it accounts for several of the major assumptions. The second is the flow characteristics of the throttle valve, since this represents the system's variable control and the third is the frictional heat generation by means of pressure reduction.

6.2 Background

6.2.1 Nomenclature

C_d - drag coefficient

C_f - friction-torque coefficient

C_s - slip coefficient

D_p - pump displacement

K - flow factor

N - shaft speed

P_1 - pump inlet pressure

P_2 - pump outlet/needle valve inlet pressure

P_3 - needle valve outlet pressure

Q - actual flowrate

Q_L - leakage flowrate

Q_{ideal} - ideal flowrate

T_1 - pump inlet temperature

T_2 - pump outlet/needle valve inlet temperature

T_3 - needle valve outlet temperature

μ - kinematic viscosity

τ - shaft torque

τ_c - constant torque

τ_o - zero-speed torque

6.2.2 Pump Characterization

In order to properly characterize the positive displacement pump the four following values must be determined:

1. Slip coefficient (C_s)
2. Drag coefficient (C_d)
3. Friction-Torque coefficient (C_f)
4. Constant torque (τ_c)

Slip Coefficient

The slip coefficient can be calculated from the slope of a leakage flow (Q_L) versus pressure differential plot, as seen in Figure 31. This plot can be generated by either directly measuring the leakage flow, or by subtracting the actual pump delivery from the ideal delivery assuming no cavitation losses. The latter will be used in this experiment, since the actual delivery needs to me measured directly for the needle valve characterization. This method is shown graphically in Figure 32.

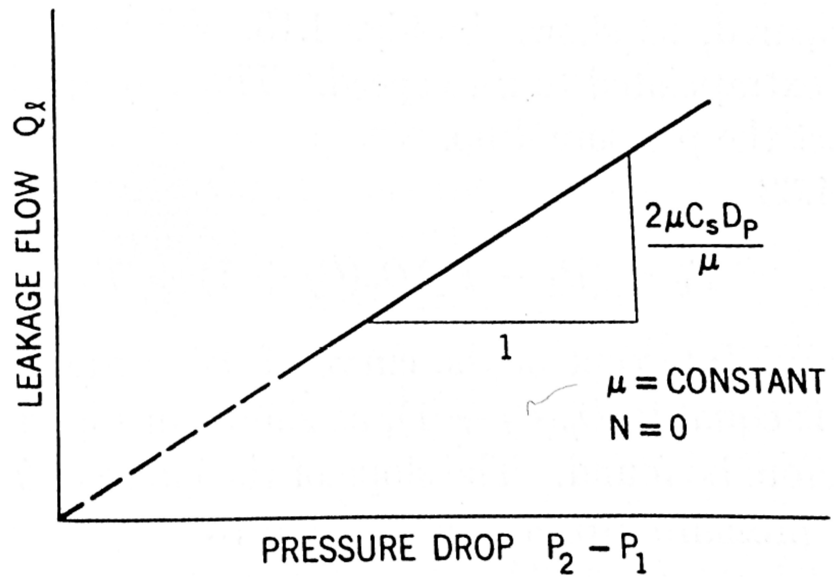

Figure 31. Leakage Flow vs. Pressure Differential (Reethof, Characteristics of Positive-Displacement Pumps and Motors, 1960)

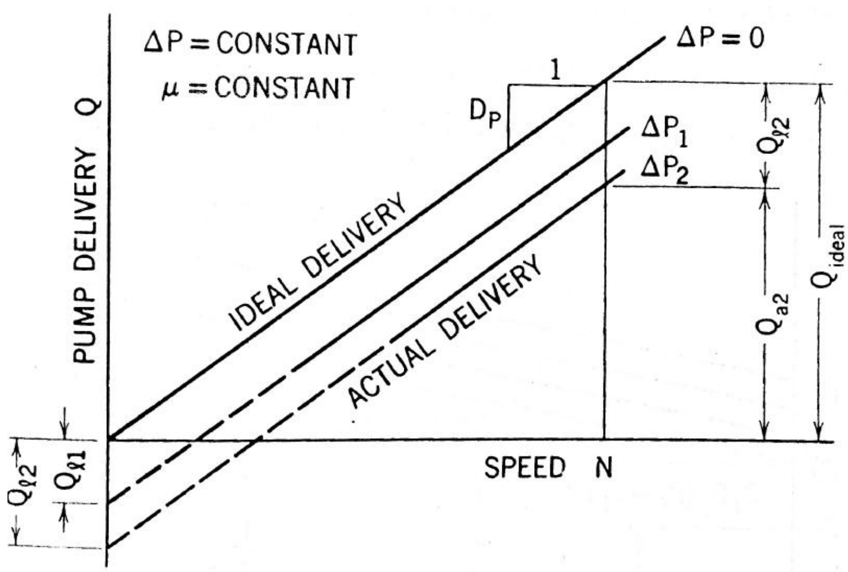

Figure 32. Pump Delivery vs. Shaft Speed (Reethof, Characteristics of Positive-Displacement Pumps and Motors, 1960)

Drag Coefficient

The drag coefficient can be determined from the slope of an applied torque versus speed plot as seen in Figure 33. This plot must be generate at a constant viscosity, with multiple runs conducted over a range of differential pressures.

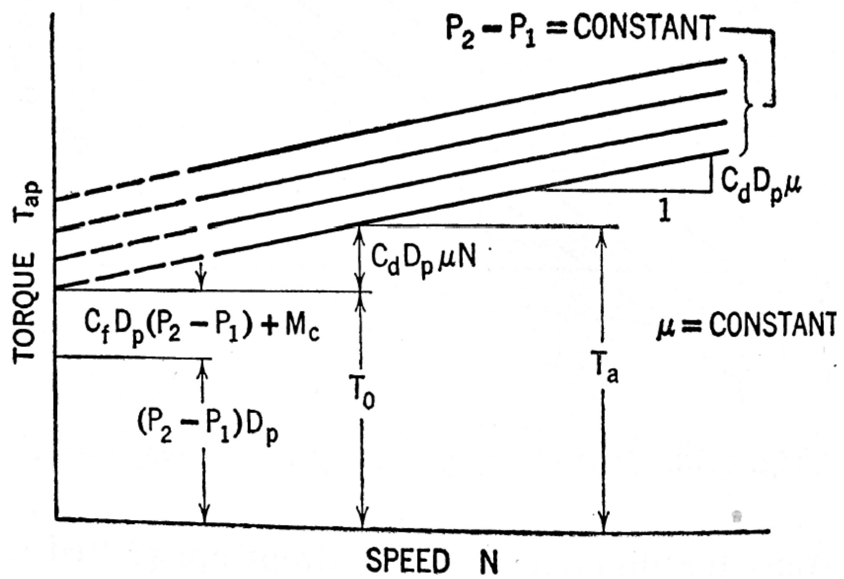

Figure 33. Shaft Torque vs. Shaft Speed (Reethof, Characteristics of Positive-Displacement Pumps and Motors, 1960)

Friction-Torque Coefficient

Similarly to the drag coefficient, the friction-torque coefficient can be determined from the slope of the zero-pressure curve shown in Figure 34. This plot is generated using the zero-speed torque extrapolated from the data gathered for Figure 33.

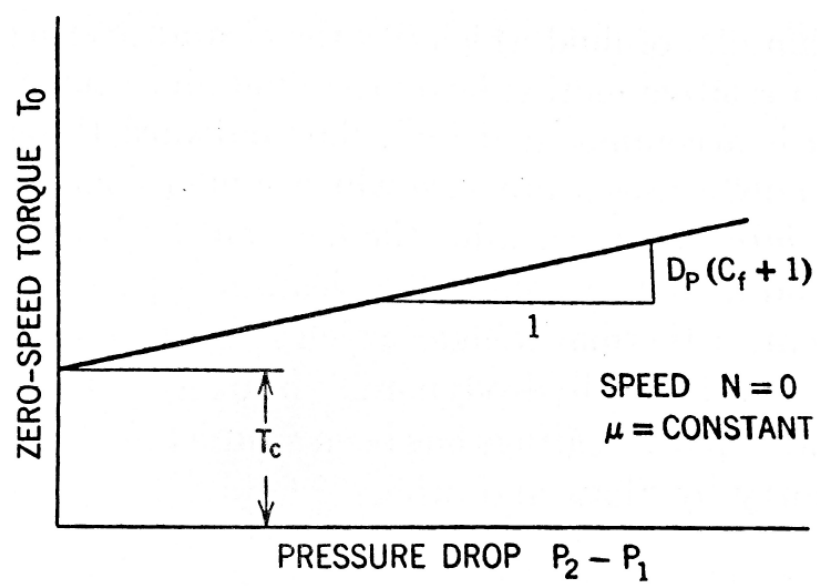

Figure 34. Zero Speed Torque vs. Pressure Differential (Reethof, Characteristics of Positive-Displacement Pumps and Motors, 1960)

Constant Torque

The constant torque is the y-intercept of the zero-speed torque curve shown in Figure 34, therefore it will also be determined from the extrapolation of data in Figure 33.

6.2.3 Throttle Valve Characterization

To characterize the throttle valve, standard convention will be observed by determining an experimental flow factor (K) for a range of needle positions (Lab 3: Pressure Flow Relation Across a Needle Valve).

6.2.4 Heat Generation

To determine the relationship between heat generation and pressure reduction within the hydraulic fluid, temperature rise across the throttle valve will be recorded along with the corresponding pressure differential and mass flowrate.

6.3 Safety Precautions

High Pressure: Pressures up to 2500psig are expected in components between the pump outlet and the needle valve inlet. Any leakage under these pressures could cause serious injury. Furthermore pressurized hydraulic fluid could cause the hydraulic hoses to move suddenly.

Protection: To protect against high pressure leaks, testing of the system will begin at the lowest pressure setting (10psig) in order to identify any potential leaks early on. At each pressure setting, the system will be visually inspected for leaks before adjusting needle valve to increase the systems pressure.

Safety glasses, face shields, and protective clothing will be worn at all times; in addition, a layer of Plexiglas will be positioned between the system and operator during testing. Also, to prevent pressures from exceeding the 2500psig limit, a pressure relief valve will be installed between the pump outlet and the needle valve.

In order to prevent injury resulting from sudden movement of hydraulic hoses, all hoses will be restrained. The only hose that will be operated under high pressure is the approximately 1.5ft long section between the pump outlet and needle valve. In the event of a rupture this short length of hose will be behind the Plexiglas shield that protects the operators; however, the operators must move past the shield to adjust the needle valve. Therefore, it is imperative that this hose be adequately restrained.

Note: The max pressure of 2500psig, was selected to provide a full range of data; however, lowering this value will not severely impacted the test results. Therefore, if the 2500psig is deemed unsafe by any Cal Poly faculty, these test procedures will be altered to reflect a safer maximum operating pressure.

High Temperature: The maximum expected system temperature is 85 degrees Celsius. Contact with oil at this temperature can cause severe burns.

Protection: The system temperature will be monitored constantly throughout the testing procedure; if the system approaches unsafe temperatures, the test can be terminated until the oil has time to cool. As mentioned before, all operators will be wearing safety glasses, face shield, and protective clothing as well as being behind a Plexiglas barrier for the majority of the testing. Everyone exposed to the system will be made aware that the metal components will be hot to the touch and components will be labeled accordingly.

Rotating Machinery/Projectile: The dynamometer will be rotating the input shaft at speeds up to 300 rpm and presents a hazard to operators near the spinning shaft. If the system is misaligned, the coupling between the pump and shaft could become a projectile.

Protection: To avoid injury, no loose clothing may be worn during testing and hair must be put up or tucked away. To prevent injury from failure of the shaft coupling, all operators will remain behind the Plexiglas barrier will the shaft speed is increased. Only after the shaft is safely operating at the desired speed and there are no signs of misalignment can an operator adjust the needle valve.

High Levels of Noise: The dynamometer and pump could produce a high level of noise at the high shaft speeds.

Protection: To guard against ear damage ear protection will be worn whenever the system is being operated.

6.4 Model Validation Testing Apparatus

Prior to model validation testing, some pieces of equipment will be manufactured including a mounting frame for the pump, a coupler for connection of the pump to the dynamometer, and support brackets for all hoses and the needle valve.

The pump frame must support the pump and attach to the mounts of the dynamometer 31" apart. To ensure that the frame is able to withstand all forces from static and dynamic loading during the testing procedure, the frame was designed and then verified using Finite Element Analysis (FEA). The pump frame was tested under the following conditions (all applied loads focused on the center of the mounting bracket):

- Torque applied by the dynamometer of 22,000 lb-in.
- Static moment caused the pump of 3,000 lb-in.
- Static force of the pump of 250 lb.

The reaction forces of the frame were focused on each corner of the support pieces mounted to the dynamometer. The pump frame was designed with 1"x 0.125" steel square tubing, 0.1875" steel sheet metal, and 1.5"x1.5"x0.125" steel angle iron. The FEA results from the test can be seen below in Figure 35.

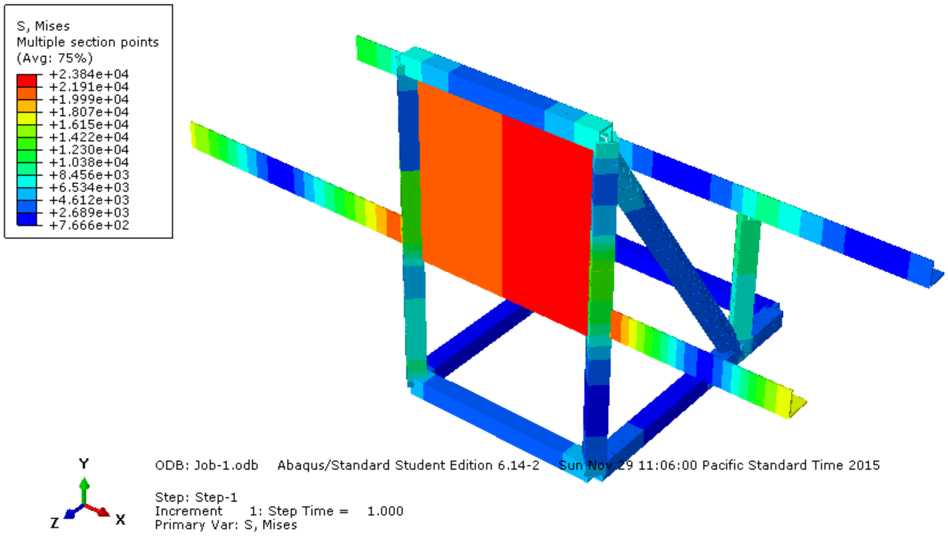

Figure 35. Finite Element Model for the Pump Frame.

From the FEA results we found that the designed pump frame was able to withstand all static and dynamic forces with a factor of safety of 1.5. The pump frame was manufactured and the pump mounted to the dynamometer mounts. The installed pump and pump frame can be seen below in Figure 36.

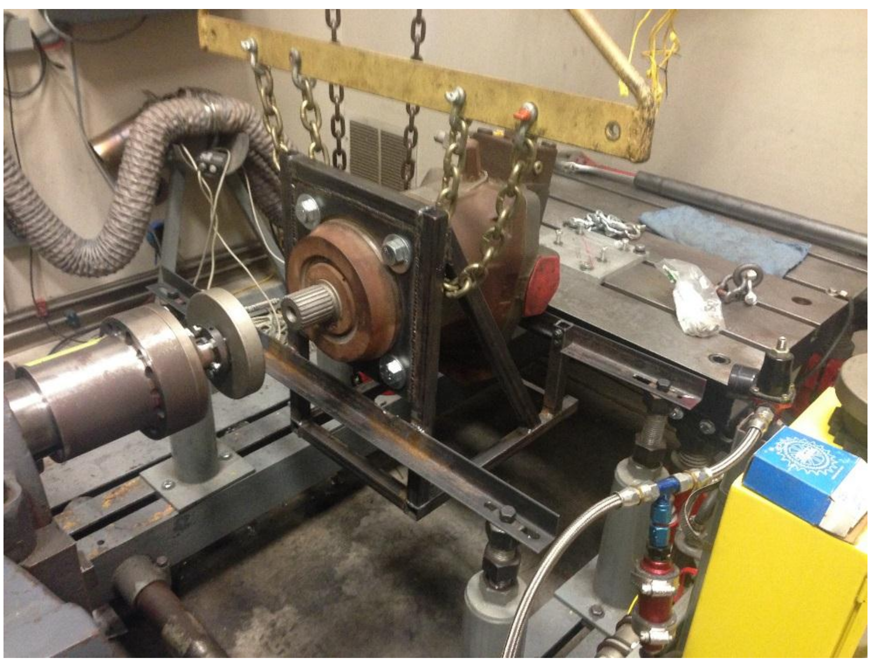

Figure 36. Installed Pump Frame Test Set-Up.

The angle iron support pieces were slotted on each corner to allow adjustment horizontal to dynamometer shaft. The bottle jacks used to support the angle iron allows adjustment vertically to the dynamometer shaft. The bottle jacks are also free to move along slotted supports to allow adjustment in parallel to the dynamometer shaft.

The coupler meant for connecting the pump's shaft to the dynamometer's shaft did not arrive in time for manufacturing and testing the model. Had it arrived, we would have used a 3.25" solid steel rod of 6" length to machine the coupler from. Due to this time constraint the model verification was not able to be completed and thus the predictions made of how the system would function could not be confirmed. If the coupler material had arrived, we would have followed the test procedure given in the next section.

6.5 Procedure

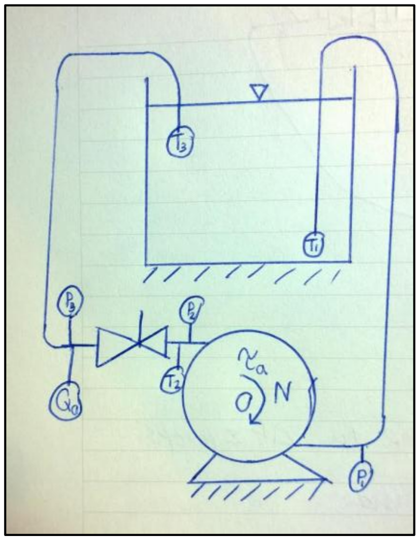

Figure 37. Test Setup

1. Set the dyno to a constant speed and adjust the needle valve to get desired pressure drop.
2. Check for any leaks in the system.
3. Record pump inlet pressure, pump inlet temperature, shaft speed, shaft torque, valve inlet temperature, valve inlet pressure, needle position, valve exit temperature, valve exit pressure, and the actual flowrate in data sheet. An example of the data sheet can be seen in Figure 38.
4. Make sure that the temperature differential across the pump is small to maintain a constant viscosity and that the maximum temperature is below upper limit of 85 [C].
5. Open needle valve, increase shaft speed, and repeat steps 1-3 for speeds from 10-50 [rpm] and 50-300 [rpm].
6. Repeat steps 1-4 for corresponding pressure differentials from 100-2500 [psig] and 10-1000 [psig].

Target ΔP_{pump} = 10 [psig]									
N	Valve Position	P_1	P_2	P_3	T_1	T_2	T_3	Q	τ
[rpm]	[turns]	[psig]	[psig]	[psig]	[F]	[F]	[F]	[gpm]	[ft.lbf]
50									
60									
70									
80									
90									
100									
110									
120									
130									
140									
150									
160									
170									
180									
190									
200									
210									
220									
230									
240									
250									
260									
270									
280									
290									
300									

Figure 38. Example of Constant Pressure Differential Test Data Sheet

7. Future Manufacturing and Testing:

Should the test above confirm the validity of the Thermal-Hydraulic Turbine Dynamometer and funds become available to build it, here is the recommended procedure for future tests.

7.1 Concept Manufacture and Installation:

Prior to any manufacturing of parts, the dimensions of the existing nacelle frame or any parts which directly impact the hydraulic system must be confirmed for accuracy. If the "As Built" dimensions are not properly measured, the system may require adjustment in order to function well inside the already built frame.

1. Confirm dimensions and build pump mounting bracket. Attach the bracket to the nacelle frame, and then attach pump to the mounting bracket.
2. Confirm dimensions and build rear bird plate mounting bracket. Attach the bracket to the nacelle frame, and then attach the rear bird plate to the mounting bracket.
3. Install Code 62 flanges and the input/output hoses. Refer to assembly drawings for approximate direction of Code 62 elbows.
4. Attach Pressure Relief Valve #1. Attach Pressure Relief Valve #1 outlet hose.
5. Attach Load Bearing Needle Valve. Attach Load Bearing Needle Valve outlet hose.
6. Attach Pressure Reducing Valve #1 Attach Pressure Reducing Valve #1 outlet hose.
7. Attach Pressure Reducing Valve #2 Attach Pressure Reducing Valve #2 outlet hose.
8. Attach Pressure Relief Valve #2. Attach Pressure Relief Valve #2 to heat exchanger outlet hose. Place the hose through the left hole of the rear bird plate.
9. Install hydraulic reservoir to the rear bird plate mounting brackets as shown in the assembly drawings. Attach pump inlet hose to the appropriate reservoir bung.
10. Attach flushing needle valve to the Flushing Tee with the appropriate adapter.
11. Attach Heat Exchanger to Flushing Tee hose.
12. Confirm dimensions and build heat exchanger mounting bracket. Attach heat exchanger. Install hoses to heat exchanger.
13. Attach all drain, flushing, and relief hoses to the reservoir.

7.2 Concept Testing:

1. Fill the hydraulic reservoir with hydraulic fluid. Spin the pump slowly while continuing to fill the hydraulic reservoir.
2. Once the hydraulic oil completes its run through the system and returns to the reservoir, stop the pump and fill the reservoir to capacity.
3. Adjust both relief valves to the middle of their operational range. Adjust both pressure reducing valves to the low end of their operating range.
4. Power the pump. Turn the load bearing needle valve until the first pressure transducer reads the relief pressure and the first relief valve opens. Adjust the first relief valve and needle valve simultaneously to set the first relief valve to 5,000 psi.
5. Once the relief valve is set, adjust the load bearing needle valve until the flow is restricted enough to balance against the relief valve.
6. Adjust the second relief valve until the relief valve activates at 225 psi.
7. Once the second relief valve is set, adjust the second pressure reducing valve to the point where the second pressure transducer reads 200 psi.

8. All primary valves are now set. Let the pump run for some time while monitoring pressures and the fluid temperature after the heat exchanger.
9. Adjust the flushing needle valve to force more hydraulic fluid to flush the pump.

Table 8. Major manufacturing resources, costs, and estimated time to completion.

Manufacture			
Object	Company/ Resource	Cost ($)	Estimated Time to Completion (hrs)
Pump Mounting Bracket	N/A	0	5
Rear Bird Plate	N/A	0	5
Rear Bird Plate Mounting Bracket	N/A	0	3
Heat Exchanger Mounting Bracket	N/A	0	3
Valve Mounting Brackets	N/A	0	5

Table 9. Major testing resources, equipment, cost, and estimated time to completion.

Testing				
Objective	Company/ Resource	Equipment Required	Cost ($)	Estimated Time to Completion (hrs)
Confirm pump function and flow direction	Cal Poly Engine Lab	Dynamometer	0	5
Set valves. Test valve function	Cal Poly Engine Lab	Dynamometer, Voltmeter	0	10
Heat exchanger function	Cal Poly Engine Lab	Dynamometer, Thermocouple, Voltmeter	0	3
Valve adjustme nt for various input speeds	Cal Poly Engine Lab	Dynamometer, Thermocouple, Voltmeter	0	12
Function in real wind conditions	Cal Poly Wind Turbine	Voltmeter	0	10+

8. Management Plan:

8.1 Method of Approach:

8.1.1 CVT:

Background Research: As with any project, our first and most crucial step was to familiarize ourselves with all aspects of the project including current wind turbine power transmission techniques, hydrostatic CVT fundamentals, previous research into hydrostatic CVTs for wind turbines, and the specific challenges of our project. We began our background research at the onset of the project, and gained a sufficient understanding of the project to begin moving forward. That being said, as we progressed through the design process we continued our research to ensure we produced the best design.

Idea Generation: After we fully defined the problem at hand, we used the design requirements and considerations to determine several feasible designs. Once we had generated numerous designs, we selected the design which best met our objectives. At the request of our sponsor, our original concepts/designs all involved a hydraulic CVT.

Preliminary Analysis: After we selected the best design for our CVT, we performed an analysis of all crucial elements to vet the design and confirm its legitimacy. The preliminary analysis confirmed this design to be valid; however, due to budget limitations we were forced to make modifications to our design and move away from the concept of a hydraulic CVT.

Design Modification: During the preliminary analysis, it became clear that our sponsor's initial request for a hydraulic CVT was not feasible, so after redefining our scope, we altered our design to meet our original requirements without accommodating the request for a hydraulic CVT.

8.1.2 Thermal-Hydraulic Turbine Dynamometer:

Idea Generation (part 2): With a new scope, we began a second round of idea generation. Once a pump had been donated to us, we had no choice but to design around that - all ideas generated incorporated the donated pump.

Design Modification (part 2): Since we will be using primarily off-the-shelf components in our design it is crucial that we modify our design to incorporate the commercially available components. This includes designing any custom fixtures, fittings, etc. that we will manufacture in house.

Selection of Components: Using off-the-shelf components requires us to design and select components concurrently. We selected components to meet our design requirements while designing concepts to accommodate available components. Once components were selected we began an in-depth analysis.

In-depth Analysis of Final Design: After we completed our design we did a final analysis of all elements to confirm our design's validity.

Validation: Due to our limited budget, we were unable to construct our final design. Instead, we designed a low-cost testing system that would confirm our calculated models.

Design of Test System: When designing our test system we designed, once again, around the pump we had and they parts we could get on campus - to save as much money as possible. Because of this design strategy, we were forced to go through many different iterations before reaching our final test system design.

Manufacturing/Testing: Unfortunately, a critical part of our design did not arrive in time and we were forced to present our design without testing data to confirm our model predictions.

8.2 Team Management

For the purpose of organization and clarity for you, the sponsor, we assigned the following general responsibilities:

Communications – Alexander Campbell

Point of contact for the team. Responsible for coordinating with sponsor and advisor.

Document Manager – Ryan Baskett

Responsible for documentation and management of all documents including online files.

Treasurer – Andrew Puntorno-Carlberg

Manages budget and controls funds.

Aside from those titles and responsibilities we believed in a collaborative approach to tackling the problems that we faced. For the most part, we worked as a team on most tasks; however, some tasks were handled primarily by individual members of the group. Andrew was in charge of the Solidworks model and manufacturing, Ryan was in charge of the EES analysis, and Alex was in charge of most of the report organization and .

Time Estimate: ~11 months

Work Estimate:1500-3000 man-hours

9. Conclusion:

Over the last eleven months, CVTeam has performed an in-depth analysis of the applications of CVT's in wind turbines - along the way learning about the characteristics of many different types of positive displacement pumps and their behavior as motors, the effects of pressure regulators (pressure relief valves, needle valves, pressure reducing valves, counter balancing valves, etc.) on fluid systems, mechanical gear boxes and their benefits/drawbacks as compared to hydraulic transmissions, fluid flow around stationary objects, how to communicate with many different vendors - discussing objectives and negotiating deals, analysis of hydraulic systems using EES, Solidworks modeling, shop manufacturing, dynamometer operations, and, above all else, how to work together in the face of adversity.

With what we have learned, we would not recommend the use of a CVT in Cal Poly's wind turbine. Due to the low input RPM, any tolerable system efficiency would require a very large pump and motor

- parts that were too expensive for the scope of this project and something that our current tower would not be able to handle structurally. However; we believe that the Thermal-Hydraulic Turbine Dynamometer that we designed would be a feasible option for the purposes of researching the affects and performance of CVT's in wind turbine applications. Unfortunately, due to shipping complications, we were unable to test our model and confirm our beliefs, but with the analysis we performed, based on widely accepted models and equations, we trust that our test would have confirmed our predictions.

In the future, if the desire to further pursue this project exists, we recommend finishing our testing apparatus and completing the testing procedure we have laid out in this report. If the results of the tests confirm our predictions, it will be up to the sponsor whether or not to pursue our design - while we don't recommend the use of CVT's with our current wind turbine, we do not oppose the use of our design for research.

Overall, the result of this project was not ideal - we were not able to deliver results as a confirmation of our design's validity. However; we were able to deliver an ideal concept for a CVT and design/performance predictions for a Thermal-Hydraulic Turbine Dynamometer that could be used to research CVT's and their applications in wind turbines. We are satisfied with the knowledge and experiences we have gained through this project and wish the best of luck to future teams, should this project be continued.

Bibliography

(2015). Retrieved from Engineeringpage.com.

Cros, P. (1979). *United States Patent No. US4149092.*

(n.d.). *Lab 3: Pressure Flow Relation Across a Needle Valve.* University of Minnesota.

MacKay, G. (n.d.). *Europe Patent No. EP2535581A2.*

Neutrium. (2012, April 29). Retrieved June 6, 2015, from https://neutrium.net/fluid_flow/pressure-loss-in-pipe/

Ragheb, A., & Ragheb, M. (2010). *Wind Turbine Gearbox Technologies.* Urbana: University of Illinois.

Reethof, G. (1960). Characteristics of Positive-Displacement Pumps and Motors. In J. F. Blackburn, G. Reethof, & J. L. Shearer, *Fluid Power Control* (pp. 90-129). Cambridge, Massachusetts: The M.I.T Press.

Reethof, G. (1960). Characteristics of Postive Displacment Pumps and Motors. In J. F. al., *Fluid Power Control* (pp. 90-129). Cambridge : The M.I.T. Press.

Stelson, D. K. (2015). Director of the Center of Compact Fluid Design. (CVTeam, Interviewer)

Streeter, V. (1966). *Fluid Mechanics, 4th edition.* Tokyo: McGraw-Hill.

Watton, J. (2009). *Fundamentals of Fluid Power Control.* Cambridge: Cambride University Press.

Appendix A: House of Quality

QFD: House of Quality

Project: Cal Poly Hydrostatic CVT
Revision: 1
Date: 1/29/2015

Correlations	
Positive	+
Negative	−
No Correlation	

Relationships	
Strong	●
Moderate	○
Weak	▽

Direction of Improvement	
Maximize	▲
Target	◇
Minimize	▼

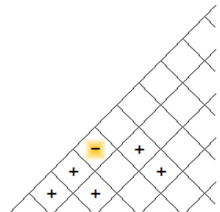

WHO: Customers

NOW: Current Product Assesment - Customer Requirements

Row #	Weight Chart	Relative Weight	Dr. Lemieux & Cal Poly Wind World	Dr. Stelson	Wind Turbine Industry		Maximum Relationship	WHAT: Customer Requirements (explicit & implicit) / HOW: Engineering Specifications	Package Dimensions	Gear Ratio Range	Power Capacity	Support Structure F.S.	Efficiency	Current System: Direct Drive	Mechanical Gearbox	Row #
								Column #	1	2	3	4	5			
								Direction of Improvement	▼	▲	▲	▲	▲			
1		9%	7	4	1		9	Must Operate with both Rotors		●	▽			2	3	1
2		21%	9	9	8		9	Must Maintain Constant Rotor Speed		●	○			0	1	2
3		19%	7	8	9		9	Needs to Operate in Low Wind Speed		●	▽			2	4	3
4		13%	6	3	7		9	Off-the-Shelf Parts	●	○		▽		4	3	4
5		4%	5	0	1		9	No Alterations to the Nacelle	●			○		5	4	5
6		14%	6	5	6		9	Must be Safe			●	●		4	4	6
7		20%	8	8	9		9	Output Power ≥ Current System		●	○		●			7

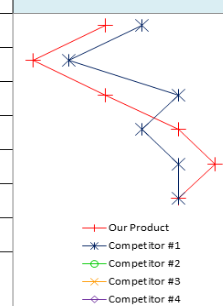

	1	2	3	4	5	Row #
HOW MUCH: Target	6 in.	Varia ble from	6kW +	2	80%	8
Max Relationship	9	9	9	9	9	9
Technical Importance Rating	151.611	664.127	273.432	147.359	180.719	10
Relative Weight	11%	47%	19%	10%	13%	11
Weight Chart						12
Our Product	5	5	5	4	3	13
Current Product: Direct Drive	5	0	5	5	5	14
Mechanical Gearbox	3	4	5	3	4	15
						16

Current Product Assesment - Engineering Specifications

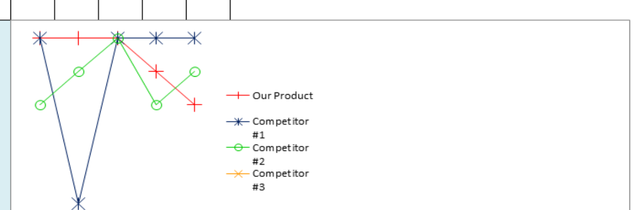

Column #	1	2	3	4	5

Appendix B: Calculations

Hydraulic Power

$$\wp = P \times Q \div 600 \tag{1.1}$$

Where $\wp$ is hydraulic power [kW], P is pressure [bar], and Q is flowrate $\left[\frac{\text{L}}{\text{min}}\right]$. Solving for the needed pressure to transmit a certain power at a certain flowrate:

$$P = \frac{\wp \times 600}{Q} \tag{1.2}$$

Q is the flowrate generated by the pump and is equivalent to the displacement of the pump multiplied by speed of the pumps rotation. Substituting this into Equation 1.2 gives:

$$P = \frac{\wp \times 600}{\frac{D}{1000} \times n} \tag{2}$$

Where D is the displacement of the pump in cubic centimeters [cc] and n is the speed of the pump in revolution per minute [rpm]. Using the values from an on-the-market pump provides a baseline for the needed pressure in the hydraulic lines. Parker's MR 400 E fixed displacement, radial piston pump fits many of the needs that the project requires. The MR 400 E has a displacement of 400.6 cc.

$$P = \frac{(6\ \text{kW}) \times 600}{\frac{400.6\ \frac{\text{cc}}{\text{rev}}}{1000} \times 25\ \text{rpm}}$$

$$P = 359\ \text{bar or} \sim 5200\ \text{psi}$$

The needed pressure is within the maximum pressure value for the pump, so it is a feasible solution.

Head Loss in Hydraulic Lines

To calculate the head loss in the hydraulic lines, first the Reynolds number for the hydraulic fluid flow must be found.

$$Re = \frac{v \times D}{\vartheta} \tag{3}$$

Where v is the characteristic velocity of the fluid flow, D is the diameter of the hydraulic lines, and ϑ is the kinematic viscosity of the hydraulic fluid. For this calculation, v is calculated below, D is 9.525 mm (for 3/8" line), and ϑ is 40 $\left[\frac{mm^2}{s}\right]$ (an average value for the kinematic viscosity for most hydraulic fluids in the desired operating range).

$$v = 1.274 \times \frac{Q}{D^2} \tag{3.1}$$

Where: Q is the flowrate, 10.015 $\frac{\mathrm{L}}{\mathrm{min}}$ ~ $0.010015\ \frac{\mathrm{m}^3}{\mathrm{min}}$

D is the line diameter, 0.009525 m

$$v = 1.274 \times \frac{0.010015\ \frac{\mathrm{m}^3}{\mathrm{min}}}{(0.009525\ \mathrm{m})^2}$$

$$v = 140.6\ \frac{\mathrm{m}}{\mathrm{min}} \sim 2.344\ \frac{\mathrm{m}}{\mathrm{s}}$$

Substituting values into the Equation 3:

$$Re = \frac{\left(2.344\ \frac{\mathrm{m}}{\mathrm{s}}\right) \times (0.009525\ \mathrm{m})}{\left(40 \times 10^{-6}\ \frac{\mathrm{m}^2}{\mathrm{s}}\right)}$$

$$Re = 558.2$$

Any Reynolds number below ~ 2,000 is laminar flow, which for this case allows us to use a simplified friction factor equation to find head loss. The total head loss over a certain length of line is:

$$h_f = f\frac{L}{D} \times \frac{v^2}{2g} \tag{4}$$

Where : f is the friction factor

L is the length of hydraulic line

D is the line diameter

v is the characteristic velocity

g is the acceleration due to gravity

The approximate friction factor is given by:

$$f = \frac{64}{Re} \tag{4.1}$$

$$f = \frac{64}{558.2}$$

$$f = 0.115$$

Assuming a line length of 55 m (~180 ft; number found for generator outside nacelle for 70 ft tower plus 20 ft of extra length), line diameter of 9.525 x 10^{-3}m, characteristic velocity of $2.344\ \frac{\mathrm{m}}{\mathrm{s}}$, and gravitational acceleration of 9.81 $\frac{\mathrm{m}}{\mathrm{s}^2}$. Substitute values into Equation 4:

$$h_f = (0.115)\frac{55\ \mathrm{m}}{9.525\ \times\ 10^{-3}\ \mathrm{m}} \times \frac{\left(2.344\ \frac{\mathrm{m}}{\mathrm{s}}\right)^2}{2\ \times 9.81\ \frac{\mathrm{m}}{\mathrm{s}^2}}$$

$$h_f = 185.9\ \mathrm{m}$$

For an assumed specific gravity of 0.87, converting head loss to pressure gives:

$$P_{loss} = \frac{h_f}{10.197} \times SG \tag{4.2}$$

$$P_{loss} = \frac{185.9\ \mathrm{m}}{10.197} \times 0.87$$

$$P_{loss} = 15.86\ \mathrm{bar}$$

A pressure loss of this size when compared to the working pressure calculated in Equation 2 represents 4.4 % of the working pressure.

Appendix C shows the tabulated results of the above calculations for a variety of line diameters and kinematic viscosities. Appendix C shows the total head loss, equivalent pressure drop, and the percent of the operating pressure that the pressure drop represents. These values were found using the same assumptions made for the above equations.

Appendix C: Head Loss for Varying Kinematic Viscosity and Line Diameters

Constant Values					
Pump Operating Point			Line Property	Hydraulic Oil Properties	
Displacement Volume	Angular Velocity	Operating Pressure	Line Length	Density	Manufacture Suggested Viscosity Operating Range
[cm^2]	[rpm]	[bar]	[m]	[kg/m^3]	[mm^2/s]
400.6	25	360	55	860	30-50

Variable Values							
Line Diameter	Fluid Velocity	Fluid Kinematic Viscosity @ 20 °C	Reynolds Number	Friction Factor	Major Head Loss	Pressure Drop	% Pressure Loss
[mm]	[m/s]	[mm^2/s]	[unitless]	[unitless]	[m]	[bar]	[%]
6.35	5.27	20	1673	0.038	469	39.6	11.0
		25	1339	0.048	586	49.5	13.7
		30	1116	0.057	704	59.4	16.5
		35	956	0.067	821	69.2	19.2
		40	837	0.076	938	79.1	22.0
		45	744	0.086	1055	89.0	24.7
		50	669	0.096	1173	98.9	27.5
		55	609	0.105	1290	108.8	30.2
		60	558	0.115	1407	118.7	33.0
[mm]	[m/s]	[mm^2/s]	[unitless]	[unitless]	[m]	[bar]	[%]
9.525	2.34	20	1116	0.057	93	7.8	2.2
		25	892	0.072	116	9.8	2.7
		30	744	0.086	139	11.7	3.3
		35	637	0.100	162	13.7	3.8
		40	558	0.115	185	15.6	4.3
		45	496	0.129	208	17.6	4.9
		50	446	0.143	232	19.5	5.4
		55	406	0.158	255	21.5	6.0
		60	372	0.1721	278	23.4	6.5
[mm]	[m/s]	[mm^2/s]	[unitless]	[unitless]	[m]	[bar]	[%]
12.7	1.32	20	837	0.076	29	2.47	0.69
		25	669	0.096	37	3.09	0.86
		30	558	0.115	44	3.71	1.03
		35	478	0.134	51	4.33	1.20
		40	418	0.153	59	4.95	1.37
		45	372	0.172	66	5.56	1.55
		50	335	0.191	73	6.18	1.72
		55	304	0.210	81	6.80	1.89
		60	279	0.229	88	7.42	2.06

Appendix D: Base EES Model Formatted Equations

System Model

Cal Poly Wind Turbine CVT Senior Project Team

Cal Poly San Luis Obispo

5/26/2015

Assumptions

-Hydraulic oil is incompressible (i.e. neglecting effect of temperature or pressure on oil density)

-The system is adiabatic except for the heat exchanger

-Neglecting effects of temperature on pressure in oil

Using ISO 32 Oil

User Defined Functions

Function **PressureRegulator** (P_{in}, P_{set}, $\dot{V}$)

If $[P_{in} > P_{set}]$ Then

sets pressure drop based on outlet prssure

PressureRegulator := $P_{in} - P_{set}$

Else

Calculates pressure drop based on empirical data

PressureRegulator := **Interpolate** ['Fully Open Pressure RegulatorFlowRate', 'PressureDrop', 'FlowRate' = $\dot{V}$]

EndIf

End **PressureRegulator**

Constants

$g = 9.81$ [m/s^2]

Air Properties

$$T_{air} = 65 \cdot \left| 0.55555556 \cdot \frac{C}{F} \right|$$

$P_{air} = 101.3$ [kPa]

$$u_{wind} = 8 \cdot \left| 0.44704 \cdot \frac{m/s}{mph} \right|$$

$\rho_{air} = \rho\left[Air_{ha}, T = T_{air}, P = P_{air}\right]$

$cp_{air} = \mathbf{Cp}\left[Air_{ha}, T = T_{air}, P = P_{air}\right]$

Rotor Properties

$R_{rotor} = 10$ [m]

$lamda_{rotor} = 7$ [-]

$C_{power} = 0.45$ *Power Coefficient*

Actuator Disk Theory

$Power_{wind} = 0.5 \cdot \rho_{air} \cdot \pi \cdot R_{rotor}^{2} \cdot u_{wind}^{3}$

$Power_{rotor} = C_{power} \cdot Power_{wind}$

Rotor Speed

$$lamda_{rotor} = R_{rotor} \cdot \frac{\omega_{rotor}}{u_{wind}}$$

Rotor Torque

$$Torque_{rotor} = \frac{Power_{rotor}}{\omega_{rotor}}$$

Max Load Torque

$$\Delta P_{max} = 5000 \cdot \left| 6.895 \cdot \frac{kPa}{lbf/in^2} \right|$$

$$Torque_{load,max} = \Delta P_{max} \cdot \left| 1000 \cdot \frac{Pa}{kPa} \right| \cdot D_p + Torque_r + Torque_f + Torque_c$$

Load Power

$Power_{load} = Torque_{load} \cdot \omega_{rotor}$

Load Torque

$C_d = 10^{5}$ [-] *Drag Coefficient based on (eq 4.57), C_{do}, & (Figure 4.11) pg. 109{1}*

$C_f = 0.07$ [-] *Friction Torque Coefficent, value of 0.04-0.1 is common pg. 109{1}*

$Torque_c = 10$ [N*m] *Constant Friction Torque (independent of pressure and speed)*

Eq. 4.1 [1]

$Torque_{load} = Torque_t + Torque_r + Torque_f + Torque_c$ *Actual Torque*

Eq. 4.14 [1]

$$Torque_t = \Delta P_{pump} \cdot \left| 1000 \cdot \frac{Pa}{kPa} \right| \cdot D_p$$ *Ideal Torque (i.e. no losses)*

Eq. 4.29 [1]

$Torque_r = C_d \cdot D_p \cdot 2 \cdot \pi \cdot \omega_{rotor} \cdot \mu$ *Viscous Friction Torque*

Eq. 4.31 [1]

$$Torque_f = C_f \cdot \Delta P_{pump} \cdot \left| 1000 \cdot \frac{Pa}{kPa} \right| \cdot D_p$$ *Mechanical Friction Torque*

$$\eta_m = \frac{Torque_t}{Torque_{load}}$$

Max Temperature

$$T_{max} = \mathbf{Max}\left[T_1, T_2, T_3, T_4, T_5, T_6, T_7, T_8, T_9, T_{10}, T_{11}, T_{12}, T_{13}, T_{14}, T_{15}, T_{16}\right]$$

Max Pressure

$$P_{max} = \mathbf{Max}\left[P_1, P_2, P_3, P_4, P_5, P_6, P_7, P_8, P_9, P_{10}, P_{11}, P_{12}, P_{13}, P_{14}, P_{15}, P_{16}\right]$$

Ideal Flow

Oil Properties

$T_0 = 20$ [C] *Set for most viscous case, start up*

$\mu = 0.08$ [kg/m-s]

$\rho = 857$ [kg/m^3]

$cp = 1950$ [J/kg-K]

Pump Properties

$$D_p = 250 \cdot \left| 1.59155 \times 10^{-7} \cdot \frac{m^3/rad}{cm^3/rev} \right|$$ *Displacement per Radian*

Volumetric Efficiency

$\eta_v = 0.6$

Ideal Flow Rate (i.e. no losses)

Eq 4.10 [1]

$$\dot{V}_t = D_p \cdot \omega_{rotor}$$

Actual Flow

$$\dot{V}_a = \eta_v \cdot \dot{V}_t$$

Leakage Flow

$$\dot{V}_l = [1 - \eta_v] \cdot \dot{V}_t$$

Temperature Rise in Pump 0-->1

Heat Transfered to fluid exiting port

$$q_{0,1} = [1 - \eta_m] \cdot Power_{load}$$

Frist Law, Assuming adiabatic boundry

$$q_{0,1} = \dot{V}_a \cdot \rho \cdot cp \cdot \Delta T_{pump}$$

$$T_1 = T_0 + \Delta T_{pump}$$

Pressure at Pump Outlet (1)

$$P_1 = P_{16} + \Delta P_{pump} - P_{11}$$ *inlet pressure plus pressure rise from shaft work-case pressure*

Pressure Drop in Pipe 1-->2

Pipe DImensions

$$D_{1,2} = 1 \cdot \left| 0.0254 \cdot \frac{m}{in} \right|$$

$$L_{1,2} = 17 \cdot \left| 0.0254 \cdot \frac{m}{in} \right|$$

$$RR = 0$$

Minor Loss Coefficents

$$K_{1,2} = 2 \cdot \mathbf{K_{90deg,Elbow}}\ [RR] + \mathbf{K_{Tee,Straight}}\ [RR]$$

Major Loss Friction Factor

$$u_{1,2} = \frac{\dot{V}_a}{\frac{\pi}{4} \cdot D_{1,2}^2}$$

$$Re_{1,2} = \frac{\rho \cdot u_{1,2} \cdot D_{1,2}}{\mu}$$

$$f_{1,2} = \mathbf{MoodyChart}[Re_{1,2}, RR]$$ *moody uses churchhill correlation, is it valid for laminat flow?looks like it*

Modified Bernoulli

$$\Delta P_{1,2} = -\rho \cdot \left[f_{1,2} \cdot \frac{L_{1,2}}{D_{1,2}} + K_{1,2} \right] \cdot \frac{u_{1,2}^2}{2} \cdot \left| 0.001 \cdot \frac{kPa}{Pa} \right|$$

Temperature Rise in Pipe 1-->2

Heat Transfered to fluid

$$q_{1,2} = -\Delta P_{1,2} \cdot \left| 1000 \cdot \frac{Pa}{kPa} \right| \cdot \dot{V}_a$$

Frist Law, Assuming adiabatic boundry

$$q_{1,2} = \dot{V}_a \cdot \rho \cdot cp \cdot \Delta T_{1,2}$$

$$T_2 = T_1 + \Delta T_{1,2}$$

Pressure at (2)

$$P_2 = P_1 + \Delta P_{1,2}$$

Pressure Drop Across Needle Valve

$N_{knob} = 0$ [-] *Number of Knob Turns, Ranges from 0-4.75(almost closed)*

$$K_{needle,2,3} = -3.94 \cdot 10^{-8} \cdot N_{knob} + 1.89 \cdot 10^{-7}$$

$$\dot{V}_a = K_{needle,2,3} \cdot \left[-\Delta P_{2,3} \cdot \left| 1000 \cdot \frac{Pa}{kPa} \right| \right]^{0.5}$$

Temperature Rise Needle Valve 2-->3

Heat Transfered to fluid

$$q_{2,3} = -\Delta P_{2,3} \cdot \left| 1000 \cdot \frac{Pa}{kPa} \right| \cdot \dot{V}_a$$

Frist Law, Assuming adiabatic boundry

$$q_{2,3} = \dot{V}_a \cdot \rho \cdot cp \cdot \Delta T_{2,3}$$

$$T_3 = T_2 + \Delta T_{2,3}$$

Pressure at (3)

$$P_3 = P_2 + \Delta P_{2,3}$$

Pressure Drop in Pipe 3-->4

Pipe DImensions

$$D_{3,4} = 0.75 \cdot \left| 0.0254 \cdot \frac{m}{in} \right|$$

$$L_{3,4} = 10 \cdot \left| 0.0254 \cdot \frac{m}{in} \right|$$

Minor Loss Coefficents

$$K_{3,4} = 0$$

Major Loss Friction Factor

$$u_{3,4} = \frac{\dot{V}_a}{\frac{\pi}{4} \cdot D_{3,4}^{\,2}}$$

$$Re_{3,4} = \frac{\rho \cdot u_{3,4} \cdot D_{3,4}}{\mu}$$

$f_{3,4} = \textbf{MoodyChart}\left[Re_{3,4},\ RR\right]$ *moody uses churchhill correlation*

Modified Bernoulli

$$\Delta P_{3,4} = -\rho \cdot \left[f_{3,4} \cdot \frac{L_{3,4}}{D_{3,4}} + K_{3,4}\right] \cdot \frac{u_{3,4}^2}{2} \cdot \left|0.001 \cdot \frac{kPa}{Pa}\right|$$

Temperature Rise in Pipe 3-->4

Heat Transfered to fluid

$$q_{3,4} = -\Delta P_{3,4} \cdot \left|1000 \cdot \frac{Pa}{kPa}\right| \cdot \dot{V}_a$$

Frist Law, Assuming adiabatic boundry

$$q_{3,4} = \dot{V}_a \cdot \rho \cdot cp \cdot \Delta T_{3,4}$$

$$T_4 = T_3 + \Delta T_{3,4}$$

Pressure at (4)

$$P_4 = P_3 + \Delta P_{3,4}$$

Pressure Drop Arcoss Pressure Regulator #1 4-->5

$$\Delta P_{4,5} = -\textbf{PressureRegulator}\left[P_4,\ P_{set,1},\ \dot{V}_a\right]$$

$$P_{set,1} = 1000 \cdot \left|6.895 \cdot \frac{kPa}{lbf/in^2}\right|$$

Temperature Rise in Pressure Regulator 1

Heat Transfered to fluid

$$q_{4,5} = -\Delta P_{4,5} \cdot \left|1000 \cdot \frac{Pa}{kPa}\right| \cdot \dot{V}_a$$

Frist Law, Assuming adiabatic boundry

$$q_{4,5} = \dot{V}_a \cdot \rho \cdot cp \cdot \Delta T_{4,5}$$

$$T_5 = T_4 + \Delta T_{4,5}$$

Pressure at (5)

$$P_5 = P_4 + \Delta P_{4,5}$$

Pressure Drop in Pipe 5-->6

Pipe DImensions

$$D_{5,6} = 0.75 \cdot \left|0.0254 \cdot \frac{m}{in}\right|$$

$$L_{5,6} = 14 \cdot \left| 0.0254 \cdot \frac{m}{in} \right|$$

Minor Loss Coefficents

$$K_{5,6} = \mathbf{K_{90deg,Elbow}} \left[RR \right]$$

Major Loss Friction Factor

$$u_{5,6} = \frac{\dot{V}_a}{\frac{\pi}{4} \cdot D_{5,6}^{\ 2}}$$

$$Re_{5,6} = \frac{\rho \cdot u_{3,4} \cdot D_{5,6}}{\mu}$$

$$f_{5,6} = \mathbf{MoodyChart} \left[Re_{5,6} , RR \right]$$

Modified Bernoulli

$$\Delta P_{5,6} = -\rho \cdot \left[f_{5,6} \cdot \frac{L_{5,6}}{D_{5,6}} + K_{5,6} \right] \cdot \frac{u_{5,6}^{\ 2}}{2} \cdot \left| 0.001 \cdot \frac{kPa}{Pa} \right|$$

Temperature Rise in Pipe 5-->6

Heat Transfered to fluid

$$q_{5,6} = -\Delta P_{5,6} \cdot \left| 1000 \cdot \frac{Pa}{kPa} \right| \cdot \dot{V}_a$$

Frist Law, Assuming adiabatic boundry

$$q_{5,6} = \dot{V}_a \cdot \rho \cdot cp \cdot \Delta T_{5,6}$$

$$T_6 = T_5 + \Delta T_{5,6}$$

Pressure at (6)

$$P_6 = P_5 + \Delta P_{5,6}$$

Pressure Drop Arcoss Pressure Regulator #2 6-->7

$$\Delta P_{6,7} = -\mathbf{PressureRegulator} \left[P_6 , P_{set,2} , \dot{V}_a \right]$$

$$P_{set,2} = 200 \cdot \left| 6.895 \cdot \frac{kPa}{lbf/in^2} \right|$$

Temperature Rise in Pressure Regulator 2

Heat Transfered to fluid

$$q_{6,7} = -\Delta P_{6,7} \cdot \left| 1000 \cdot \frac{Pa}{kPa} \right| \cdot \dot{V}_a$$

Frist Law, Assuming adiabatic boundry

$$q_{6,7} = \dot{V}_a \cdot \rho \cdot cp \cdot \Delta T_{6,7}$$

$$T_7 = T_6 + \Delta T_{6,7}$$

Pressure at (5)

$$P_7 = P_6 + \Delta P_{6,7}$$

Pressure Drop in Pipe 7-->8

Pipe DImensions

$$D_{7,8} = 1 \cdot \left| 0.0254 \cdot \frac{m}{in} \right|$$

$$L_{7,8} = 5 \cdot \left| 0.3048 \cdot \frac{m}{ft} \right|$$

$$\Delta Z_{7,8} = -1.5 \cdot \left| 0.3048 \cdot \frac{m}{ft} \right|$$

Minor Loss Coefficents

$$K_{7,8} = 2 \cdot \mathbf{K}_{\mathbf{90deg,Elbow}} \quad [RR]$$

Major Loss Friction Factor

$$u_{7,8} = \frac{\dot{V}_a}{\frac{\pi}{4} \cdot D_{7,8}^2}$$

$$Re_{7,8} = \frac{\rho \cdot u_{7,8} \cdot D_{7,8}}{\mu}$$

$$f_{7,8} = \mathbf{MoodyChart}\left[Re_{7,8}, RR\right]$$

Modified Bernoulli

$$\Delta P_{7,8} = -\rho \cdot \left[g \cdot \Delta Z_{7,8} + \left(f_{7,8} \cdot \frac{L_{7,8}}{D_{7,8}} + K_{7,8} \right) \cdot \frac{u_{7,8}^2}{2} \right] \cdot \left| 0.001 \cdot \frac{kPa}{Pa} \right|$$

Temperature Rise in Pipe 7-->8

Heat Transfered to fluid

$$q_{7,8} = -\Delta P_{7,8} \cdot \left| 1000 \cdot \frac{Pa}{kPa} \right| \cdot \dot{V}_a$$

Frist Law, Assuming adiabatic boundry

$$q_{7,8} = \dot{V}_a \cdot \rho \cdot cp \cdot \Delta T_{7,8}$$

$$T_8 = T_7 + \Delta T_{7,8}$$

Pressure at (8)

$$P_8 = P_7 + \Delta P_{7,8}$$

F39: Pressure Drop Across Heat Exchanger 8-->9

$$\Delta P_{8,9} = 4 \cdot 10^6 \cdot \dot{V}_a^{1.5909}$$

Temperature Drop Across Heat Exchanger

$$UA_{fouled} = 230 \quad [W/K]$$

$$\dot{C}_H = cp \cdot \dot{V}_a \cdot \rho$$

$$\dot{C}_C = 0.04497 \quad [m^2] \cdot u_{wind} \cdot \rho_{air} \cdot cp_{air}$$

$$C_{min} = \mathbf{Min}\left[\dot{C}_H, \dot{C}_C\right]$$

$$Ntu = \frac{UA_{fouled}}{C_{min}}$$

$$\varepsilon = \mathbf{HX}\left['crossflow_{both,unmixed}', Ntu, \dot{C}_H, \dot{C}_C, 'epsilon'\right]$$

$$\varepsilon = \frac{q_{8,9}}{C_{min} \cdot \left[T_{air} - T_8\right]}$$

$$q_{8,9} = \dot{C}_H \cdot \left[T_9 - T_8\right]$$

Pressure at (9)

$$P_9 = P_8 + \Delta P_{8,9}$$

Pressure Drop in Pipe 9-->10

Pipe Dimensions

$$D_{9,10} = 1 \cdot \left|0.0254 \cdot \frac{m}{in}\right|$$

$$L_{9,10} = 5 \cdot \left|0.3048 \cdot \frac{m}{ft}\right|$$

$$\Delta Z_{9,10} = 20 \cdot \left|0.0254 \cdot \frac{m}{in}\right|$$

Minor Loss Coefficents

$$K_{9,10} = \mathbf{K_{Tee,Branched}}\left[RR\right] + \mathbf{K_{90deg,Elbow}}\left[RR\right]$$

Major Loss Friction Factor

$$u_{9,10} = \frac{\dot{V}_a}{\frac{\pi}{4} \cdot D_{9,10}^{\,2}}$$

$$Re_{9,10} = \frac{\rho \cdot u_{9,10} \cdot D_{9,10}}{\mu}$$

$$f_{9,10} = \textbf{MoodyChart}\left[Re_{9,10}, RR\right]$$

Modified Bernoulli

$$\Delta P_{9,10} = -\rho \cdot \left[g \cdot \Delta Z_{9,10} + \left(f_{9,10} \cdot \frac{L_{9,10}}{D_{9,10}} + K_{9,10}\right) \cdot \frac{u_{9,10}^{\ 2}}{2}\right] \cdot \left|0.001 \cdot \frac{kPa}{Pa}\right|$$

Temperature Rise in Pipe 9-->10

Heat Transfered to fluid

$$q_{9,10} = -\Delta P_{9,10} \cdot \left|1000 \cdot \frac{Pa}{kPa}\right| \cdot \dot{V}_a$$

Frist Law, Assuming adiabatic boundry

$$q_{9,10} = \dot{V}_a \cdot \rho \cdot cp \cdot \Delta T_{9,10}$$

$$T_{10} = T_9 + \Delta T_{9,10}$$

Pressure at (10)

$$P_{10} = P_9 + \Delta P_{9,10}$$

Pressure Drop in Pipe 10-->11

Pipe DImensions

$$D_{10,11} = 3 / 8 \cdot \left|0.0254 \cdot \frac{m}{in}\right|$$

$$L_{10,11} = 20 \cdot \left|0.0254 \cdot \frac{m}{in}\right|$$

$$\Delta Z_{10,11} = 0$$

Minor Loss Coefficents

$$K_{10,11} = \mathbf{K_{SwingCheckValve}}\left[RR\right]$$

Major Loss Friction Factor

$$u_{10,11} = \frac{\dot{V}_a}{\frac{\pi}{4} \cdot D_{10,11}^{\ 2}}$$

$$Re_{10,11} = \frac{\rho \cdot u_{10,11} \cdot D_{10,11}}{\mu}$$

$$f_{10,11} = \textbf{MoodyChart}\left[Re_{10,11}, RR\right]$$

Modified Bernoulli

$$\Delta P_{10,11} = -\rho \cdot \left[g \cdot \Delta Z_{10,11} + \left(f_{10,11} \cdot \frac{L_{10,11}}{D_{10,11}} + K_{10,11} \right) \cdot \frac{u_{10,11}^{\ 2}}{2} \right] \cdot \left| 0.001 \cdot \frac{kPa}{Pa} \right|$$

Temperature Rise in Pipe 10-->11

Heat Transfered to fluid

$$q_{10,11} = -\Delta P_{10,11} \cdot \left| 1000 \cdot \frac{Pa}{kPa} \right| \cdot \dot{V}_{flush}$$

Frist Law, Assuming adiabatic boundry

$$q_{10,11} = \dot{V}_{flush} \cdot \rho \cdot cp \cdot \Delta T_{10,11}$$

$$T_{11} = T_{10} + \Delta T_{10,11}$$

Pressure at (11)

$$P_{11} = P_{10} + \Delta P_{10,11}$$

Pressure Drop in Case Flushing 11-->12

Effective Pipe DImensions

$$D_{11,12} = 3 / 8 \cdot \left| 0.0254 \cdot \frac{m}{in} \right|$$

$$L_{11,12} = 6 \cdot \left| 0.3048 \cdot \frac{m}{ft} \right|$$

$$\Delta Z_{11,12} = 0$$

Minor Loss Coefficents

$$K_{11,12} = 0$$

$$\dot{V}_{case} = \dot{V}_{flush} + \dot{V}_l$$ *Case Exiting flow*

Major Loss Friction Factor

$$u_{11,12} = \frac{\dot{V}_{case}}{\frac{\pi}{4} \cdot D_{11,12}^{\ 2}}$$

$$Re_{11,12} = \frac{\rho \cdot u_{11,12} \cdot D_{11,12}}{\mu}$$

$$f_{11,12} = \textbf{MoodyChart}\left[Re_{11,12} , RR \right]$$

Modified Bernoulli

$$\Delta P_{11,12} = -\rho \cdot \left[g \cdot \Delta Z_{11,12} + \left(f_{11,12} \cdot \frac{L_{11,12}}{D_{11,12}} + K_{11,12} \right) \cdot \frac{u_{11,12}^{\ 2}}{2} \right] \cdot \left| 0.001 \cdot \frac{kPa}{Pa} \right|$$

Temperature Rise in Case Flushing 11-->12

Heat Transfered to fluid

$$q_{11,12} = -\Delta P_{11,12} \cdot \left| 1000 \cdot \frac{Pa}{kPa} \right| \cdot \dot{V}_{case} + [1 - \eta_v] \cdot Power_{rotor}$$

Frist Law, Assuming adiabatic boundry

$$q_{11,12} = \dot{V}_{case} \cdot \rho \cdot cp \cdot \Delta T_{11,12}$$

$$T_{12} = T_{11} + \Delta T_{11,12}$$

Pressure at (12)

$$P_{12} = P_{11} + \Delta P_{11,12}$$

Pressure Drop in Pipe 12-->13

Pipe DImensions

$$D_{12,13} = 3 / 8 \cdot \left| 0.0254 \cdot \frac{m}{in} \right|$$

$$L_{12,13} = 6 \cdot \left| 0.0254 \cdot \frac{m}{in} \right|$$

$$\Delta Z_{12,13} = 0$$

Minor Loss Coefficents

$$K_{12,13} = \mathbf{K}_{SwingCheckValve} [RR] + \mathbf{K}_{Sharp,Edged,Pipe,Exit} ['LAMINAR']$$

Major Loss Friction Factor

$$u_{12,13} = \frac{\dot{V}_{case}}{\frac{\pi}{4} \cdot D_{12,13}^{2}}$$

$$Re_{12,13} = \frac{\rho \cdot u_{12,13} \cdot D_{12,13}}{\mu}$$

$$f_{12,13} = \mathbf{MoodyChart} [Re_{12,13} , RR]$$

Modified Bernoulli

$$\Delta P_{12,13} = -\rho \cdot \left[g \cdot \Delta Z_{12,13} + \left(f_{12,13} \cdot \frac{L_{12,13}}{D_{12,13}} + K_{12,13} \right) \cdot \frac{u_{12,13}^{2}}{2} \right] \cdot \left| 0.001 \cdot \frac{kPa}{Pa} \right|$$

Temperature Rise in Pipe 12->13

Heat Transfered to fluid

$$q_{12,13} = -\Delta P_{12,13} \cdot \left| 1000 \cdot \frac{Pa}{kPa} \right| \cdot \dot{V}_{case}$$

Frist Law, Assuming adiabatic boundry

$$q_{12,13} = \dot{V}_{case} \cdot \rho \cdot cp \cdot \Delta T_{12,13}$$

$$T_{13} = T_{12} + \Delta T_{12,13}$$

Pressure at (13)

$$P_{13} = P_{12} + \Delta P_{12,13}$$

Pressure Drop in Pipe 10-->14

Pipe DImensions

$$D_{10,14} = 3 \; / \; 8 \cdot \left| 0.0254 \cdot \frac{m}{in} \right|$$

$$L_{10,14} = 40 \cdot \left| 0.0254 \cdot \frac{m}{in} \right|$$ *pressure drop across filter facotored in as effective length*

$$\Delta Z_{10,14} = 0$$

Pressure Drop Across Needle Valve

$N_{knob,resevoir} = 0$ [-] *Number of Knob Turns, Ranges from 0-4.75(almost closed)*

$$K_{needle,resevoir} = -3.94 \cdot 10^{-8} \cdot N_{knob,resevoir} + 1.89 \cdot 10^{-7}$$

$$\dot{V}_{resevoir} = K_{needle,resevoir} \cdot \left[-\Delta P_{resevoir} \cdot \left| 1000 \cdot \frac{Pa}{kPa} \right| \right]^{0.5}$$

Major Loss Friction Factor

$$u_{10,14} = \frac{\dot{V}_a}{\frac{\pi}{4} \cdot D_{10,14}^{\;2}}$$

$$Re_{10,14} = \frac{\rho \cdot u_{10,14} \cdot D_{10,14}}{\mu}$$

$$f_{10,14} = \textbf{MoodyChart}\left[Re_{10,14} \; , \; RR \right]$$

Modified Bernoulli

$$\Delta P_{10,14} = -\rho \cdot \left[g \cdot \Delta Z_{10,14} + f_{10,14} \cdot \frac{L_{10,14}}{D_{10,14}} \cdot \frac{u_{10,14}^{\;2}}{2} \right] \cdot \left| 0.001 \cdot \frac{kPa}{Pa} \right| + \Delta P_{resevoir}$$

$\dot{V}_{resevoir} = \dot{V}_a - \dot{V}_{flush}$ *Flow to Resevoir*

Temperature Rise in Pipe 10-->14

Heat Transfered to fluid

$$q_{10,14} = -\Delta P_{10,14} \cdot \left| 1000 \cdot \frac{Pa}{kPa} \right| \cdot \dot{V}_{resevoir}$$

Frist Law, Assuming adiabatic boundry

$$q_{10,14} = \dot{V}_{resevoir} \cdot \rho \cdot cp \cdot \Delta T_{10,14}$$

$$T_{14} = T_{10} + \Delta T_{10,14}$$

Pressure at (14)

$$P_{14} = P_{10} + \Delta P_{10,14}$$

Pressure in Resevoir

Make resevoir vented

$$P_{13} = P_{15}$$

$$P_{14} = P_{15}$$

$$P_{15} = P_{air}$$

Temperature in Resevoir

$$T_{15} = \frac{T_{14} \cdot \dot{V}_{resevoir} + T_{13} \cdot \dot{V}_{case}}{\dot{V}_t}$$

Pressure Drop in Pipe 15-->16

Pipe DImensions

$$D_{15,16} = 1 \cdot \left| 0.0254 \cdot \frac{m}{in} \right|$$

$$L_{15,16} = 20 \cdot \left| 0.0254 \cdot \frac{m}{in} \right|$$

$$\Delta Z_{15,16} = 0$$

Minor Loss Coefficents

$$K_{15,16} = \mathbf{K}_{Sharp,Edged,Pipe,Inlet} \left[D_{15,16} \right]$$

Major Loss Friction Factor

$$u_{15,16} = \frac{\dot{V}_t}{\frac{\pi}{4} \cdot D_{15,16}^{\ 2}}$$

$$Re_{15,16} = \frac{\rho \cdot u_{15,16} \cdot D_{15,16}}{\mu}$$

$$f_{15,16} = \mathbf{MoodyChart} \left[Re_{15,16} , RR \right]$$

Modified Bernoulli

$$\Delta P_{15,16} = -\rho \cdot \left[g \cdot \Delta Z_{15,16} + \left(f_{15,16} \cdot \frac{L_{15,16}}{D_{15,16}} + K_{15,16} \right) \cdot \frac{u_{15,16}^{2}}{2} \right] \cdot \left| 0.001 \cdot \frac{kPa}{Pa} \right|$$

Temperature Rise in Pipe 15->16

Heat Transfered to fluid

$$q_{15,16} = -\Delta P_{15,16} \cdot \left| 1000 \cdot \frac{Pa}{kPa} \right| \cdot \dot{V}_t$$

Frist Law, Assuming adiabatic boundry

$$q_{15,16} = \dot{V}_t \cdot \rho \cdot cp \cdot \Delta T_{15,16}$$

$$T_{16} = T_{15} + \Delta T_{15,16}$$

Pressure at (16)

$$P_{16} = P_{15} + \Delta P_{15,16}$$

Lookup Table: Fully Open Pressure Regulator

	FlowRate [m³/s]	PressureDrop [kPa]
Row 1	0.00001035	16.82
Row 2	0.00009057	39.24
Row 3	0.0001604	33.63
Row 4	0.0002303	50.45
Row 5	0.0003286	84.09
Row 6	0.0004502	157
Row 7	0.0005537	224.2
Row 8	0.0006676	302.7
Row 9	0.0007892	364.4
Row 10	0.0009212	465.3
Row 11	0.001045	577.4
Row 12	0.001162	706.3
Row 13	0.001281	868.9
Row 14	0.001402	1076
Row 15	0.001503	1244
Row 16	0.001599	1441
Row 17	0.001679	1592
Row 18	0.001749	1743
Row 19	0.001811	1861
Row 20	0.001871	2001
Row 21	0.00192	2091

Appendix E: Thermal-Hydraulic Dynamometer Bill of Materials

Bill of Materials

REF	Item	QTY	Description	Manufacturer/Vendor	Item Number	Cost	Total Cost
1	Code 62 Captive Flange (1.25)	2	Code 62 Captive Flange. Attaches to pump. Flange size = 1.25	Discount Hydraulic Hose	62SF-KIT-20	$19.29	$38.58
2	90° Flange Elbow	2	Code 62 1.25 Flange to 1" ID Tube.	Discount Hydraulic Hose	C6290-16-20W	$40.53	$81.06
			Drain				
3	Drain male	2	M22-1.5. Male hook up to drain ports. 3/8 hose.	Discount Hydraulic Hose	MDH-06-14-22	$7.59	$15.18
			Needle Valve				
4	Needle Valve Cartridge	1	Simple Needle Valve	Sun Hydraulics	NFCD	$28.60	$28.60
5	Needle Valve manifold	1	GADS. Steel manifold. 3/4" NPTF Ports	Sun Hydraulics	GADS	$54.90	$54.90
6	3/4" NPTF Fitting	2	MPX-12-12W. Male 3/4" NPTF swivel fitting. 3/4" Hose.	Discount Hydraulic Hose	MPX-12-12W	$9.94	$19.88
			Pressure Reducing 1				
7	Pressure Reducing Valve (Fixed)	1	PRFRLAN. Pressure reduction adjustment range: 750-3000 psi.	Sun Hydraulics	PRFRLAN	$101.80	$101.80
8	Pressure Reducing Valve Cartridge	1	BCDS. 3/4" NPTF.	Sun Hydraulics	BCDS	$75.70	$75.70
9	3/4" NPTF Fitting	1	MPX-12-12W. Male 3/4" NPTF swivel fitting. 3/4" Hose.	Discount Hydraulic Hose	MPX-12-12W	$9.94	$9.94
10	3/4" NPTF 90 Fitting	1	MPX90-12-12W. Male 3/4" NPTF 90 Swivel fitting. 3/4" Hose.	Discount Hydraulic Hose	MPX90-12-12W	$29.70	$29.70
11	1/4" NPTF Fitting for Port 3	1	MPX90-06-04. 1/4" NPTF Male 90 fitting swivel for port 3.	Discount Hydraulic Hose	MPX90-06-04	$9.47	$9.47
			Pressure Reducing 2				
12	Pressure Reducing Valve	1	PRFRLSN	sun Hydraulics	PRFRLSN	$104.80	$104.80
13	Pressure Reducing Valve Cartridge	1	BCDS. 3/4" NPTF.	Sun Hydraulics	BCDS	$75.70	$75.70
14	3/4" NPTF Fitting	1	MPX-12-12W. Male 3/4" NPTF swivel fitting. 3/4" Hose.	Discount Hydraulic Hose	MPX-12-12W	$9.94	$9.94
15	3/4" NPTF 90 Fitting	1	MPX90-12-12W. Male 3/4" NPTF 90 Swivel fitting. 3/4" Hose.	Discount Hydraulic Hose	MPX90-12-12W	$29.70	$29.70
16	1/4" NPTF Fitting for Port 3	1	MPX-06-04. 1/4" NPTF Male fitting for port 3.	Discount Hydraulic Hose	MPX-06-04	$4.26	$4.26
			Pressure Transducer				
24	Pressure Transducer	2	1/4" NPT male connection	AST	AST 4100	$230.00	$460.00
			Heat Exchanger				
25	Heat Exchanger	1	C-18 w/ Bypass	Grainger	4UJD7	$332.00	$332.00
26	ORB #16 Fitting to JIC elbow	2	#16 SAE to 1" JIC Male 90	Discount Hydraulic Hose	6801-16-16	$7.80	$15.60
27	JIC Female Fitting	2	1" Swivel Female JIC Fitting	Discount Hydraulic Hose	FJX-16-16W	$15.67	$31.34
			Flushing				
28	1" NPT T Female	1	1" Tee leads to flushing or reservoir from heat exchanger	Discount Hydraulic Hose	5605-16-16-16	$10.31	$10.31
29	1" NPTF Fitting T inlet	1	1" NPTF swivel Fitting for 1" Hose	Discount Hydraulic Hose	MPX-16-16W	$15.10	$15.10
30	1" to 3/8" NPTF reducer	2	1" M NPTF to 3/8" F NPTF reducer	Discount Hydraulic Hose	SS-5406-16-06	$28.78	$57.56
31	3/8" NPTF Swivel fitting	2	3/8" Male NPTF Swivel fitting	Discount Hydraulic Hose	MPX-06-06	$3.76	$7.52
32	NEEDLE	1	3/8 NPTF FEMALE. 5000 PSI	MCMASTER	7824K23	$40.02	$40.02
33	3/8" NPTF MALE Nipple	2	3/8" Male NPTF Nipple	Discount Hydraulic Hose	6/6/5404	$0.97	$1.94
			Relief 1				
34	5000 psi relief for after pump	1	5000 psi direct relief valve. 2 ports.	Sun Hydraulics	RDDALCN	$47.00	$47.00
35	5000 psi manifold	1	Steel relief manifold 3/4" NPTF with .25 NPTF gauge port.	Sun Hydraulics	FEDS	$71.20	$71.20
36	3/4 NPTF Male Fittings	1	3/4 NPTF male fittings	Discount Hydraulic Hose	MP-16-12W	$14.33	$14.33
37	Swivel Joint	1	3/4" swivel joint	Discount Hydraulic Hose	S8-PF12-P12	$36.60	$36.60
38	3/4 NPTF Swivel	2	3/4" NPTF Male Swivel	Discount Hydraulic Hose	MPX-12-12w	$9.94	$19.88
			Relief 2				
39	100-400 psi relief before heat x	1	400 psi direct relief valve. 2 ports.	Sun Hydraulics	RDDALEN	$46.00	$46.00
40	3000 psi manifold	1	Aluminum relief manifold 3/4" NPTF with .25 NPTF gauge port.	Sun Hydraulics	FED	$38.80	$38.80
41	3/4 NPTF Male Fittings	1	3/4 NPTF male fittings	Discount Hydraulic Hose	MP-16-12W	$14.33	$14.33
42	Swivel Joint	1	3/4" swivel joint	Discount Hydraulic Hose	S8-PF12-P12	$36.60	$36.60
43	3/4 NPTF Swivel for Relief	1	3/4" NPTF Male Swivel	Discount Hydraulic Hose	MPX-12-12w	$9.94	$9.94
44	3/4" NPTF Fitting	1	MPX-12-12W. Male 3/4" NPTF swivel fitting. 3/4" Hose.	Discount Hydraulic Hose	MPX-12-12W	$9.94	$9.94
			Tank (ALUMINUM)				
45	PR 1 IN BUNG	1	1/4" NPTF	METAL TANKS	260-0001	$3.00	$3.00
46		1	MPX-06-04. 1/4" NPTF Male fitting.	Discount Hydraulic Hose	MPX-06-04	$4.26	$4.26
47	PR2 IN	1	1/4" NPTF	METAL TANKS	260-0001	$3.00	$3.00
48		1	MPX-06-04. 1/4" NPTF Male fitting.	Discount Hydraulic Hose	MPX-06-04	$4.26	$4.26
49	TO PUMP	1	1" NPTF	METAL TANKS	260-0007	$5.00	$5.00
50		1	1" NPTF Male Swivel	Discount Hydraulic Hose	MPX-16-16w	$15.10	$15.10
51	FROM FLUSH	1	3/8" NPTF	METAL TANKS	260-0003	$4.00	$4.00
52		1	3/8" Male NPTF Swivel fitting	Discount Hydraulic Hose	MPX-06-06	$3.76	$3.76
53	RELIEF 1	1	3/4" NPTF	METAL TANKS	260-0006	$5.00	$5.00
54		1	3/4" NPTF Male Swivel	Discount Hydraulic Hose	MPX-12-12w	$9.94	$9.94
55	RELIEF 2	1	3/4" NPTF	METAL TANKS	260-0006	$5.00	$5.00
56		1	3/4" NPTF Male Swivel	Discount Hydraulic Hose	MPX-12-12w	$9.94	$9.94
64	Drain	1	3/8" NPTF	METAL TANKS	260-0003	$4.00	$4.00
65		1	3/8" Male NPTF Swivel fitting	Discount Hydraulic Hose	MPX-06-06	$3.76	$3.76
57	FILLER CAP	1	FILLER CAP+BUNG. VENTED	BUNG KING	VFCBAL	$28.75	$28.75
58	TANK MOUNTS	4	3/8" BLIND TANK BUNGS	BUNG KING	BTB38CAL	$4.00	$16.00
			FILTER				
59	FILTER	1	3/4" NPTF. Inline.	MCMASTER	4453K12	$42.21	$42.21
60	HEAT X to Filter	2	1" NPTF swivel Fitting for 1" Hose	Discount Hydraulic Hose	MPX-16-16W	$15.10	$30.20
			Raw Materials				
	Tank	1	24" x 36" 0.125 thick 6061	Online Metals		$71.55	$71.55
	RBP Mount + RBP + HX Mount	1	12" x 24" 0.25" thick 6061	Online Metals		$59.65	$59.65
						PARTS TOTAL:	**$2,333.60**
						HOSE TOTAL:	**$279.50**
						GRAND TOTAL:	**$2,613.10**

Appendix F: Final Design Drawings and Assemblies

Final Design Drawings:

Pump:

Drawings of Rexroth A6VM-250 acquired from Bosch-Rexroth. The control system installed for this pump is Rexroth's EP2 electrical control system which will not be implemented at the present. The drive shaft is the splined option shown below.

Dimensions size 250

Before finalizing your design, request a binding installation drawing. Dimensions in mm.

HD1, HD2 – Proportional control hydraulic

HZ – Two-point control hydraulic

Port plate 02 – SAE flange ports A and B at side, opposite

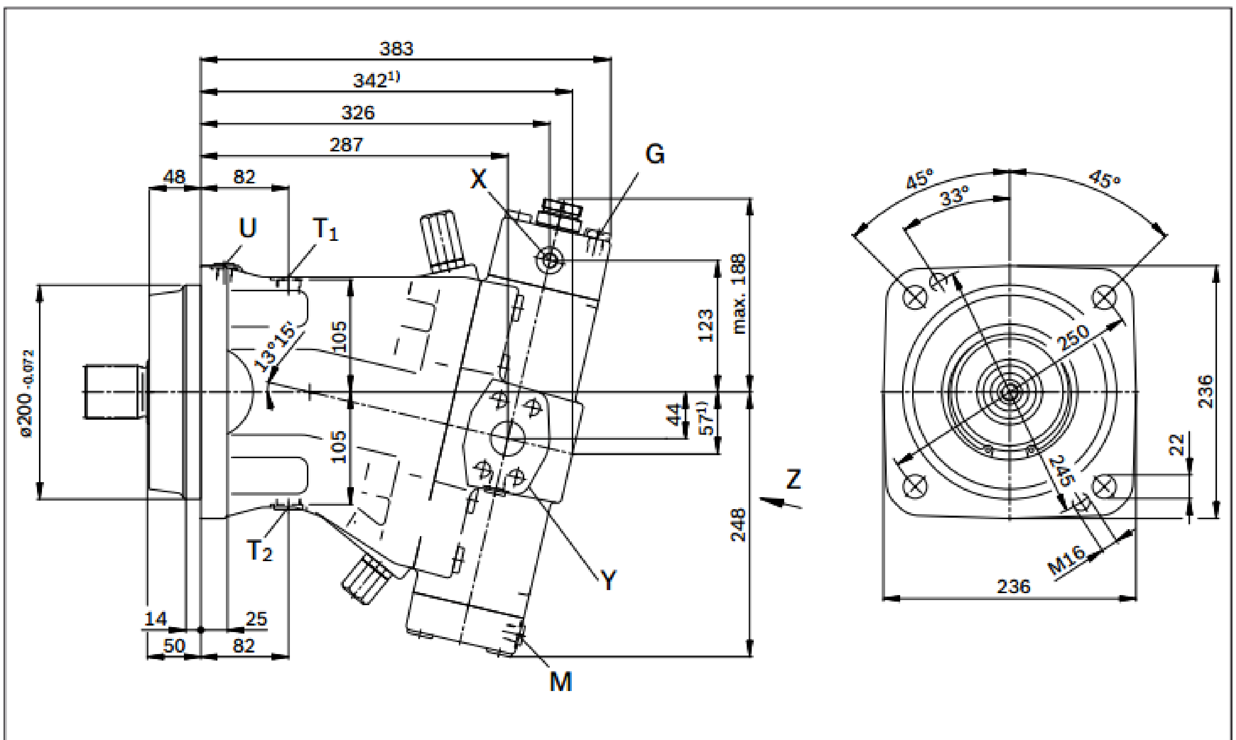

1) Port plate 01/15 – SAE flange ports A and B at rear

Drive shafts

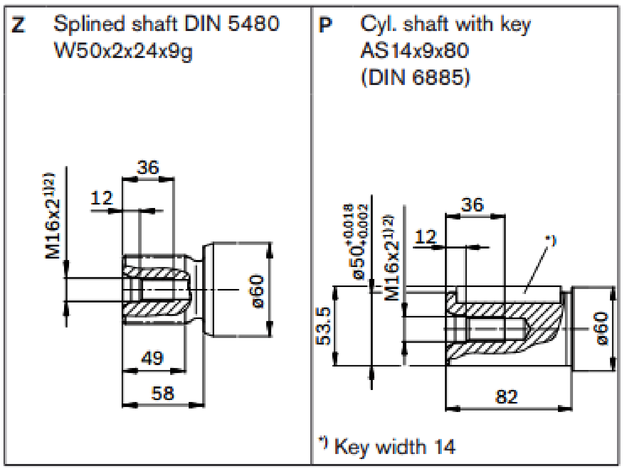

Service line port (detail Y)

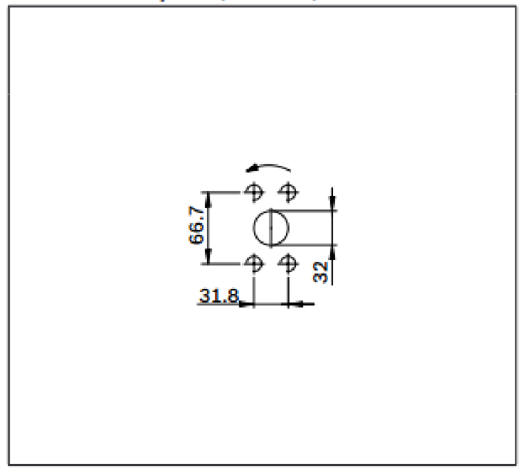

1) Observe the general instructions on page 80 for the maximum tightening torques.

2) Center bore according to DIN 332 (thread according to DIN 13)

Location of the service line ports on the port plates (view Z)

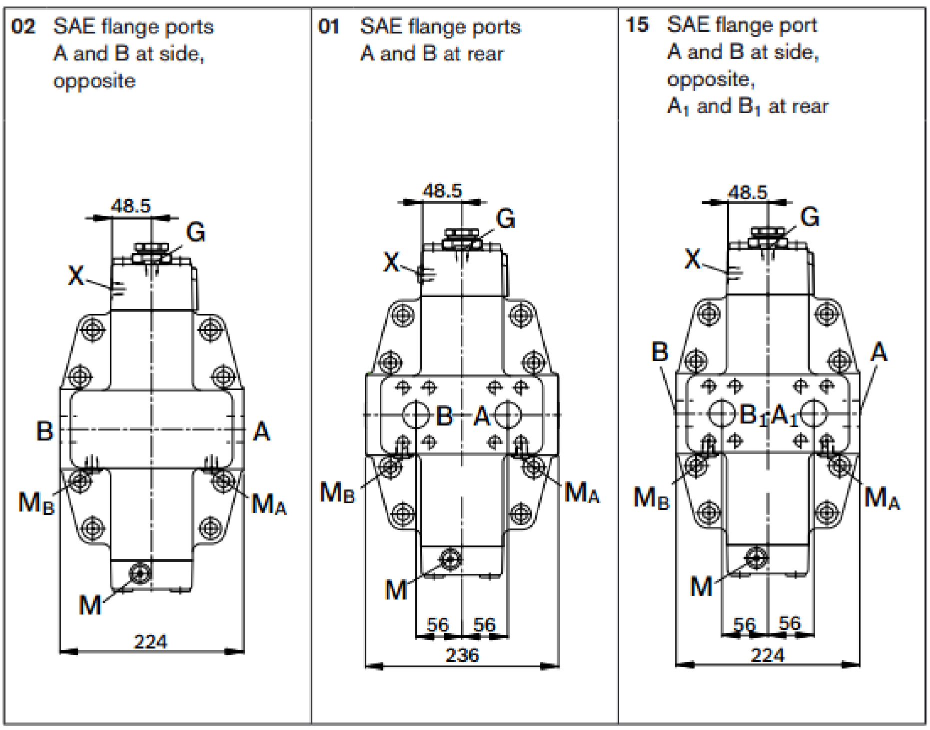

Ports

Designation	Port for	Standard	Size[1]	Maximum pressure [bar][2]	State[6]
A, B	Service line Fastening thread A/B	SAE J518[3] DIN 13	1 1/4 in M14 x 2; 19 deep	400	O
A_1, B_1	Additional service line for plate 15 Fastening thread A_1/B_1	SAE J518[3] DIN 13	1 1/4 in M14 x 2; 19 deep	400	O
T_1	Drain line	DIN 3852[5]	M22 x 1.5; 14 deep	3	X[4]
T_2	Drain line	DIN 3852[5]	M22 x 1.5; 14 deep	3	O[4]
G	Synchronous control	DIN 3852[5]	M14 x 1.5; 12 deep	400	X
G_2	2nd pressure setting (HD.D, EP.D)	DIN 3852[5]	M14 x 1.5; 12 deep	400	X
P	Pilot oil supply (EP)	DIN 3852[5]	M14 x 1.5; 12 deep	100	O
U	Bearing flushing	DIN 3852[5]	M14 x 1.5; 12 deep	3	X
X	Pilot signal (HD, HZ, HA1T/HA2T)	DIN 3852[5]	M14 x 1.5; 12 deep	100	O
X	Pilot signal (HA1 and HA2)	DIN 3852[5]	M14 x 1.5; 12 deep	3	X
X_1, X_2	Pilot signal (DA)	DIN 2353-CL	8B-ST	40	O
X_3	Remote control valve (HD.G, EP.G)	DIN 3852[5]	M14 x 1.5; 12 deep	400	O
M	Measuring stroking chamber	DIN 3852[5]	M14 x 1.5; 12 deep	400	X
M_A, M_B	Measuring pressure A/B	DIN 3852[5]	M14 x 1.5; 12 deep	400	X
M_{St}	Measuring pilot pressure	DIN 3852[5]	M14 x 1.5; 12 deep	400	X

1) Observe the general instructions on page 80 for the maximum tightening torques.
2) Momentary pressure spikes may occur depending on the application. Keep this in mind when selecting measuring devices and fittings.
3) Only dimensions according to SAE J518, metric fastening thread is a deviation from standard.
4) Depending on installation position, T_1 or T_2 must be connected (see also installation instructions on page 79).
5) The spot face can be deeper than specified in the appropriate standard.
6) O = Must be connected (plugged on delivery)
X = Plugged (in normal operation)

Valves:

All Sun Hydraulic dimensions and specifications are found on their site.

Load Bearing Needle Valve: Sun Hydraulic NFCD Needle Valve w/ GADS Manifold

NFCD Needle Valve Dimensions and Specifications:

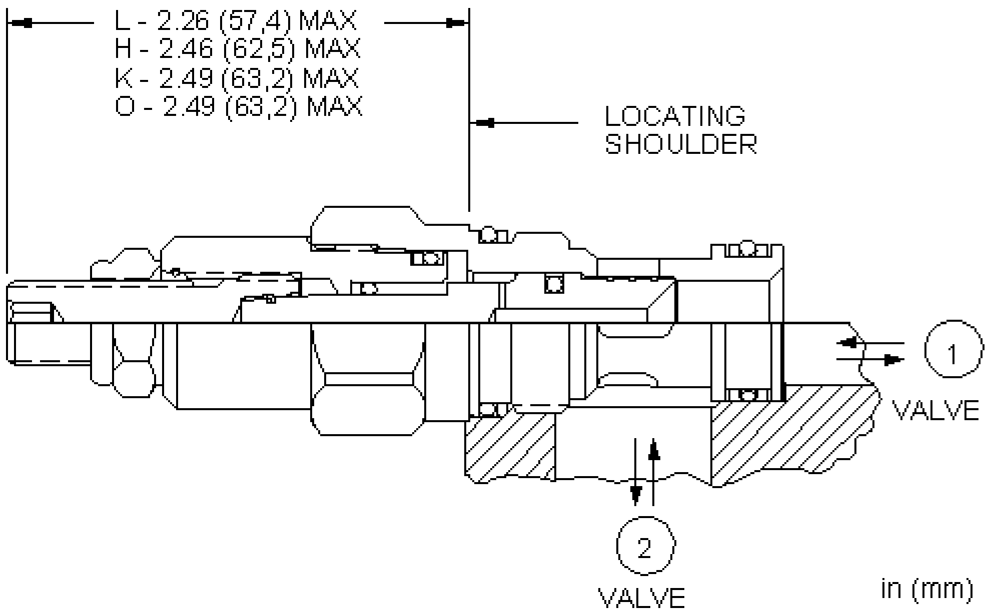

Cavity	T-13A
Series	1
Capacity	20 gpm (.33 inch)
Maximum Operating Pressure	5000 psi
Adjustment - Number of Counterclockwise Turns - Fully Closed to Fully Open	5
Valve Hex Size	7/8 in.
Valve Installation Torque	30 - 35 lbf ft
Adjustment Screw Internal Hex Size	5/32 in.
Locknut Hex Size	9/16 in.
Locknut Torque	80 - 90 lbf in.
Model Weight	0.32 lb.
Seal kit - Cartridge	Buna: 990-010-007

GAD Manifold Dimensions and Specifications:

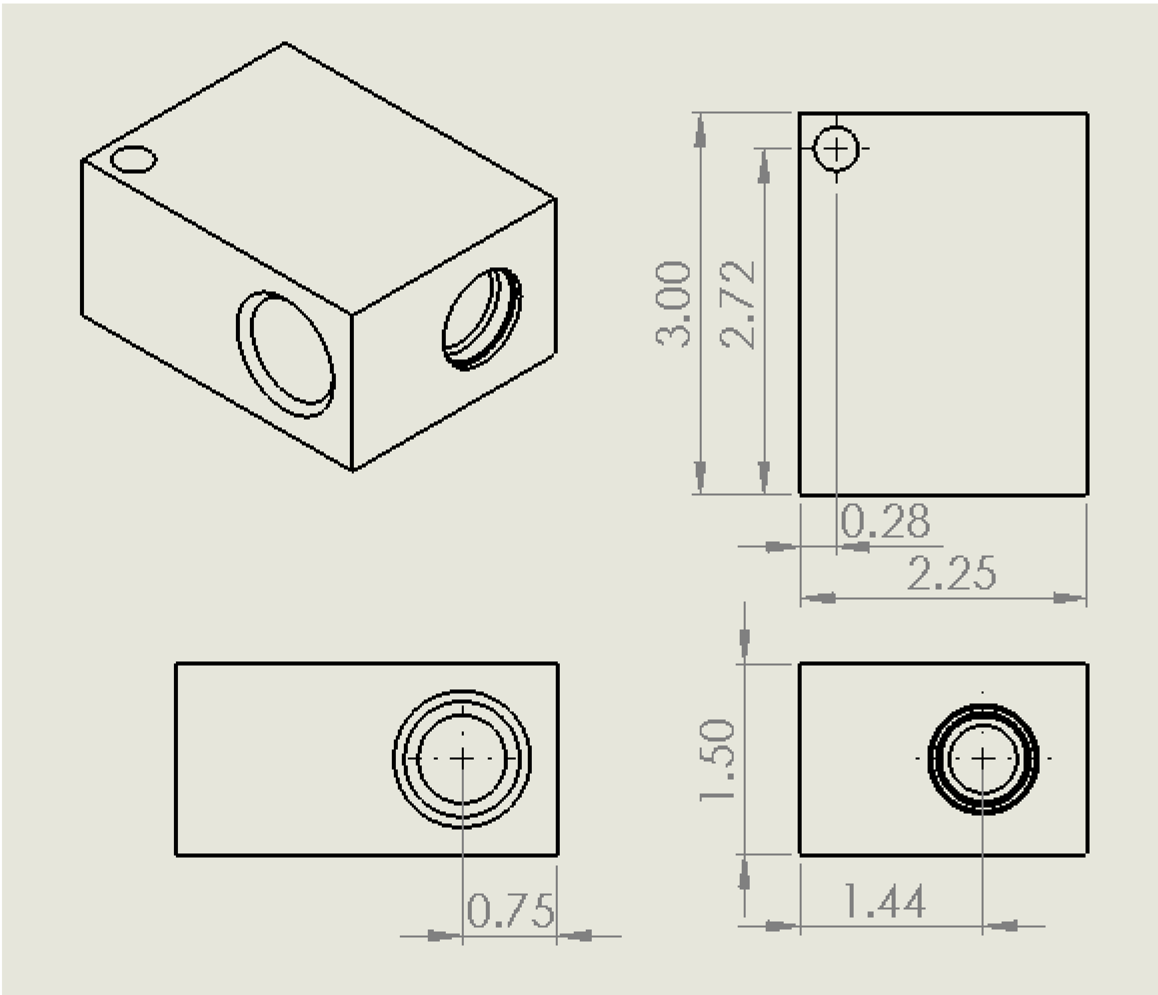

Modifiers	Ports
GAD	All Ports: 3/4" NPTF;

Body Type	Line mount
Interface	None
Body Features	Ninety degree
Mounting Hole Diameter	.34 in.
Mounting Hole Depth	Through
Mounting Hole Quantity	1
Open Cavities	1
Cavity	T-13A
Port Size	3/4" NPTF
Model Weight	0.77 lb.

Pressure Reducing Valve #1: Sun Hydraulic PRFRLAN w/ BCDS Manifold

PRFRLAN Pressure Reducing Valve Dimensions and Specifications:

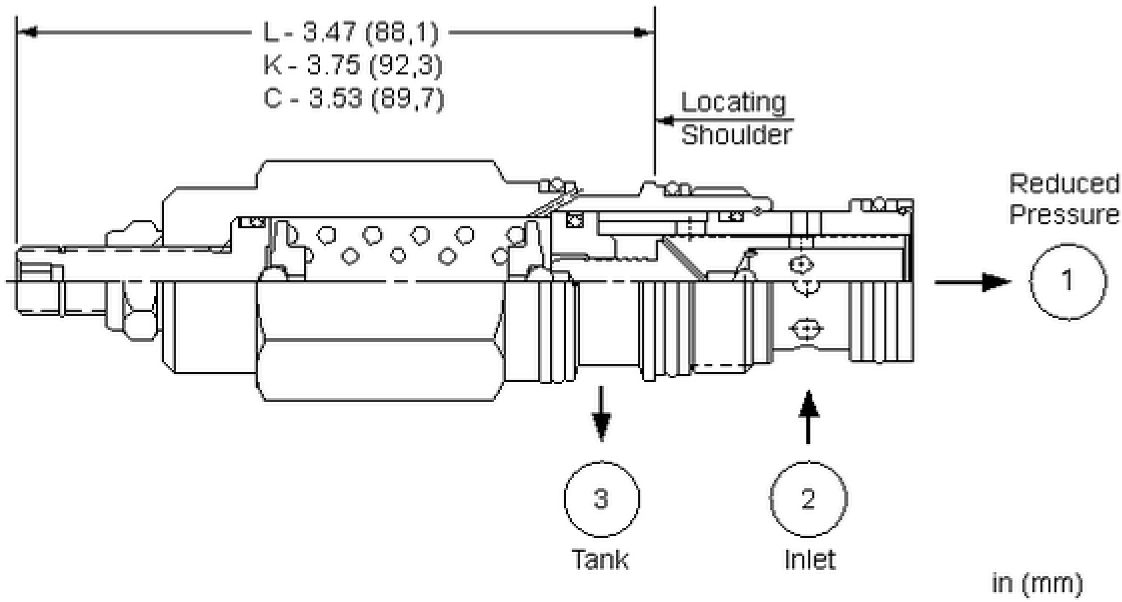

Cavity	T-2A
Series	2
Capacity	20 gpm
Factory Pressure Settings Established at	2 in^3/min.
Maximum Operating Pressure	5000 psi
Maximum Valve Leakage at 110 SUS (24 cSt)	3 in^3/min.
Adjustment - Number of Clockwise Turns to Increase Setting	5
Valve Hex Size	1 1/8 in.
Valve Installation Torque	45 - 50 lbf ft
Adjustment Screw Internal Hex Size	5/32 in.
Locknut Hex Size	9/16 in.
Locknut Torque	80 - 90 lbf in.
Model Weight	0.79 lb.
Seal kit - Cartridge	Buna: 990-202-007

BCDS Manifold Dimensions and Specifications:

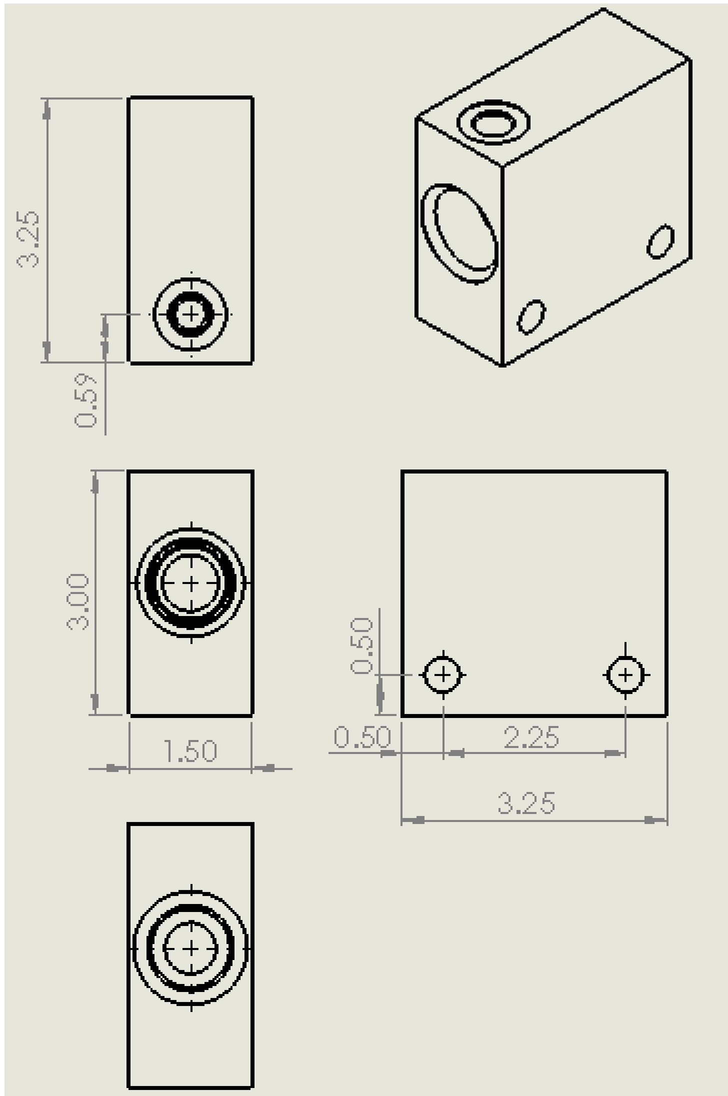

Modifiers	Ports
BCD	Ports 1 & 2: 3/4" NPTF; Port 3: 1/4" NPTF;

Body Type	Line mount
Interface	None
Body Features	Ninety degree
Mounting Hole Diameter	.42 in.
Mounting Hole Depth	Through
Mounting Hole Quantity	2
Open Cavities	1
Cavity	T-2A
Port Size	3/4" NPTF
Model Weight	2.94 lb.

Pressure Reducing Valve #2: Sun Hydraulic PRFRLSN w/ BCDS Manifold

PRFRLSN Pressure Reducing Valve Dimensions and Specifications:

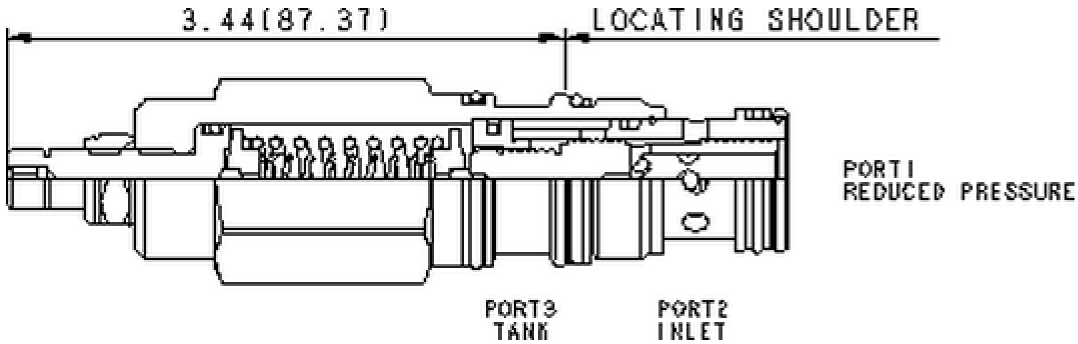

Cavity	T-2A
Series	2
Capacity	20 gpm
Factory Pressure Settings Established at	2 in³/min.
Maximum Operating Pressure	5000 psi
Maximum Valve Leakage at 110 SUS (24 cSt)	3 in³/min.
Adjustment - Number of Clockwise Turns to Increase Setting	5
Valve Hex Size	1 1/8 in.
Valve Installation Torque	45 - 50 lbf ft
Adjustment Screw Internal Hex Size	5/32 in.
Locknut Hex Size	9/16 in.
Locknut Torque	80 - 90 lbf in.
Model Weight	0.76 lb.
Seal kit - Cartridge	Buna: 990-202-007

Pressure Relief Valve #1: Sun Hydraulic RDDALCN w/ FEDS Manifold

RDDALCN Pressure Relief Valve Dimensions and Specifications:

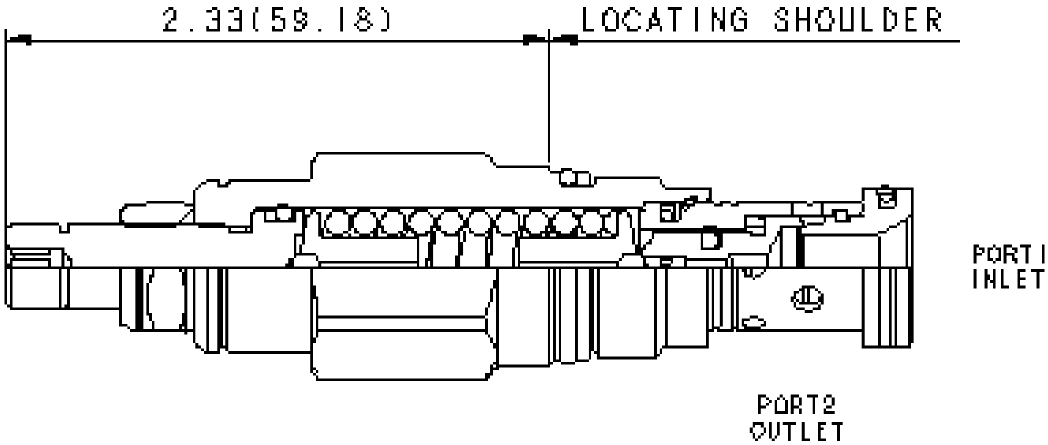

Cavity	T-10A
Series	1
Capacity	25 gpm
Factory Pressure Settings Established at	4 gpm
Maximum Operating Pressure	5000 psi
Response Time - Typical	2 ms
Maximum Valve Leakage at Reseat	10 drops/min.
Reseat	>90% of setting
Adjustment - Number of Clockwise Turns to Increase Setting	6
Valve Hex Size	7/8 in.
Valve Installation Torque	30 - 35 lbf ft
Adjustment Screw Internal Hex Size	5/32 in.
Locknut Hex Size	9/16 in.
Locknut Torque	80 - 90 lbf in.
Model Weight	0.37 lb.
Seal kit - Cartridge	Buna: 990-310-007

FEDS Manifold Dimensions and Specifications:

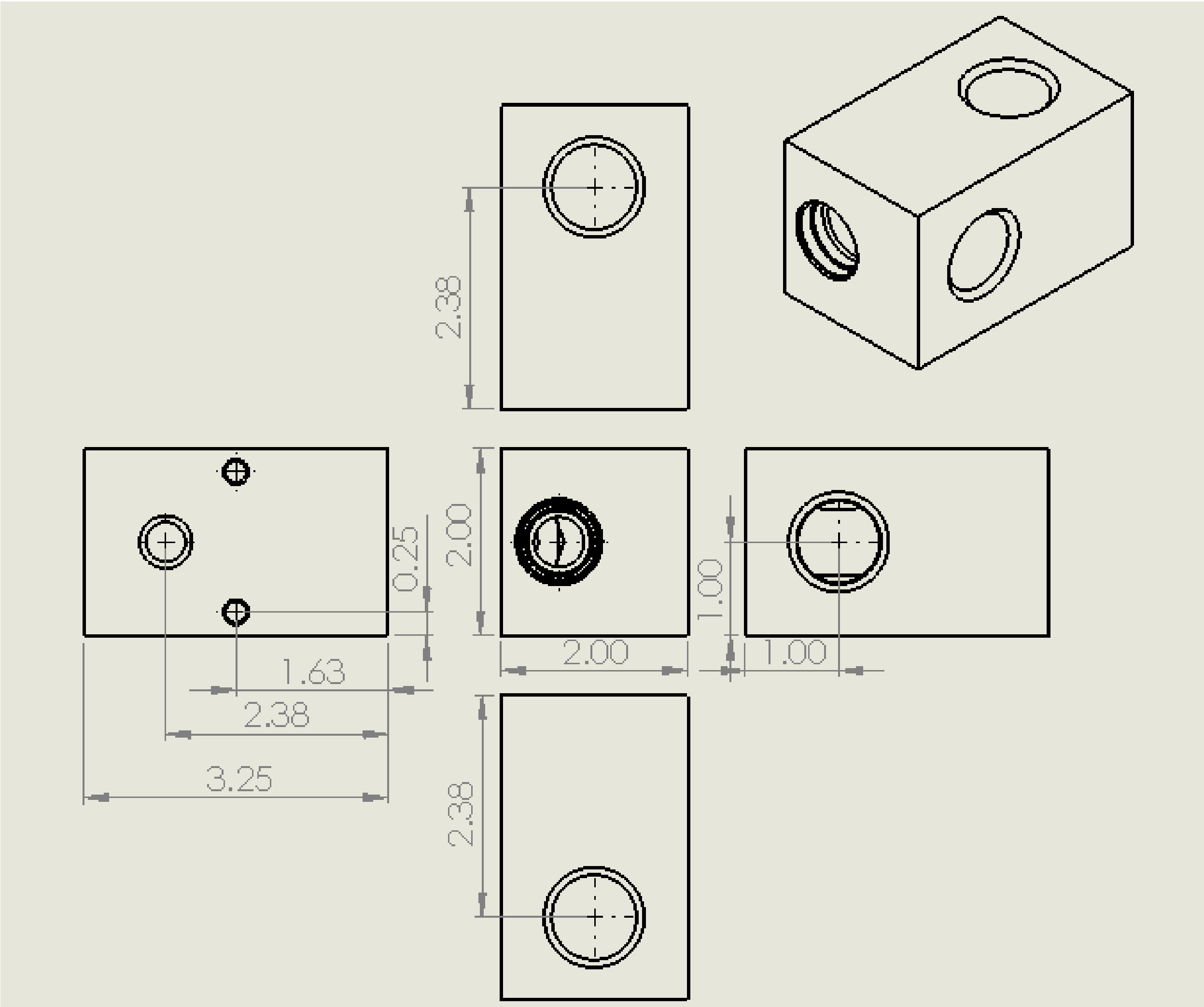

Modifiers	Ports
FED	Ports 1 & 2: 3/4" NPTF; Gage Port: 1/4" NPTF;

Body Type	Line mount
Interface	None
Body Features	Through port with gauge port
Mounting Hole Thread	.250-20 UNC - 2B in.
Mounting Hole Depth	.50 in.
Mounting Hole Quantity	2
Open Cavities	1
Cavity	T-10A
Port Size	3/4" NPTF
Model Weight	2.55 lb.

Pressure Relief Valve #2: Sun Hydraulic RDDALEN w/ FED Manifold

RDDALEN Pressure Relief Valve Dimensions and Specifications:

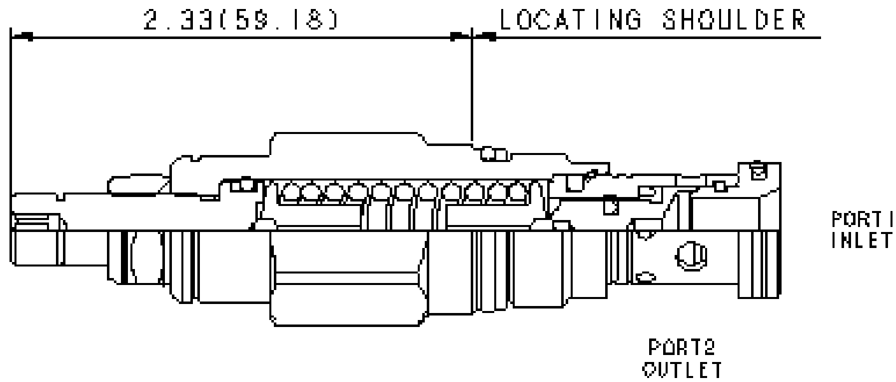

Cavity	T-10A
Series	1
Capacity	25 gpm
Factory Pressure Settings Established at	4 gpm
Maximum Operating Pressure	5000 psi
Response Time - Typical	2 ms
Maximum Valve Leakage at Reseat	10 drops/min.
Reseat	>90% of setting
Adjustment - Number of Clockwise Turns to Increase Setting	6
Valve Hex Size	7/8 in.
Valve Installation Torque	30 - 35 lbf ft
Adjustment Screw Internal Hex Size	5/32 in.
Locknut Hex Size	9/16 in.
Locknut Torque	80 - 90 lbf in.
Model Weight	0.36 lb.
Seal kit - Cartridge	Buna: 990-310-007

Hydraulic Hoses:

Hydraulax EN 856 4SH 1" and ¾" Hoses

Hose Number	Inside Diameter	Outside Diameter	Maximum Working Pressure (MWP)	Minimum Burst Pressure	Minimum Bend Radius
4SH-12	3/4"	1.21"	6,095	24,380	9.5"
4SH-16	**1"**	**1.50"**	**5,515**	**22,060**	**12"**
4SH-20	1-1/4"	1.85"	5,000	20,000	16.5"
4SH-24	1-1/2"	2.11"	4,200	16,800	20"
4SH-32	2"	2.63"	3,625	14,500	25"

Hydraulax SAE 100R1AT ⅜" Hoses

Hose Number	Inside Diameter	Outside Diameter	Maximum Working Pressure (MWP)	Minimum Burst Pressure	Minimum Bend Radius
R1-04	1/4"	0.53"	2,750 psi	11,000 psi	4"
R1-06	**3/8"**	**0.69"**	**2,250 psi**	**9,000 psi**	**5"**
R1-08	1/2"	0.82"	2,000 psi	8,000 psi	7"
R1-10	5/8"	0.94"	1,500 psi	6,000 psi	8"
R1-12	3/4"	1.10"	1,250 psi	5,000 psi	9.5"
R1-16	1"	1.41"	1,000 psi	4,000 psi	12"

Brackets:

Pump Mounting Bracket

Pump Mounting Bracket made from ¼" Steel.

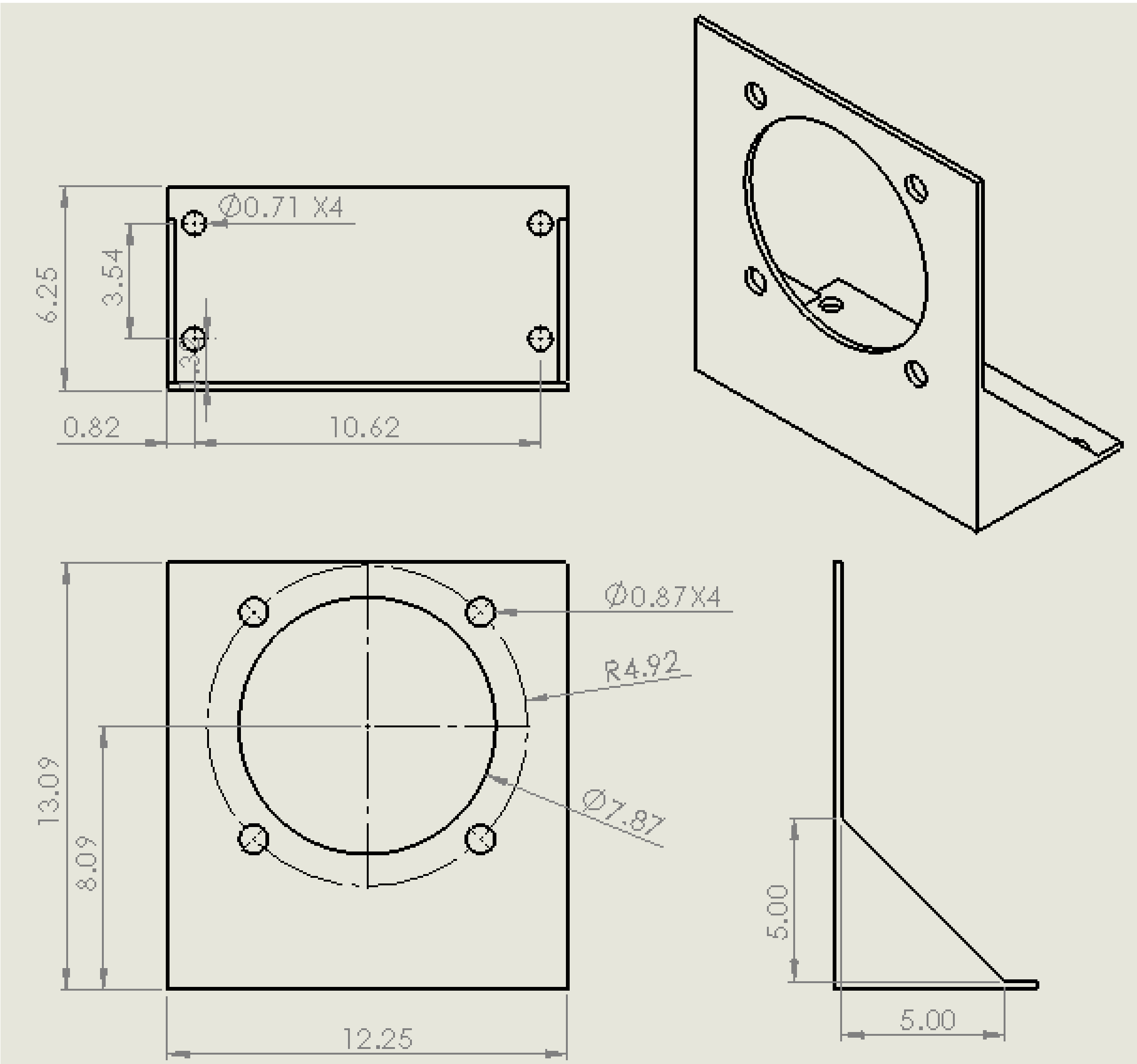

Rear Bird Plate Mounting Brackets

Rear Bird Plate Mounts made from ¼" 6061 Aluminum.

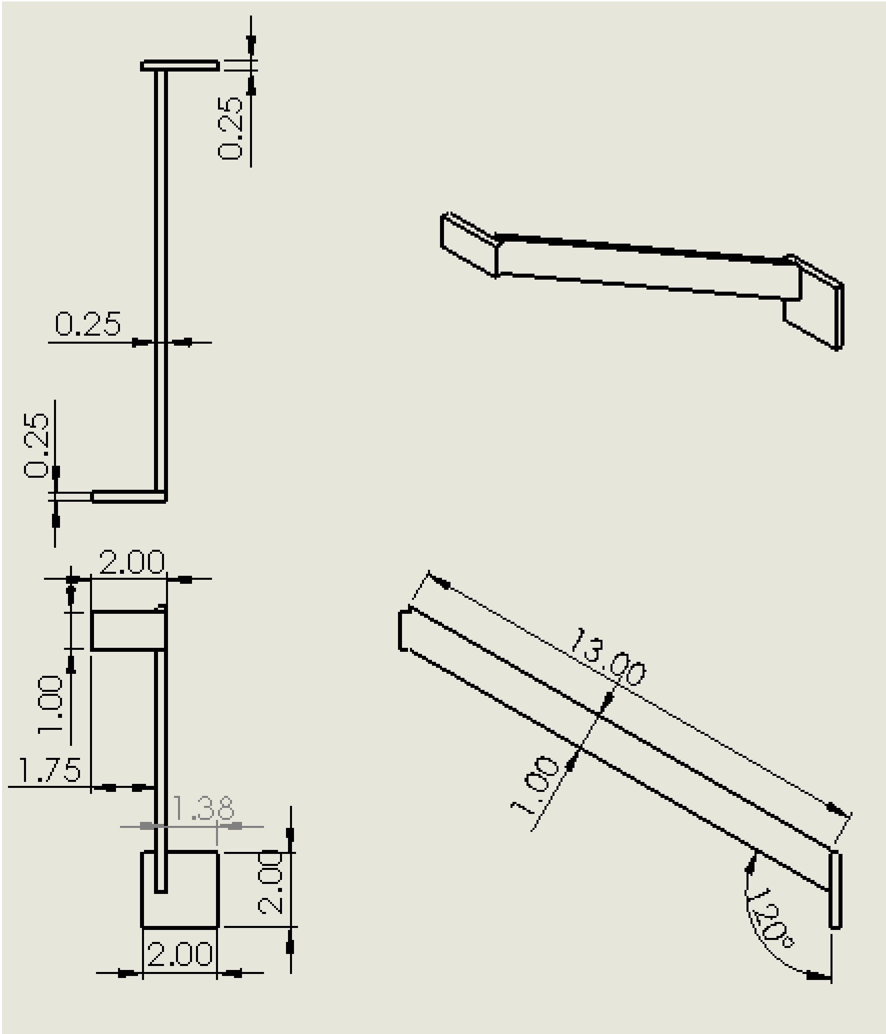

Heat Exchanger Mounting Brackets

Heat Exchanger Mount made from ¼" 6061 Aluminum.

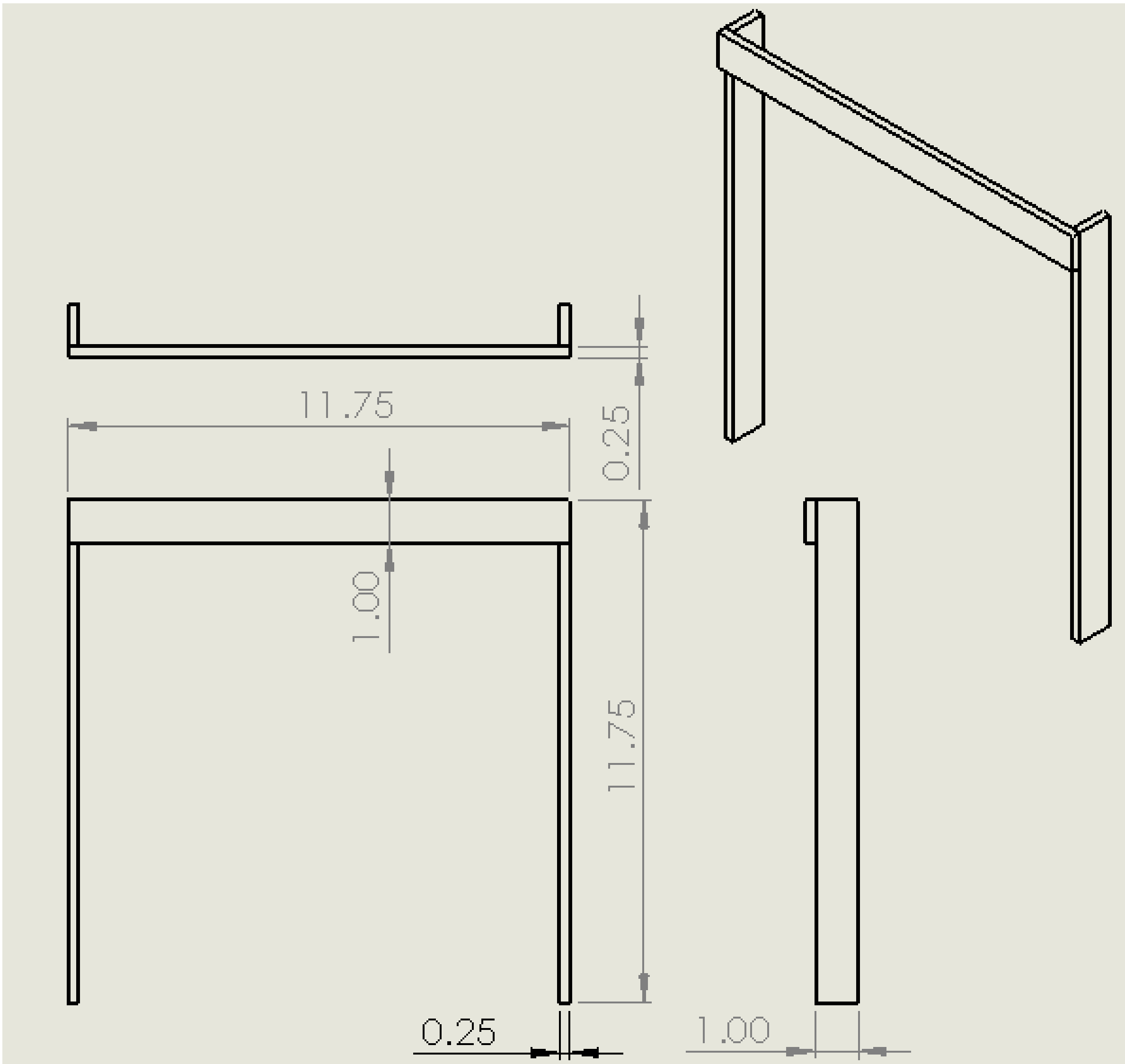

Rear Bird Plate:

Rear Bird Plate made from 6061 Aluminum. Vent holes and mounting holes not shown.

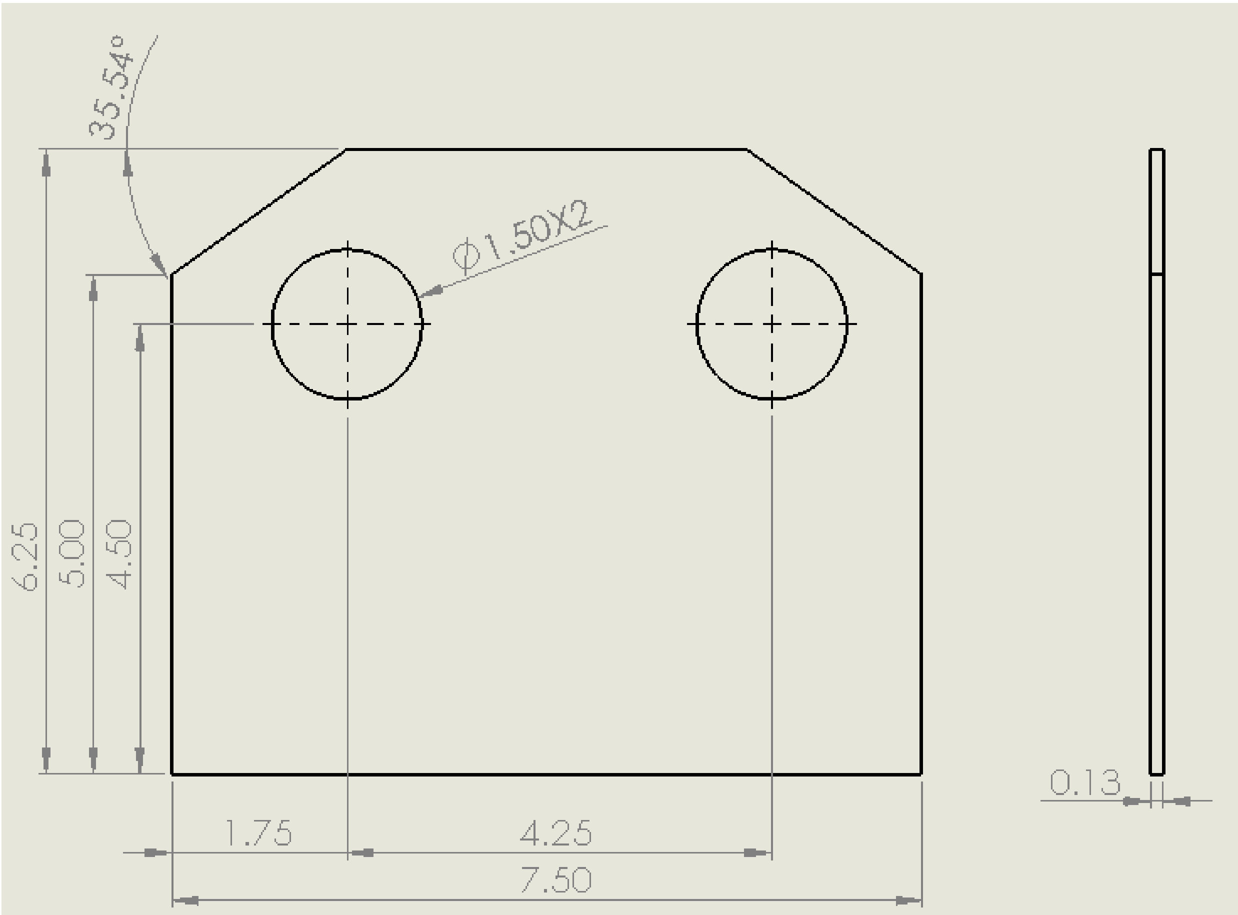

Hydraulic Reservoir:
The hydraulic reservoir will be made from 0.1" 6061 Aluminum. The threaded holes and mounting points shown below will be weld-in bungs.

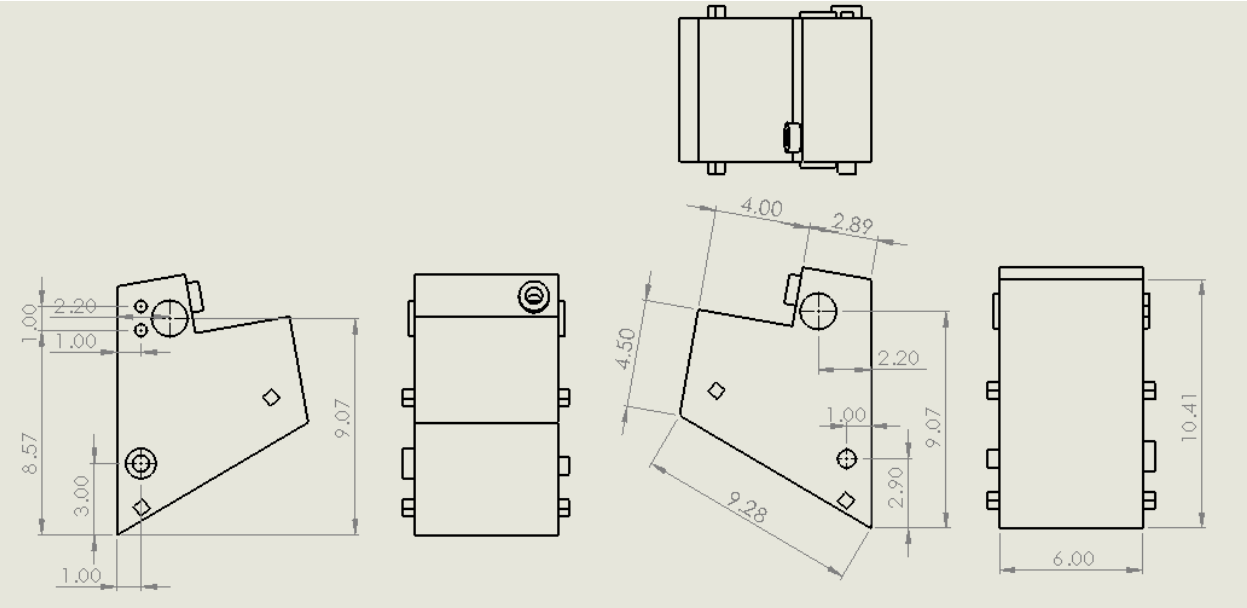

Final Design Assemblies:

Due to the large number of parts associated with this project, the entire assembly will be broken into sections to show more detail in separate parts. After these sections are shown, an entire assembly view will be visible to show detail in how the separate section fit together. Datum will be placed at junctions to show the connection points between assemblies.

Section 1: Pump

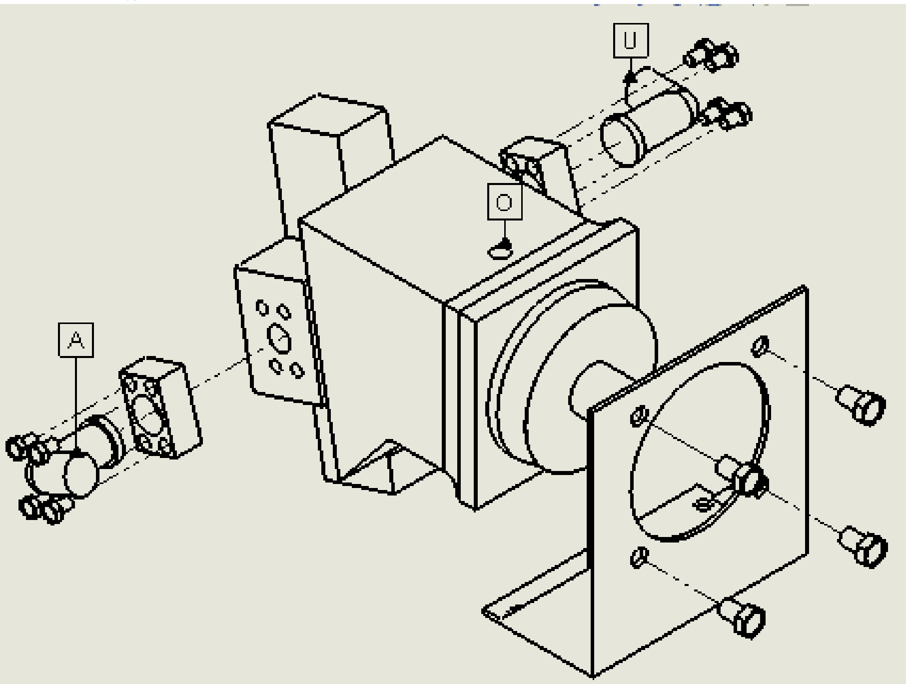

ITEM NO.	PART NUMBER	DESCRIPTION	QTY.
1	A6VM-250	PUMP	1
2	motor_bracket	Custom Built Mounting Bracket	1
3	90 alt Code 62 Flange		2
4	Code 62 Flange 1.25		2
5	B18.2.3.2M - Formed hex screw, M14 x 2.0 x 20 --20WN	Attaches Code 62 Flanges (Item #4) to A6VM-250 (Item #1)	8
6	B18.2.3.2M - Formed hex screw, M20 x 2.5 x 30 --30WN	Attaches Motor Bracket (Item #2) to A6VM-250 (Item #1)	4

Section 2: Pump Outlet Hose, Pressure Relief #1, Pressure Relief #1 Outlet Hose

Valve mounts not shown. Pressure Transducer attached to the bottom.

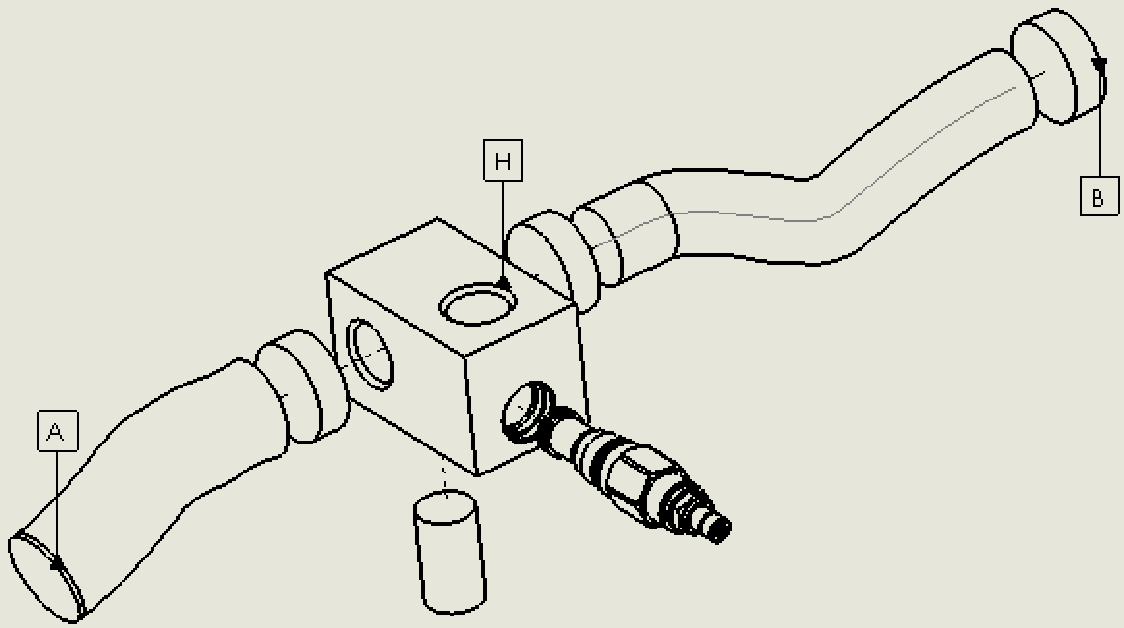

ITEM NO.	PART NUMBER	DESCRIPTION	QTY.
1	FEDS	Sun Hydraulic Manifold	1
2	RDDA-LEN	Sun Hydraulic Pressure Relief Valve	1
3	1" Hose	1" Hose. Outlet of Pump	1
4	3/4" Hose	3/4" Hose. Outlet of Pressure Relief #1	1
5	3/4" Male NPTF Fitting	For 1" Hose	1
6	3/4" Male NPTF Swivel Fitting	For 3/4" Hose	2
7	Pressure Transducer		1

Section 3: Load Bearing Needle Valve and Needle Valve Outlet Hose

Valve mounts not shown.

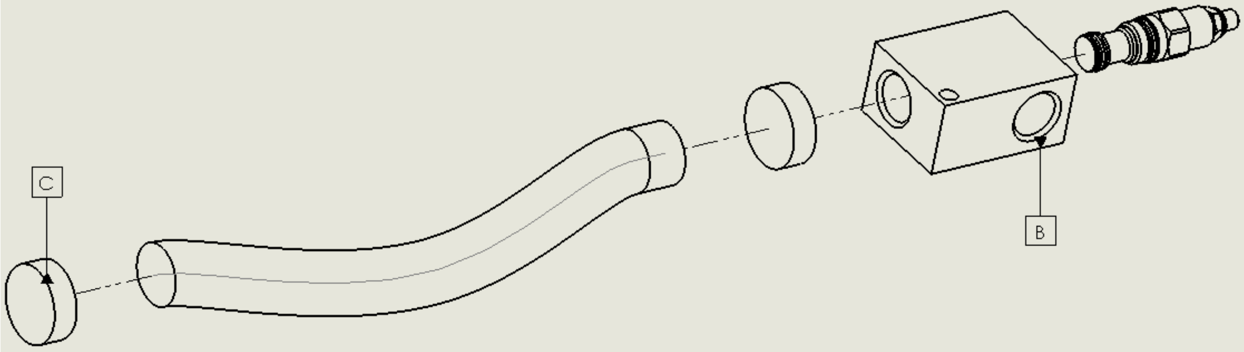

ITEM NO.	PART NUMBER	DESCRIPTION	QTY.
1	GAD	Sun Hydraulic Manifold	1
2	NFCD-LFN	Sun Hydraulic Needle Valve	1
3	3/4" Hose	3/4" Hose. Outlet of Needle Valve	1
4	3/4" Male NPTF Swivel Fitting	For 3/4" Hose	2

Section 4: Pressure Reducing Valve #1and Pressure Reducing Valve Outlet Hose

Valve mounts not shown.

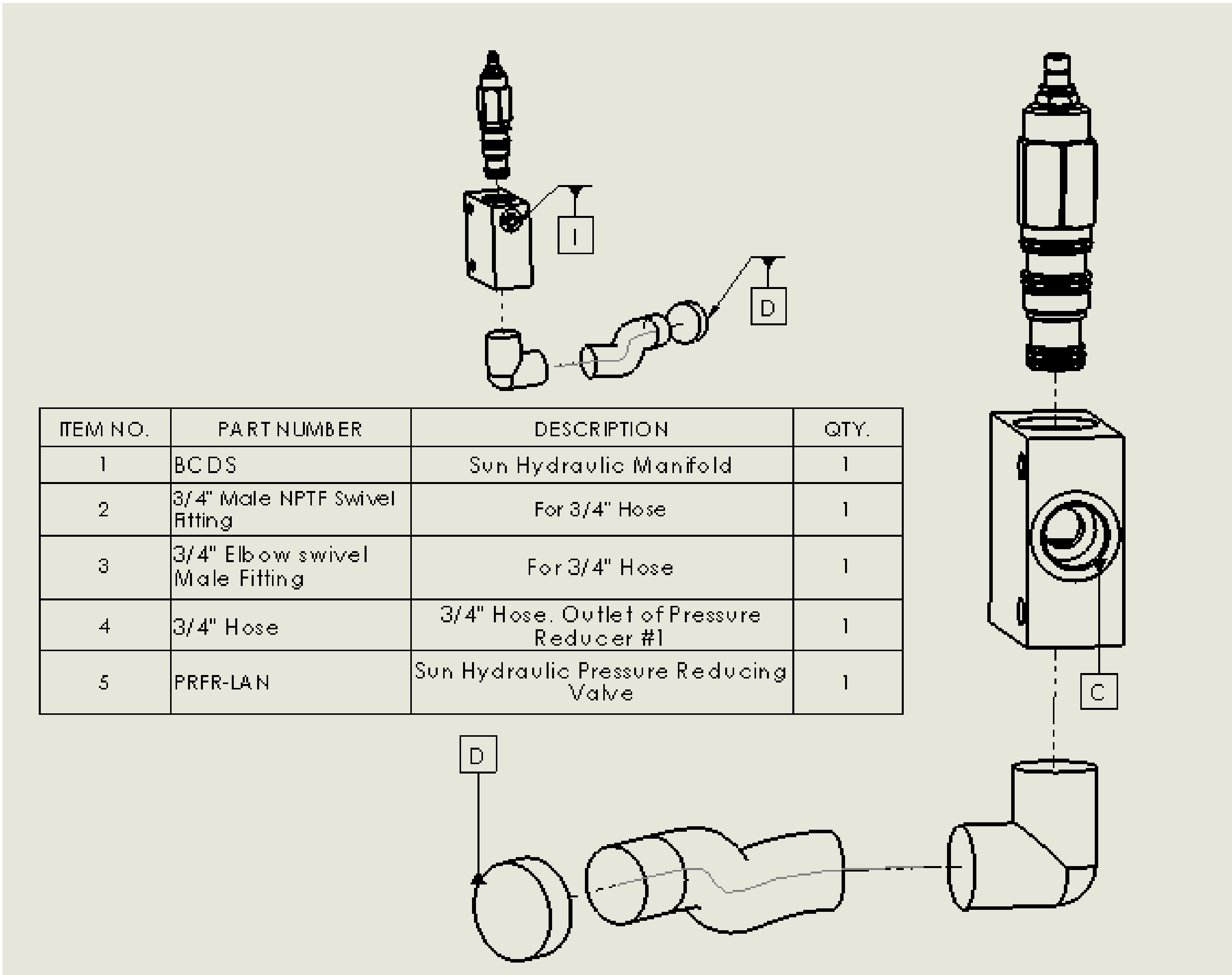

ITEM NO.	PART NUMBER	DESCRIPTION	QTY.
1	BCDS	Sun Hydraulic Manifold	1
2	3/4" Male NPTF Swivel Fitting	For 3/4" Hose	1
3	3/4" Elbow swivel Male Fitting	For 3/4" Hose	1
4	3/4" Hose	3/4" Hose. Outlet of Pressure Reducer #1	1
5	PRFR-LAN	Sun Hydraulic Pressure Reducing Valve	1

Section 5: Pressure Reducing Valve #2 and Pressure Reducing Valve Outlet Hose

Valve mounts not shown.

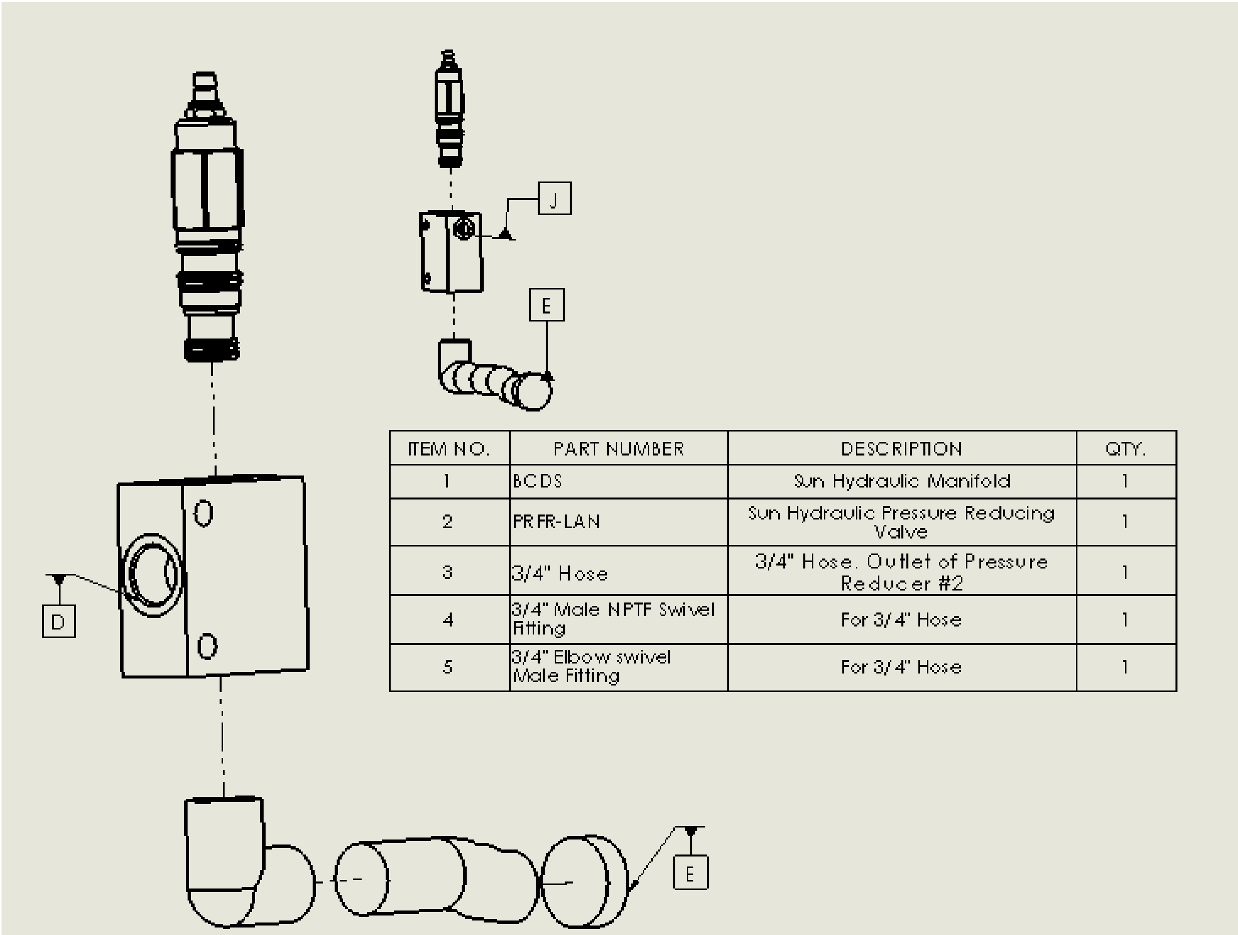

ITEM NO.	PART NUMBER	DESCRIPTION	QTY.
1	BCDS	Sun Hydraulic Manifold	1
2	PRFR-LAN	Sun Hydraulic Pressure Reducing Valve	1
3	3/4" Hose	3/4" Hose. Outlet of Pressure Reducer #2	1
4	3/4" Male NPTF Swivel Fitting	For 3/4" Hose	1
5	3/4" Elbow swivel Male Fitting	For 3/4" Hose	1

Section 6: Pressure Relief Valve #2

Valve mounts not shown.

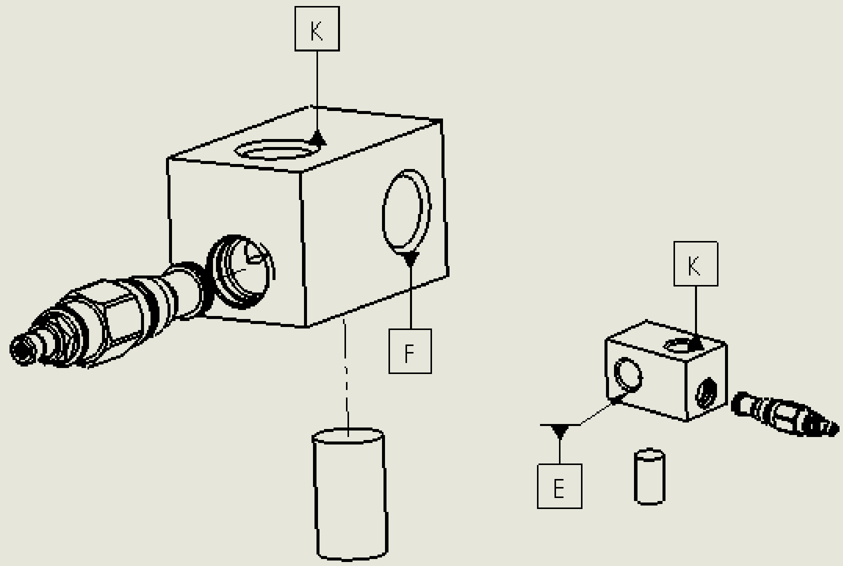

ITEM NO.	PART NUMBER	DESCRIPTION	QTY.
1	FED	Sun Hydraulic Manifold	1
2	Pressure Transducer		1
3	RDDA-LSN	Sun Hydraulic Pressure Relief Valve	1

Section 7: Heat Exchanger and Heat Exchanger Inlet and Outlet Hoses

Heat Exchanger mounts not shown. Oil filter not shown.

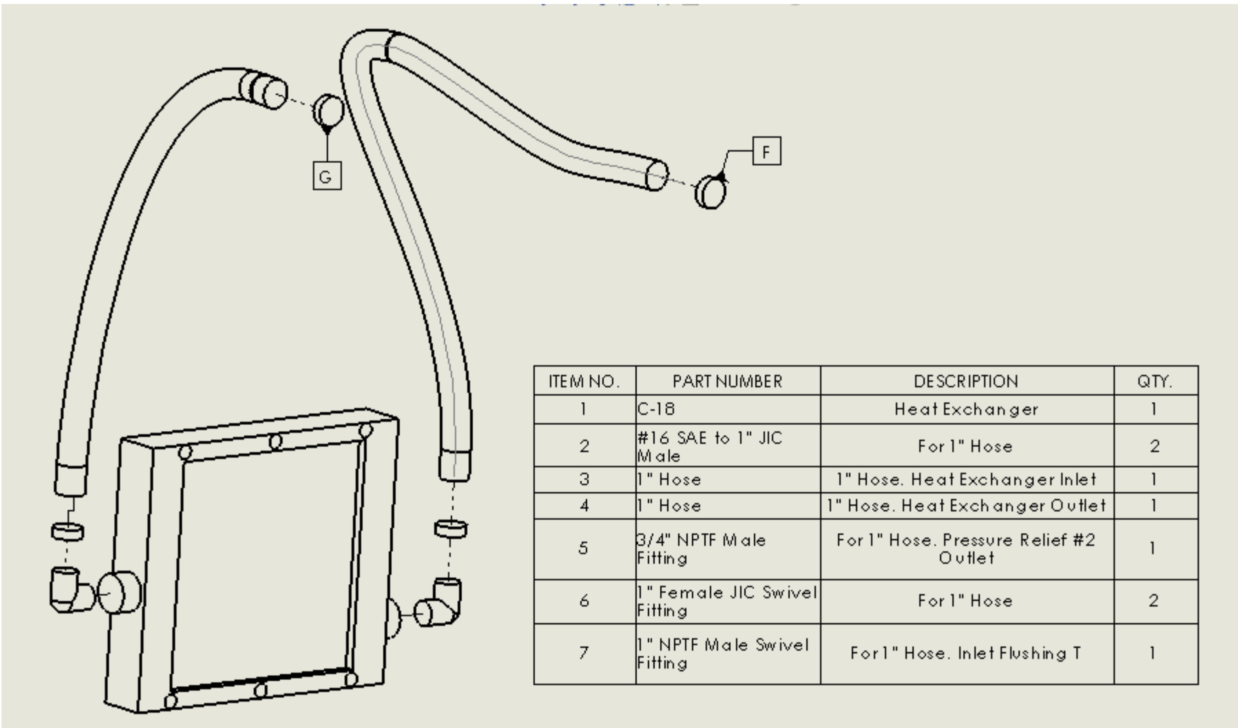

ITEM NO.	PART NUMBER	DESCRIPTION	QTY.
1	C-18	Heat Exchanger	1
2	#16 SAE to 1" JIC Male	For 1" Hose	2
3	1" Hose	1" Hose. Heat Exchanger Inlet	1
4	1" Hose	1" Hose. Heat Exchanger Outlet	1
5	3/4" NPTF Male Fitting	For 1" Hose. Pressure Relief #2 Outlet	1
6	1" Female JIC Swivel Fitting	For 1" Hose	2
7	1" NPTF Male Swivel Fitting	For 1" Hose. Inlet Flushing T	1

Section 8: Flushing Tee, Flushing Needle Valve, and Flushing Hose

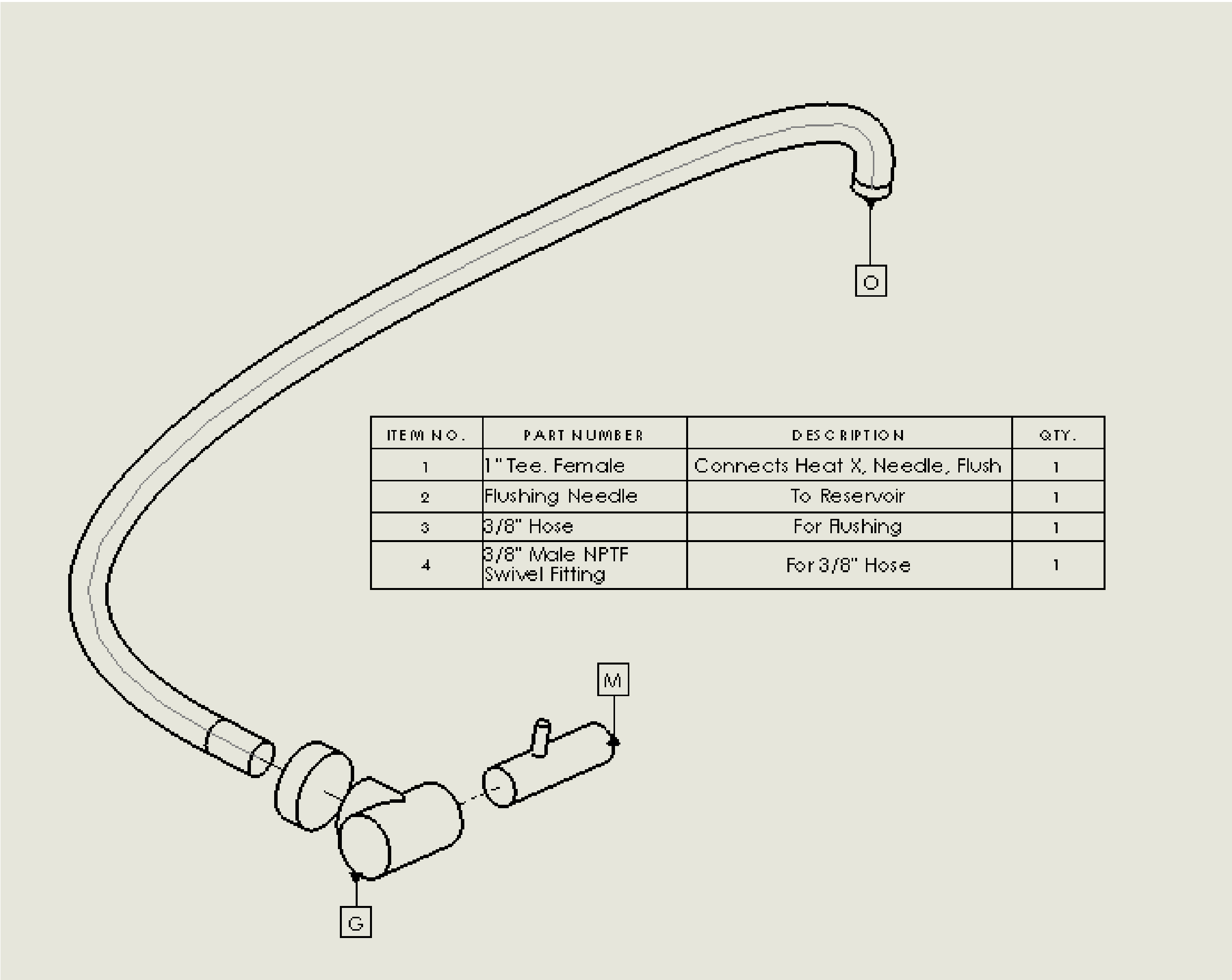

ITEM NO.	PART NUMBER	DESCRIPTION	QTY.
1	1" Tee. Female	Connects Heat X, Needle, Flush	1
2	Flushing Needle	To Reservoir	1
3	3/8" Hose	For Flushing	1
4	3/8" Male NPTF Swivel Fitting	For 3/8" Hose	1

Section 8: Reservoir and Connected Hoses

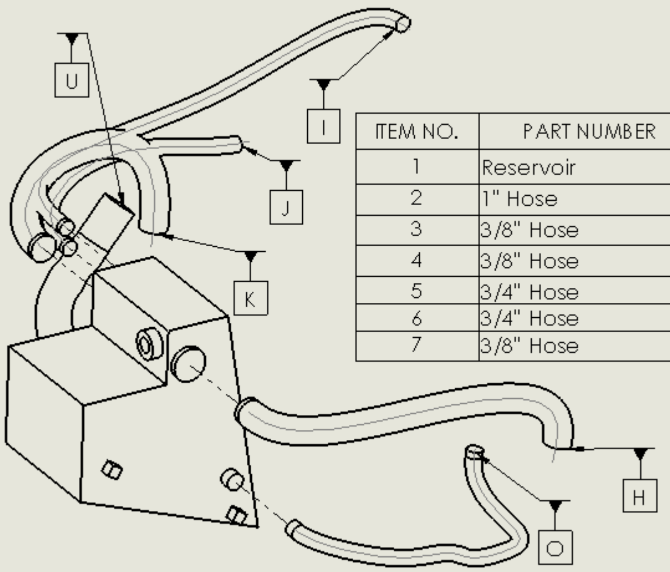

ITEM NO.	PART NUMBER	DESCRIPTION	QTY.
1	Reservoir		1
2	1" Hose	Pump Inlet	1
3	3/8" Hose	Pressure Reducing #1 Drain	1
4	3/8" Hose	Pressure Reducing #2 Drain	1
5	3/4" Hose	Pressure Relief #2 Port 3	1
6	3/4" Hose	Pressure Relief #1 Port 3	1
7	3/8" Hose	Pump Drain	1

Full Assembly:

Right:

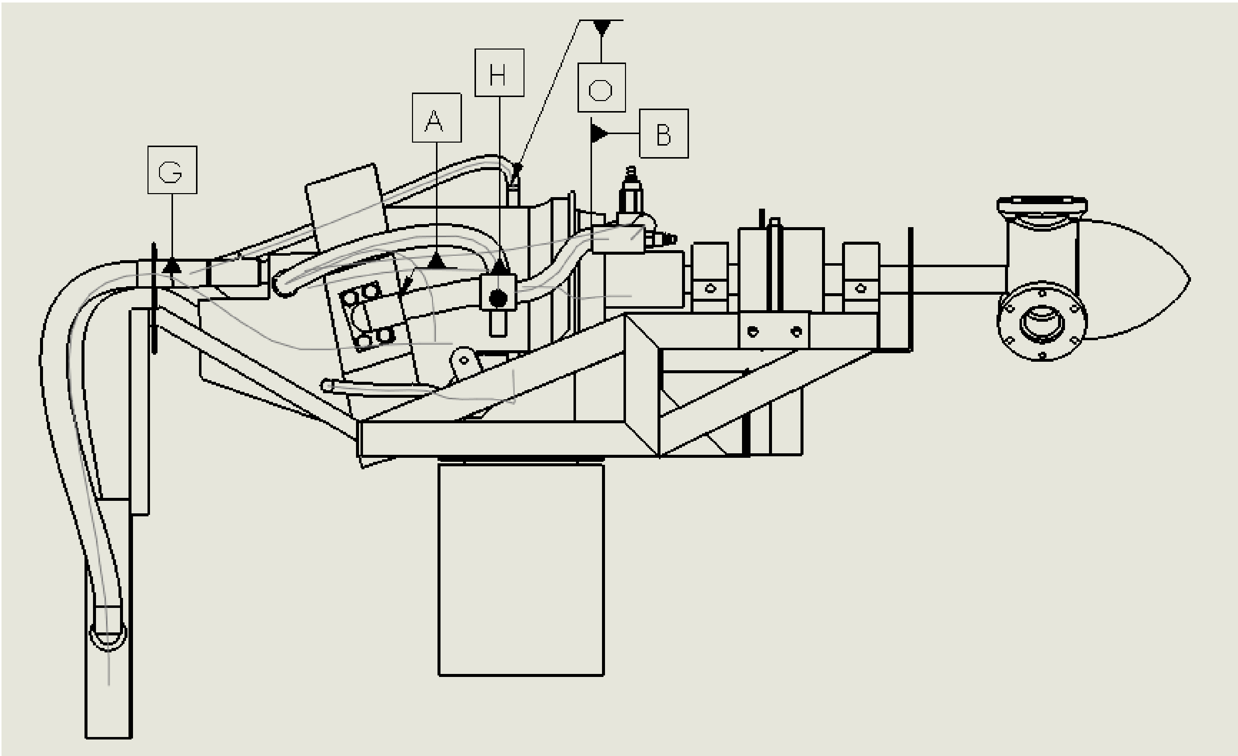

Left:

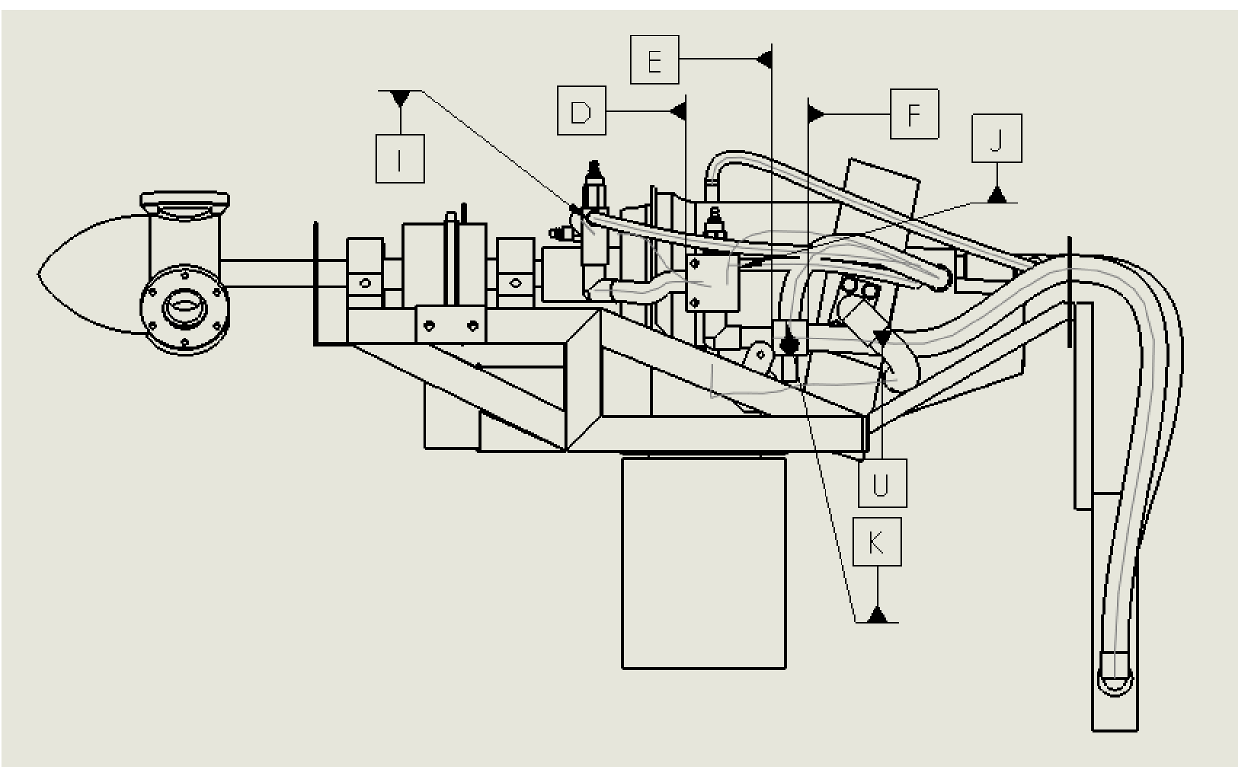

Top:

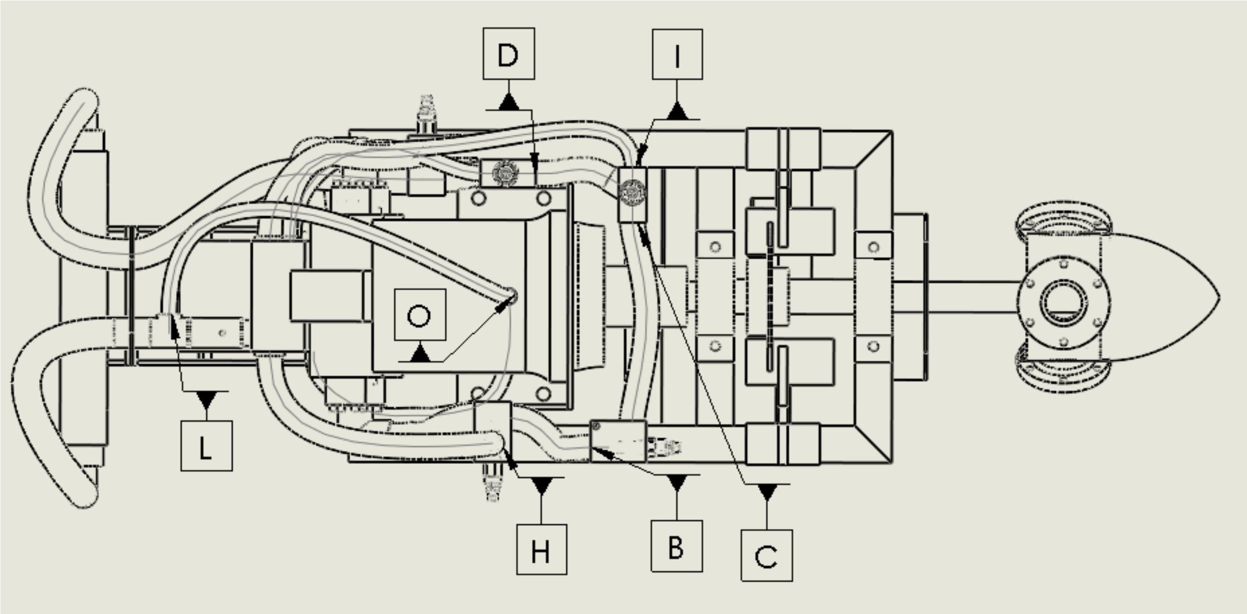

Isometric: